Calibration and Verification of a Mathematical Model for the Simulation of Blackwater/Biowaste Digestion

Master Thesis

A u t h o r : Yucheng Feng

Supervisors: Prof. Dr.-Ing. Ralf Otterpohl

Prof. Dr.-Ing. Rainer Stegmann

Dr.-Ing. Joachim Behrendt

Institute of Wastewater Management

Institute of Waste Management

Hamburg University of Technology

December 2004, Hamburg Germany

Preface

I found that I became a butterfly in my dream last night. Morning I woke up. I really do not know that it is just a butterfly in my dream or I am just a person in the dream of the butterfly.

Chinese philosopher – Zhuangzi (B.C. 369 – B.C. 286)

URN urn:nbn:de:gbv:830-tubdok-5750

URL http://doku.b.tu-harburg.de/volltexte/2009/575/

y.feng@gmx.net

Contents

Acknowledgement

I would like to thank Prof. Dr. -Ing. Ralf Otterpohl very much. Though he is always so busy, he still tries to talk to me and help me. He taught me the scientific knowledge. He also taught me how to touch the world in a different way.

I would like to thank Prof. Dr. -Ing. Rainer Stegmann to be my examiner.

I would like to thank Dr. -Ing. Joachim Behrendt so much. He is a very good teacher, as well as a very good friend. He shared not only knowledge, but also experience with me. He helped me to face the confront difficulties. He talked to me breezily and sprightly in order to make tough and bald studies become comfortable and enjoyable. I should say that without his help, I could not achieve the work readily and opportunely.

I would like to thank International Postgraduate Studies in Water Technologies (IPSWaT), Prof. Dr. -Ing. Uwe Neis and Dipl. -Ing. Torben Blume for awarding and taking care of my financial support. Without their sustainment, I have no chance to entirely concentrate on my study, and I can not have more opportunities to touch the German spirits.

Thanks to Dipl. -Ing. Claudia Wendland, Dipl. -Ing. Stefan Deegener and Dipl. -Ing. Jörn Heerenklage. Because of their cordial and zealous help, the experiments parts of this study can be executed smoothly and approvingly.

I want to thank Mr. Damien J. Batstone very much, though we do not know each other, even only contacted by email. He provided me invaluable information and help.

Special thanks to my parents and my sister. Without their support and encouragement either in spirit or in matter, I could never have chance to come here and study freely. They are the best parents and the best sister for me.

I appreciate the whole Institute of Wastewater Management for providing such a beautiful condition and ambience for scientific research.

Again, thanks to everyone who had ever helped me, encouraged me, and supported me. They are the most important parts in my life.

In North America, there is a kind of butterfly. It has only 3 weeks life. However, before it is able to become a butterfly flying in the sky, it has to be the chrysalis staying under the earth for 17 years. This is just my three-week life, and I like this beautiful life…

Abstract

The object of this work is to apply and develop IWA anaerobic digestion model No.1 (ADM1) to the blackwater anaerobic digestion (BWAD) plant. The basic theory of anaerobic digestion (AD) processes and biochemical kinetics were introduced first. Afterwards the model was calibrated based on the performance of a lab-scale BWAD plant (at the mesophilic condition). The calculation includes three scenario studies, i.e. the reference conditions, the different feeding frequency and with high NH_4^+ input concentration. In order to verify the biochemical kinetics, the batch experiments were executed. According as the Michaelis-Menten kinetics, the maximum uptake rates (k_m) of butyrate, propionate, acetate are 18, 14, 13 d^{-1}, and their half saturation concentrations (K_S) are justified as 110, 120, 160 g COD/m^3, respectively. The further two scenario studies were achieved based on the calibrated and verified model. First, the BWAD plant performance is predicted with different sludge retention time (SRT); second, the kitchen refuse (KR) was added into BWAD plant. The model successfully simulated these two scenarios and generated some suggestions for the operation of the real BWAD plant.

The model was discussed from the mathematical point of view subsequently. Disintegration and hydrolysis is not the rate-limiting step (at least not the sole step) for BWAD. They are much faster than the common mesophilic biowaste digestion. Containing disintegration and hydrolysis two steps make the model more flexible and controllable, although they are treated as one step normally. The influence from uptake processes of valerate and butyrate was checked. At least in BWAD, valerate and butyrate have very limited impact on the whole anaerobic digestion processes (ADP). Meanwhile, ADM1 uses the same degraders (i.e. the same uptake rate) to utilise these two acids. However, we suggested that these two acids are either excluded from the model (if they are not important), or included with individual uptake rates. Two methods for implementing acid-base processes were compared (equilibrium processes with differential-algebraic equation (DAE) and dynamic processes with differential equation (DE)). The same simulation results were obtained, which indicates that two methods can be arbitrarily chosen for all each acid-base. As to inhibition, different half inhibitory NH_3 concentration had to be used in order to fit in with both the reference condition and high NH_4^+ input situation. This implies that the threshold of NH_3 inhibition could be existent. The coefficients for physicochemical processes k_La and k_p were tested by the model. Both of them are not sensitive to the model, so the determination experiments are unnecessary. In our model, $k_La = 20\ d^{-1}$ and $k_p = 100\ m^3/(d \cdot bar)$, respectively. It is justified that cations and anions influence pH strongly due to the charge balance, though they do not contribute either OH^- or H^+. The startup of model needs to be careful because of minus logarithm due to the improper initial conditions.

1 Introduction

In this chapter, as the basic elements of this research work, the anaerobic digestion (AD), the ecological sanitation (ECOSAN), and the mathematical modelling are introduced firstly. Afterwards, the targets of this work are presented.

1.1 Anaerobic digestion (AD)

The anaerobic process is one of the oldest natural processes which has been existing millions years. AD is among the oldest processes used for the stabilization of solids and biosolids (Metcalf & Eddy 2003, pp1505). Two total different group species, *bacteria* and *Archaea*, work together to convert organic matter into the methane (CH_4) in the absence of molecular oxygen. In the species of *Archaea*, a large number of *Euryarchaeota* produce methane as an integral part of their energy metabolism. Such organisms are called *methanogens* and the process of methane formation called *methanogenesis* (Madigan *et al.* 2003, pp453).

Anecdotal evidence indicates that biogas was used for heating bath water in Assyria during the 10th century BC and in Persia during the 16th century. Jan Baptita Van Helmont first determined in 17th century that flammable gases could evolve from decaying organic matter[1]. The Italian physicist Alessandro Volta recognized a direct correlation between the anaerobic decomposition of organic matter and the produced flammable gas in 1776 with his famous experiment of "combustible air" (Barker 1956). About one century later, the first full-scale anaerobic treatment for domestic wastewater treatment appeared and was recorded in the French journal (McCarty 2001). At the beginning of 20 century the Imhoff tank, which was modified based on Travis tank, came into use, and the improved Imhoff tank was widely used in many German and American cities in the later three decades (Metcalf and Eddy 1915). The anaerobic process for industrial wastewater treatment is considered that it was started by Arthur M. Buswell and his colleagues at the beginning of 1920s (McCarty 2001).

Another leap development is the Upflow Anaerobic Suspended Batch (UASB) process conceived by G. Lettinga in the early 1970. The UASB concept and method accelerate the development and application of anaerobic biological process in wastewater treatment. The earliest publication of UASB with the general description in the international journals can be found from Lettinga *et al.* (1980).

AD has many advantages, like biogas (mainly CH_4) is a renewable energy resource, biosolids are the good soil conditioner, and anaerobic digestion processes (ADP) produce less volume biosolids with less pathogens danger as well as less energy consumption comparing to aerobic processes, etc. Both European community and U.S. consider that anaerobic treatment is the most promising approach for future in sustainable development (Lema and Omil 2001,

[1] http://www.biogasworks.com/Index/AD%20Short%20History.htm

NRC 1995). AD treatment can be the indispensable element in the sustainable sanitation concepts (Otterpohl *et al.* 1997).

1.2 Ecological sanitation (ECOSAN)

Based on the principle of separating different flows of domestic wastewater according to their characteristics, ECOSAN directs towards establishing an efficient domestic water system including nutrients recycling. It is an approach that saves water, protects water quality, prevents pollution and returns valuable nutrients into the loop on which our food security depends[2]. It represents a holistic approach towards sound ecological and economic sanitation[3]. ECOSAN is the closing loop in wastewater management and sanitation[4]. Otterpohl (2001) illustrated this new sanitation concept and gave successful examples.

With the increasing awareness of its ecological and economic value, more and more ECOSAN projects are currently built over the world. In Lübek-Flintenbreite, Germany, an innovative decentralised sanitation concept has been realised in a peri-urban area. Currently, 100 inhabitants are connected to the plant and the capacity of the system is up to the 350 persons that shall be living in the settlement when it will be finalised. Grey and black water are collected and treated separately (Otterpohl *et al.* 2002). Figure 1 is the scheme of this ECOSAN pilot project. As regards blackwater (BW), simply it is the wastewater coming from toilet. The components of the BW are mainly human feces, urine, flushing water, and toilet paper as the concomitant. Our work will be based upon the AD treatment of the BW from this project.

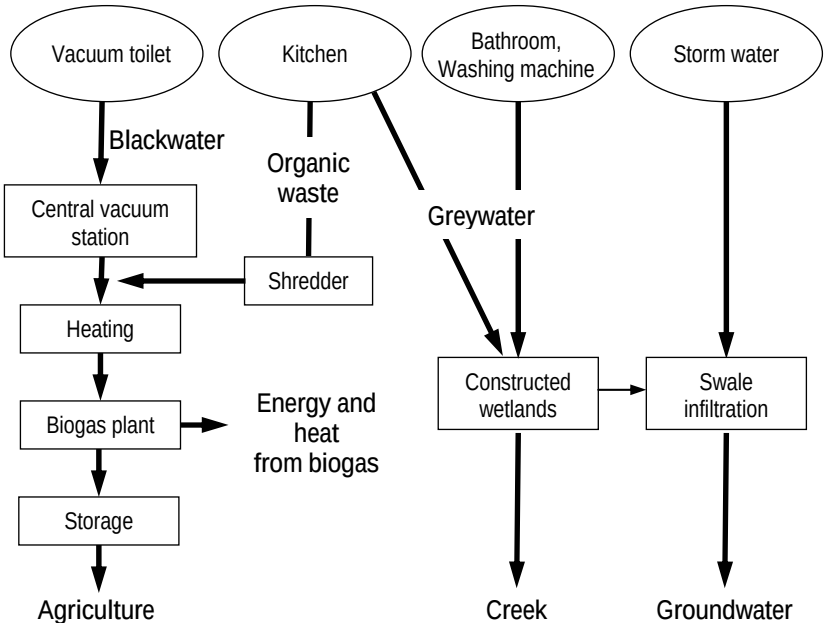

Figure 1: Scheme of the ECOSAN pilot project Lübeck-Flintenbreite (Wendland *et al.* 2004)

[2] http://www.ecosan.nl/
[3] http://www.ecosan.at/
[4] http://www2.gtz.de/ecosan/

1.3 Mathematical model

The model is a simplified representation of reality based on hypotheses and equations used to rationalize observations[5]. By providing a rational environment, models can lead to deeper and more general understanding[5].

The useful model should satisfy the following demands (Jöbses 1986):

1. adequate description of the features of interest
2. correlation of observable quantities to each other by mathematical functions
3. the mathematical functions with their parameters must be experimentally verifiable and determinable

Therefore, the more a mathematical model reflects the reality, the more opportunities it could predict the new experimental results. That is one of the primary senses of mathematical models.

The mathematical anaerobic digestion model (ADM) has been extensively investigated and developed during the last 3 decades (Gavala *et al.* 2003). The simplest ADM contains only one biological process, where the most complex ADM involves more than 20 biological and physicochemical processes. In 2002, the *International Water Association (IWA) Task Group for Mathematical Modelling of Anaerobic Digestion Processes* published one ADM, namely, IWA, Anaerobic Digestion Model No. 1 (ADM1) (Batstone *et al.* 2002). Trying to be a generic platform, ADM1 involves totally 19 biochemical processes with 7 species utilising 8 intermediates, as well as three sorts of physiochemical processes. As one of the most sophisticated model, ADM1 is chosen to be the fundamental of our work.

1.4 Tasks of this work

Our work is to implement and develop an ADM, which can be applied to anaerobic treatment of BW from vacuum toilet. All the data for calibration come from a lab-scale AD plant, which has been operating steadily for two years.

Based on above, the tasks of this work are outlined as follows:

1. implement and develop a mathematical anaerobic digestion model
2. calibrate the model by the lab-scale AD plant
3. verify kinetics parameters of the model
4. improve the performance of lab-scale AD plant by the model
5. check and enhance the capacity of the model

[5] http://www.biofilms.bt.tudelft.nl/

2 Mathematical model of Processes

In order to build up the mathematical mode, the nature anaerobic processes need to be understood first. So in this chapter, the ADP are introduced followed by the mathematical equations and the methods to construct the model. The necessary software is introduced as well.

2.1 General processes of AD

Currently, the basic steps of ADP are clear. Being very complex processes, the ADP can fall into two kinds of processes, biochemical processes (in Figure 2 following the vertical lines) and physicochemical processes (in Figure 2 following the horizontal lines). Abbreviations in Figure 2 are AA (amino acids); MS (monosaccharides); LCFA (long chain fatty acids); HVa (valeric acid); Va^- (valerate); HBu (butyric acid); Bu^- (butyrate); HPr (Propionic acid); Pr^- (propionate); HAc (acetic acid); Ac^- (acetate). HVa, HBu, HPr and HAc are classified as short chain fatty acids (SCFA).

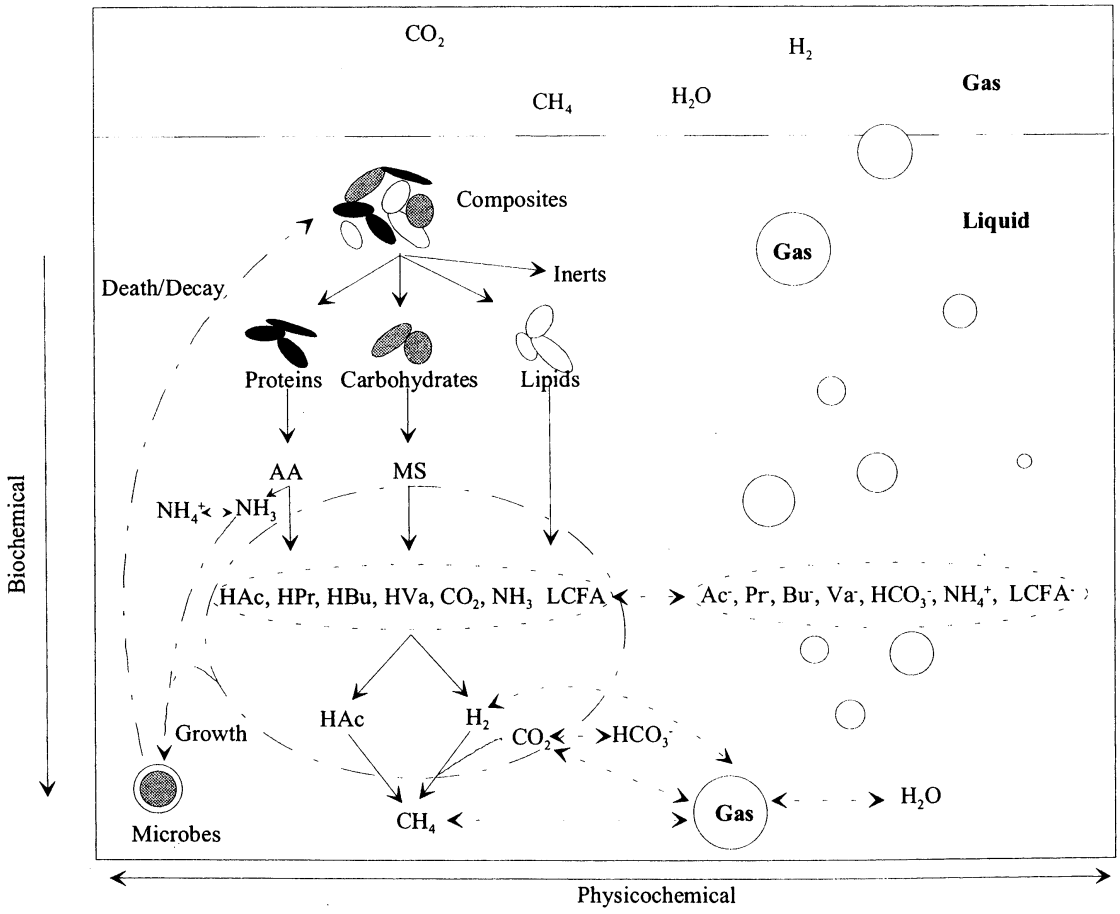

Figure 2: The general processes of AD (Batstone *et al.* 2002)

Through the biochemical processes, the raw composites are converted to CH_4, CO_2, biomass, inerts, etc. and in between there are many intermediate steps and intermediates. The

physicochemical processes mainly describe the physical phenomena and chemical reactions, such as gas transfer, precipitation, and acid-base reactions etc.

It needs to be remembered that under different conditions the different final products can be obtained through anaerobic processes. Besides CH_4, ethanol, volatile fatty acids (VFA) and H_2 also can be the main products. One side, this character makes the anaerobic processes more applicable; on the other side, the desired final products might never appear due to the improper conditions.

Though only the biological processes are expected in order to get the desired final products, the physicochemical processes also need to be looked into and controlled, as they influence the biochemical processes severely.

In ADM1, the biochemical processes are categorized into five steps: Disintegration, hydrolysis, acidogenesis, acetogenesis and methanogenesis. Figure 3 displays these steps with the mass flux. In Figure 3, the arrows represent the mass flow through the biochemical processes, and the numbers beside the lines are the ratio of the mass flux. These ratios are only the examples, as with different raw composites the ratios will be certainly different.

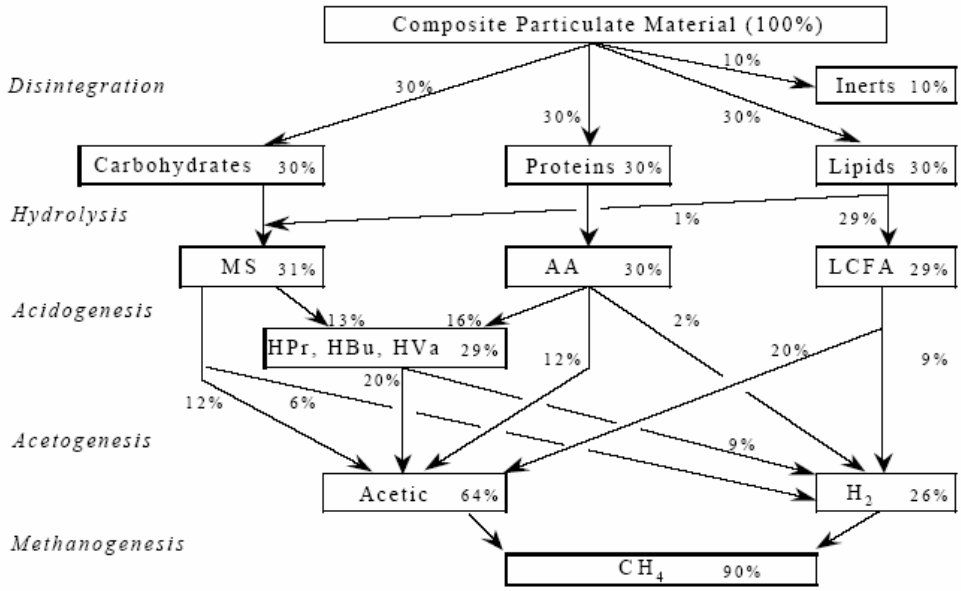

Figure 3: The biochemical processes with the mass flux of AD (Batstone *et al.* 2002)

2.2 Units, parameters and variables

The ADM1 uses the units of kg COD/m^3 and kmole/m^3 (kmole/m^3 ≡ M), though it offers the method to transfer the units. In our model the units of g COD/m^3 (g COD/m^3 ≡ mg COD/l), g N/m^3 (g N/m^3 ≡ mg N/l) and mole/m^3 (mole/m^3 ≡ mM) are used, which are universally used units for aerobic wastewater treatment. The unit of g COD/m^3 is used for the concentrations of substrates and biomass, where the g N/m^3 and mole/m^3 are for Nitrogen and inorganic carbon (IC) respectively. The other physical units of bar (pressure), m (distance), m^3 (volume) and day (time) are used.

The parameters and variables with their symbols and units are listed in Table 1.

Table 1: parameters and variables

Symbol	Description	Unit
Stoichiometric and kinetic coefficients		
Biochemical processes		
C_i	carbon content of component i	mole C·g COD^{-1}
N_i	nitrogen content of component i	mole N·g COD^{-1}
ρ_j	reaction rate of process j	varies
v_{i_j}	coefficient of component i on process j in the matrix	-
f_{i_j}	yield of product i on component j	g COD·g COD^{-1}
k_{dis}	disintegration rate (first-order)	d^{-1}
$k_{hyd,i}$	hydrolysis rate (first-order) of substrate i	d^{-1}
$k_{m,i}$	maximum specific uptake rate of process i	d^{-1}
$K_{S,i}$	half saturation value of process i	g COD·m^{-3}
Y_i	yield of biomass on substrate i	g COD·g COD^{-1}
$k_{dec,i}$	biomass decay rate (first-order) of degrader i	d^{-1}
I_{i_j}	inhibition function of inhibitor i on process j	-
K_{I,i_j}	half inhibitory coefficient of inhibitor i on process j	g COD·m^{-3}
Physico-chemical processes		
ρ_j	reaction rate of process j	varies
$K_{a,i}$	acid dissociation constant of acid i	mole·m^{-3}
$pK_{a,i}$	$-\log_{10}[K_{a,i}]$ of acid i	-
$k_{A/B,i}$	acid - base dynamic constant of acid i	m^3·$mole^{-1}$·d^{-1}
$k_{prec,i}$	precipitation rate constant of salt i	$mole^{-1}$·d^{-1}
$K_{H,i}$	henry's law coefficient of gas i	mole·m^{-3}·bar^{-1}
k_La	gas liquid transfer coefficient	d^{-1}
k_P	pipe resistance coefficient	m^3·d^{-1}·bar^{-1}
ΔG	Gibbs free energy	J·$mole^{-1}$
R	gas law constant, 8.314 x 10^{-5}	bar·m^3·$mole^{-1}$·K^{-1}
State parameters		
V	volume	m^3
T	absolute temperature	K
t	time	d
Variables		
S_i	concentration of soluble component i	g COD·m^{-3}
X_i	concentration of particulate component i	g COD·m^{-3}
pH	$-\log_{10}[S_H^+]$	-
$P_{gas,i}$	pressure of gas i	bar

2.3 Peterson Matrix

Peterson Matrix (Peterson 1965) is the widely used structure to construct chemical and biological models, which is terse and flexible. In the matrix, each row represents one process, where each column represents one component. The reaction rates of processes are displayed on the right side of the matrix, where the coefficients between processes and components are distributed inside the matrix. Formerly, the activated sludge models (ASM) from *IWA Task Group on Mathematical Modelling for Design and Operation of Biological Wastewater Treatment* was built up in the way of Peterson Matrix (Henze *et al.* 2000). ADM1 is also constructed by Peterson Matrix. Appendix B is the matrix of biochemical processes and Appendix C is the matrix of the physicochemical processes. More explanation of these matrixes is narrated in following sections.

2.4 Implementation of biochemical processes

2.4.1 Disintegration and hydrolysis

As discussed before, five steps of ADP are identified. The first two steps are disintegration and hydrolysis. These processes occur with the support of extra cellular-enzyme outside organisms in the liquid phase. Actually, in most literatures these two steps are not divided, and instead the processes are together investigated in the term of hydrolysis. From the mathematical point of view, the processes with two steps make the model easier to be adjusted in order to be seasoned with different cases.

It is generally accepted that the hydrolysis (or disintegration) is the rate-limiting step over the whole ADP if the substrates are in the particulate form (Eastman and Ferguson 1981). Several mathematical models can be used to implement hydrolysis (the same for disintegration). Vavilin *et al.* (1996) compared the four types of hydrolysis kinetics, i.e. the first-order, two-phase model (Vavilin *et al.* 1996), Monod type (Hobson 1983), and Contois model (Chen and Hashimoto 1980) with four different composites (swine waste, sewage sludge, cattle manure, cellulose), and the four kinetics gave the similar simulation results. Being a simplest and most widely applied kinetics, the first-order kinetics is easiest to implement and adopted in our model.

The common expression of first-order kinetics is shown as equation (Eqn.) (1).

$$\rho_i = k_i X_i \tag{1}$$

Where: ρ_i = uptake rate of substrate i, g COD/(m^3·d)

k_i = parameter of first order kinetics of particulate component i, d^{-1}

X_i = particulate component i, g COD/m^3

The parameter k_{dis} is used for disintegration, where the parameters k_{hyd_ch}, k_{hyd_pr} and k_{hyd_li} are used for the hydrolysis of carbohydrates (ch), proteins (pr) and lipids (li), respectively. The values of k_i can be found in Appendix E.

2.4.2 Substrates uptake

Following hydrolysis, three steps acidogenesis, acetogenesis and methanogenesis are at its heel orderly. They are used to describe the utilisation of substrates by microorganisms. Seven species are involved in three steps, namely sugar degraders, amino acids degraders, LCFA degraders, valerate and butyrate degraders, propionate degraders, acetate degraders and hydrogen degraders. Especially valerate and butyrate are utilised by the same degraders in ADM1 (it will be further discussed in section (Sec.) 4.3).

2.4.2.1 Uptake kinetics

Formerly, the ASMs use Monod Kinetics to describe the growth rate of biomass. Different from ASM, the ADM1 use Michaelis-Menten Kinetics to describe the uptake rate of substrate (Michaelis and Menten 1913). Flexibility to include the different kinetics forms (e.g. inhibition) is one of the reasons that ADM1 use Michaelis-menten kinetics (substrate uptake rate) instead of Monod function (biomass growth rate) (Batstone *et al.* 2002).

Another often used function is Haldane Kinetics (Haldane 1930), which considers that too high concentration of substrate will cause the reverse reaction (or say it will inhibit the uptake of substrate itself). Eqn. (2) and Eqn. (3) are the formulas of Michaelis-Menten Kinetics and Haldane Kinetics, respectively.

$$\text{Michaelis-Menten: } \rho_j = k_{m,j} \frac{S_i}{K_{S,j} + S_i} X_i \cdot I_{i\_j} \tag{2}$$

$$\text{Haldane Kinetics: } \rho_j = k_{m,j} \frac{S_i}{K_{S,j} + S_i + \frac{S_i^2}{K_{H,i}}} X_i \cdot I_{i\_j} \tag{3}$$

Where: ρ_j = reaction rate of process j, g COD/(m^3·d)

$k_{m,j}$ = maximum specific uptake rate of process j, d^{-1}

$K_{S,j}$ = half saturation concentration of process j, g COD/m^3

$K_{H,j}$ = Haldane saturation concentration of process j, g COD/m^3

S_i = utilised soluble component (i.e. substrate) i, g COD/m^3

X_i = particulate component (i.e. biomass) i, g COD/m^3

I_{i_j} = inhibition function from inhibitor i to process j, g COD/m^3

In our model, owing to the low concentration of intermediates, the Michaelis-Menten Kinetics is used for implementing the uptake of substrates. As the essential parameter, the biomass growth rate is attained by timing uptake rate with yield rate. Seven yield rates Y_i are included for seven different species.

In order to compare different kinds of kinetics easily, the typical curves of the zero order reaction (i.e. the reaction rate is constant), the first order reaction, the Michaelis-Menten Kinetics and Haldane Kinetics are shown in Figure 4.

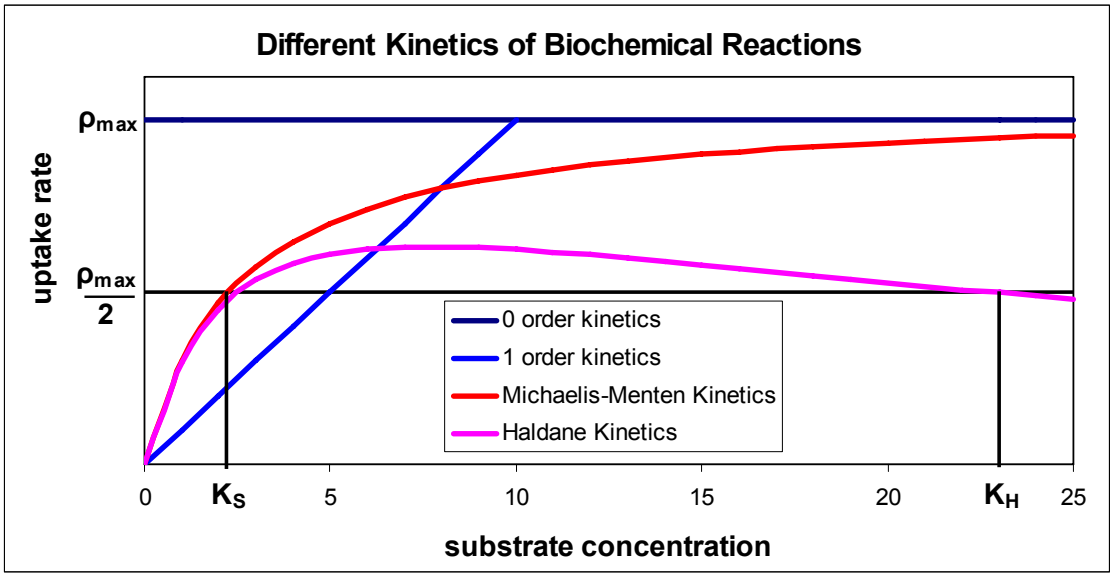

Figure 4: Different Kinetics of Biochemical Reactions

2.4.2.2 Parallel reactions of acidogenesis

In the step of acidogenesis from monosaccharides (MS), parallel reactions can occur simultaneously. ADM1 uses glucose (6 carbons) as the model monomer. Though there are many reaction possibilities of acidogenesis from MS, only following three reactions are taken into account:

$$C_6H_{12}O_6 + 2H_2O \rightarrow 2CH_3COOH + 2CO_2 + 4H_2 \quad \text{(HAc)} \quad (4)$$

$$3C_6H_{12}O_6 \rightarrow 4CH_3CH_2COOH + 2CH_3COOH + 2CO_2 + 2H_2O \quad \text{(HPr and HAc)} \quad (5)$$

$$C_6H_{12}O_6 \rightarrow CH_3CH_2CH_2COOH + 2CO_2 + 2H_2 \quad \text{(HBu)} \quad (6)$$

Suppose the fractions of MS through reaction (4), (5) and (6), are $\eta_{1,su}$, $\eta_{2,su}$ and $\eta_{3,su}$ (subscript su is the shortcut of sugar representing MS), separately. It is obvious that:

$$\eta_{1,su} + \eta_{2,su} + \eta_{3,su} = 1 \quad (7)$$

Hereby, the product coefficients from MS to SCFA and H_2 can be obtained according to above reactions (Table 2):

Table 2: Stoichiometric coefficients from MS uptake

product	coefficient	
Acetate	$f_{ac,su}$ =	0.67 $\eta_{1,su}$ + 0.22 $\eta_{2,su}$
Propionate	$f_{pro,su}$ =	0.78 $\eta_{2,su}$
Butyrate	$f_{bu,su}$ =	0.83 $\eta_{3,su}$
Hydrogen	$f_{h2,su}$ =	0.33 $\eta_{1,su}$ + 0.17 $\eta_{3,su}$

Parallel reactions take place as well during Acidogenesis from amino acids (AA). There are two main pathways for AA fermentation (Batstone *et al.* 2002):

1. Stickland oxidation-reduction paired fermentation

2. oxidation of a single amino acid with hydrogen ions or carbon dioxide as the external electron acceptor.

Only the first pathway is taken into account in ADM1. Unfortunately, due to the diversity of AA, different kinds of input substrates will have different stoichiometric coefficients from AA to SCFA and H_2. The recommended values by ADM1, which are also used in our model, are shown in Appendix E.

2.4.2.3 Carbon balance and nitrogen balance

In many cases, inorganic carbon (IC) is the carbon source or a product of catabolism or anabolism (Batstone *et al*. 2002), so the carbon balance is obligatory. ADM1 uses the following approach to keep the carbon balance:

$$\nu_{IC,j} = -\sum_{i=1\sim9,11\sim24} C_i \nu_{i,j} \tag{8}$$

Where: $\nu_{IC,j}$ = coefficient of processes j for IC in Peterson Matrix

C_i = carbon content of component i, mole C/g COD

$\nu_{i,j}$ = coefficient of processes j for component i

It means that within each biochemical step the difference of carbon contents among all components is finally compensated by IC. Use AA uptake as an example:

$$\nu_{IC,aa} = -\left[-C_{aa} + (1 - Y_{aa})\left(f_{va,aa} C_{va} + f_{bu,aa} C_{bu} + f_{pro,aa} C_{pro} + f_{ac,aa} C_{ac}\right) + Y_{aa} C_{biom}\right] \tag{9}$$

Where: C_{biom} = carbon content of biomass, mole C/g COD

Y_{aa} = biomass yield of AA degraders from AA uptake

The values of C_i are given in Appendix E.

For the same purpose, the inorganic nitrogen (IN) balance is considered with the same approach too. Due to less components contain nitrogen, the coefficients of IN in Peterson Matrix are much simpler. Only the input substance, proteins, AA and biomass contain nitrogen, so the coefficients are:

$$\nu_{IN,j} = \nu_{aa,j} \cdot N_{aa} - Y_j \cdot N_{biom} \tag{10}$$

Where: $\nu_{IN,j}$ = coefficient of processes j for IN in Peterson Matrix

$\nu_{aa,j}$ = coefficient of processes j for AA in Peterson Matrix

N_{aa} = nitrogen content of AA, g N/g COD

N_{biom} = nitrogen content of biomass, g N/g COD

Y_j = biomass yield of process j

The values of N_i are given in Appendix E as well.

2.4.3 Redox potential and free energy

Redox potential is a very important parameter for anaerobic processes. Two decades ago, Mosey (1983) already demonstrated that product formation from acidogenesis is the function of the redox state of the system. In another aspect, to obtain the energy is the primary impetus for organisms to utilise the substrates. Redox and energy are two kinds of groundwork of anaerobic processes. However, they are not directly reflected by the mathematical model. More knowledge of Redox and energy can be found in other relevant literatures.

2.4.4 Biomass decay

The decay of biomass is the indispensable step of the biochemical processes. It is described as the first-order reaction too, so the same formula as Eqn. (1) is used. Seven $k_{dec,i}$ represent the decay rates of seven different species.

Thus, the whole 19 biochemical processes are introduced and have been implemented in one Peterson Matrix (see Appendix B). From process 1 to 4 are disintegration and hydrolysis, where from process 5 to 12 are the substrate uptake processes and last 7 processes (13 to 19) are the decay of 7 species.

2.4.5 Inhibition

Inhibition is the reduction of microbial growth because of a decrease in the number of organisms present or alterations in the microbial environment (Madigan *et al.* 2003, pp696). The inhibitory effect of end products on enzyme-catalyzed reactions can be as a result of three different mechanisms: irreversible inhibition; non-competitive inhibition; and reversible competitive inhibition (Lehninger *et al.* 1993, Stryer 1988). ADP are very sensitive and fragile biological processes. Improper surroundings or changes can destroy ADP totally. Hence, it is essential to include the inhibition function in the model. In ADM1, three kinds of inhibition are involved, 1. pH inhibition, 2. non-competitive inhibition from free ammonia and hydrogen and 3. competitive inhibition between valerate and butyrate.

The inhibition factor is implemented by timing inhibition term with substrate uptake rate. The symbol I is used as the inhibition term. Two empirical equations were developed. Eqn. (11) deliberates both upper and lower pH inhibition (Angelidaki *et al.* 1993), where Eqn. (12) only considers lower pH inhibition (Ramsay 1997). ADM1 suggests using Eqn. (12) when the free ammonia inhibition is taken into account at the same time. Nevertheless, we found that Eqn. (11) should be used together with the inhibition function of free ammonia.

For upper and lower pH inhibition:
$$I_{pH\_j} = \frac{1 + 2 \times 10^{0.5(pH_{LL} - pH_{UL})}}{1 + 10^{(pH - pH_{UL})} + 10^{(pH_{LL} - pH)}} \tag{11}$$

Only for lower pH inhibition:
$$\left. \begin{aligned} I_{pH\_j} &= \exp\left(-3 \left(\frac{pH - pH_{UL}}{pH_{UL} - pH_{LL}} \right)^2 \right) \Bigg|_{pH < pH_{UL}} \\ I_{pH\_j} &= 1 \Big|_{pH > pH_{UL}} \end{aligned} \right\} \tag{12}$$

Where: I_{pH_j} = inhibition of pH on process j

pH = pH value

pH_{LL} = pH value that below this level process is 50% inhibited, in Eqn. (11); below this level process is completely inhibited, in Eqn. (12)

pH_{UL} = pH value that above this level process is 50% inhibited, in Eqn. (11); above this level process is not inhibited at all, in Eqn. (12)

The Eqn. (13) is corresponding to non-competitive inhibition (Pavlostathis and Giraldo-Gomez 1991). It is used to implement the inhibition from free ammonia and hydrogen. The free ammonia is taken in to account instead of IN, as it is widely accepted that the free ammonia in the liquid phase mainly responds to the inhibition.

$$\text{non-competitive inhibition: } I_{i\_j} = \frac{K_{I,i\_j}}{K_{I,i\_j} + S_{I,i}} \tag{13}$$

Where: I_{i_j} = inhibition from inhibitor i to process j

K_{I,i_j} = 50% inhibitory concentration of inhibitor i to process j, g N/m^3 for ammonia; g COD/m^3 for hydrogen

$S_{I,i}$ = concentration of inhibitor I, g N/m^3 for ammonia; g COD/m^3 for hydrogen

In respect that valerate and butyrate are metabolised by the same kind of microorganisms, the competition inhibition is introduced.

$$\text{competitive inhibition: } I_{i\_j} = \frac{S_j}{S_j + S_i} \tag{14}$$

Where: $I_{i,j}$ = competitive inhibition from substrate i to substrate j

S_i = concentration of substrate i (as inhibitor), g COD/m^3

S_j = concentration of substrate j (which is utilised), g COD/m^3

As another important limiting factor, C:N ratio is controlled also as a inhibition factor, i.e. when S_{IN} is too low in the reactor, the ADP will be inhibited. No doubt, this inhibition (or say limitation) exerts on uptake processes of all substrates.

$$\text{Low IN limitation: } I_{IN\_j} = \frac{S_{IN}}{K_{I,IN\_j} + S_{IN}} \tag{15}$$

Where: I_{IN_j} = inorganic nitrogen (IN) as a inhibition function when IN → 0

K_{I,IN_j} = 50% inhibitory concentration of IN to process j, g N/m^3

S_{IN} = concentration of IN, g N/m^3

As we can see in the Matrix (Appendix B), pH inhibition and IN limitation affect on uptake processes of all 8 substrates (from 5 to 12). The inhibition of hydrogen affect on the

uptake of LCFA, valerate, butyrate and propionate, and the free ammonia only exerts an influence on the uptake of acetate.

2.5 Implementation of physicochemical processes

As mentioned before, ADP are sensitive to surroundings, so physicochemical processes are integrated into the model in order to look into the physical conditions. In the model, three physicochemical processes are considered, i.e. Liquid-Liquid processes, Liquid-Gas processes, and Liquid-Solid processes. The influence of temperature is also introduced at the end of this section.

2.5.1 Liquid-liquid processes (acid-base reactions)

Since pH inhibition is involved into the model, the behaviour of pH must be verified. Liquid-Liquid processes are involved in order to look into the pH.

In the model, four short chain fatty acids (SCFA) are considered: HVa, HBu, HPr and HAc. Three inorganic acids are included: H_2CO_3, HCO_3^- (H_2CO_3 dissociates to CO_3^{2-} in two steps, so they are considered as two acids) and NH_4^+.

By the definition of pH, it is calculated as:

$$pH = -\log\left(S^N{}_{H^+}\right) \tag{16}$$

Where: S^N_{H+} = concentration of H^+ with norm unit, kmole/m^3

When unit of is not norm, the transformation is necessary. Make S^N_{H+} = 1 kmole/m^3, it can be attained as follows:

$$pH = -\log\left(\frac{S_{H^+}}{S^N{}_{H^+}}\right) = -\log\left(\frac{S_{H^+}\cdot \text{mole}/\text{m}^3}{1\cdot \text{kmole}/\text{m}^3}\right) = -\log\left(S_{H^+}\right) + 3 \tag{17}$$

Where: S_{H+} = concentration of H^+, mole/m^3

And S_{H+} is obtained from the charge balance:

$$S_{cat^+} + S_{NH_4^+} + S_{H^+} - S_{HCO_3^-} - 2\times S_{CO_3^{2-}} - \frac{S_{Ac^-}}{64} - \frac{S_{Pro^-}}{112} - \frac{S_{Bu^-}}{160} - \frac{S_{Va^-}}{208} - S_{OH^-} - S_{an^-} = 0 \tag{18}$$

Where: S_{cat+} = concentration of cations of strong bases, mole/m^3

S_{an-} = concentration of anions of strong acids, mole/m^3

In Eqn. (18), firstly because the unit of SCFA is g COD/m^3, it is converted to mole/m^3 by multiplying the coefficients; secondly, cations and anions representing ions of strong bases and acids are also included, as they are able to influence the whole charge balance and finally affect the pH.

Based on the requirements of mathematics and considering the characteristics of acid-base reactions, two methods can be used to implement the processes. The acid-base reactions can

be treated as either equilibrium processes that is implemented as Differential-Algebraic Equations (DAE), or dynamic processes that is achieved as Differential Equations (DE). The concrete explanation and how to manipulate them are given as follows.

2.5.1.1 Equilibrium Processes

Comparing to the biochemical processes, the reaction rates of physicochemical processes are much faster (in different magnitudes). The reaction time is so short that the process is reckoned always at the equilibrium state. According to this assumption, DAE can be used to describe the process. A DAE is a type of differential equation in which the derivatives are not (in general) expressed explicitly, and typically derivatives of some of the dependent variables may not appear in the equations at all[6]. The general form of a DAE system is given by $F(t,x,x')=0$, where $x'=dx/dt$. Taking H_2CO_3 as an example, it is implemented as an equilibrium process by DAE set as follows.

The chemical reaction of H_2CO_3 is:

$$H_2CO_3 \rightleftharpoons HCO_3^- + H^+ \tag{19}$$

and acid dissociation constant $K_{a,CO2}$ as well as formula is:

$$K_{a,CO_2} = \frac{[HCO_3^-]\cdot[H^+]}{[H_2CO_3]} \tag{20}$$

$$\text{with: } K_{a,CO_2} = 10^{(-pK_{a,CO2})} \tag{21}$$

Where: pK_a = acid equilibrium constant, -

Meanwhile, another equation can be obtained according to mass balance:

$$S_{H_2CO_3} = S_{IC} - S_{HCO_3^-} \tag{22}$$

Where: S_{IC} = concentration of inorganic carbon (IC), mole C/m^3

S_{H2CO3} = concentration of H_2CO_3, mole C/m^3

S_{HCO3-} = concentration of HCO_3^-, mole C/m^3

Because in the liquid phase, the ratio of dissolved H_2CO_3 : CO_2 is fixed to 99.76 : 0.24 at 25°C and is independent of pH and ionic strength (Musvoto *et al.* 2000a, 2000b), the S_{H2CO3} is used to represent both H_2CO_3 and CO_2 in liquid phase with a small error. From equation (20) and (22), the other equation can be obtained:

$$S_{HCO_3^-} - \frac{K_{a,CO_2}\cdot S_{IC}}{K_{a,CO_2} + S_{H^+}} = 0 \tag{23}$$

[6] http://mathworld.wolfram.com/Differential-AlgebraicEquation.html

So far there are three variables S_{H+}, S_{IC}, and S_{HCO3}- with three equations (18), (22) and (23), so they are resolvable. All acids can be implemented as equilibrium processes by DAE, and the relevant equations can be found in Appendix D .

However, calculation of DAE is time consuming. If the computer is not fast enough, calculating many complex DAE together can take several days. Of necessity, another method is developed, which has faster calculation speed.

2.5.1.2 Dynamic Processes

In order to understand this method, let us use H_2CO_3 as an example too. In Eqn. (19), obviously it is the double-direction reaction with the dissociation and association of acid and base. The dissociation and association take place simultaneously, but with individual reaction speeds:

dissociation rate of H_2CO_3: $$\gamma_{diss,CO_2} = k_{diss,CO_2}\left[H_2CO_3\right] \tag{24}$$

association rate of HCO_3^- and H^+: $$\gamma_{asso,CO_2} = k_{asso,CO_2}\left[HCO_3^-\right]\cdot\left[H^+\right] \tag{25}$$

The two reactions together reflect the acid dissociation constant:

$$k_{diss,CO_2} \Big/ k_{asso,CO_2} = \frac{\left[HCO_3^-\right]\cdot\left[H^+\right]}{\left[H_2CO_3\right]} = K_{a,CO_2} \Rightarrow k_{diss,CO_2} = k_{asso,CO_2}\cdot K_{a,CO_2} \tag{26}$$

Therefore, when the k_{asso} is given, the k_{diss} can be gotten automatically. Musvoto *et al.* (2000a, 2000b) suggests the values of k_{asso} for different acids in ADP. However, due to their very high reaction speeds, from the mathematical point of view, the values of k_{asso} from 10^7 to 10^{14} can bring out the same results.

Based on this double-direction reaction, the processes can be implemented by Differential Equation (DE). DE is an equation which involves the derivatives of a function as well as the function itself[7]. The disadvantage of DE is too stiff.

Regarding implementation of the dynamic processes into the mathematical model, further two ways can be used. First, the dissociation and association are considered as two independent processes in the model, so two equations (27) and (28) as two processes are used:

Dissociation of H_2CO_3: $$\rho_{diss,CO_2} = k_{diss,CO_2}\cdot S_{H_2CO_3} = k_{asso,CO_2}\cdot K_{a,CO_2}\cdot S_{H_2CO_3} \tag{27}$$

Association of HCO_3^- and H^+: $$\rho_{asso,CO_2} = k_{asso,CO_2}\cdot S_{HCO_3^-}\cdot S_{H^+} \tag{28}$$

Another way around, the speed and direction of reaction (19) depend on the difference between the dissociation and association. Therefore the whole reaction rate as one dynamic process can be given as Eqn. (29) (use $k_{A/B,CO2}$ to replace $k_{asso,CO2}$):

$$\rho_{A/B,CO_2} = k_{A/B,CO_2}\left(S_{HCO_3^-}\cdot S_{H^+} - K_{a,CO_2}\cdot S_{H_2CO_3}\right) \tag{29}$$

[7] http://mathworld.wolfram.com/DifferentialEquation.html

It has been testified that the two implementation methods work out exactly the same results. Appendix C displays the dynamic reaction rates of all acids in the form of Peterson Matrix. The pK_a constants are given in Appendix F.

Theoretically, all acid-base reactions involved in the model can be achieved by either equilibrium processes or dynamic processes. In our model, SCFA and NH_4^+ are implemented as equilibrium processes, where H_2CO_3 and HCO_3^- are implemented as dynamic processes. The comparison of these two methods is given in Sec. 4.5.

2.5.2 Liquid-gas processes

One of the most important advantages of ADP is that biogas products can be used as renewable energy resource. The biogas products from ADP contain CH_4, CO_2, and water vapour, as well as some other trace gases like H_2, N_2 and H_2S. If the ADP are artificially controlled, the H_2 also can be the main biogas product. Liquid-gas processes are implemented in order to get biogas products.

There are many theories to model the gas transfer from liquid phase to gas phase. The two film theory of Whitman (1923) is used in ADM1, which is also the most widely used theory. Meanwhile, the Henry's law can be satisfied when the liquid phase is dilute. Based on these, the gas transfer rates can be presented in the form of Eqn. (30), and K_H values of gases are given in Appendix F.

$$\rho_{T,i} = k_L a \cdot \left(S_{liq,i} - K_{H,i} P_{gas,i}\right) \tag{30}$$

Where: $\rho_{T,i}$ = specific mass transfer rate of gas i,
g COD/(m^3·d) for CH_4 and H_2; mole C/(m^3·d) for CO_2

K_La = overall mass transfer coefficient K_L times the specific transfer area a, d^{-1}

$S_{liq,i}$ = concentration of gas i in liquid phase,
g COD/m^3 for CH_4 and H_2; mole C/m^3 for CO_2

$P_{gas,i}$ = partial pressure of gas i in gas phase, bar

$K_{H,i}$ = Henry's law coefficient of gas i, mole/(m^3·bar)

For Eqn. (30), the partial pressure of each gas is necessary and can be calculated by ideal gas law:

$$P_{gas,i} = S_{gas,i} RT \tag{31}$$

Where: $S_{gas.i}$ = concentration of gas i in gas phase,
g COD/m^3 for CH_4 and H_2; mole C/m^3 for CO_2

R = gas law constant, 8.314 x 10^{-5} bar·m^3·$mole^{-1}$·K^{-1}

T = absolute temperature, K

It has to be taken care of that in Eqn. (31) the unit of CH_4 and H_2 has to be changed from g COD/m^3 to mole/m^3 in order to match the unit of K_H. Hence, the coefficients 1/64 and 1/16 are employed for CH_4 and H_2, respectively (see Eqn. (58) and (60) for calculation).

The software AQUASIM, which is used for our model (see Sec. 2.6 and 2.7 for details), provides the diffusion link between compartments, which follows the Henry's law but with the transformation of the formula (Reichert 1998, pp129). So Eqn. (30) can be easily achieved in the model, but it needs to be careful of the coefficients and the transfer sequence of compartments in AQUASIM. Three main gases CH_4, CO_2, and H_2 are transferred between two phases with the rates from Eqn. (30).

The partial pressure of water vapour in gas phase is also needed in order to calculate the total gas pressure, and it is given by the empirical equation:

$$P_{gas,H2O} = 0.0313 \cdot \exp\left(5290\left(\frac{1}{298} - \frac{1}{T}\right)\right) \tag{32}$$

So the total gas pressure $P_{gas,total}$ is as follows:

$$P_{gas,total} = P_{gas,CH_4} + P_{gas,H_2} + P_{gas,CO_2} + P_{gas,H_2O} \tag{33}$$

Introducing the pipe resistance coefficient k_p (m^3/(bar·d)), hereby the gas flowrate q_{gas} (m^3/d) can be obtained as Eqn. (34):

$$q_{gas} = k_p\left(P_{gas,total} - P_{atm}\right) \tag{34}$$

Afterwards the biogas products are dried and transformed to the standard conditions through Eqn. (35) in order to make them comparable.

$$q_{gas,norm} = q_{gas} \cdot \frac{\left(p_{gas,air} - p_{gas,H2O}\right)}{p_{gas,norm}} \cdot \frac{273.15}{T} \tag{35}$$

Where: $q_{gas,norm}$ = dried norm biogas volume, m^3_{norm}/d

q_{gas} = measured biogas volume from the gas counter, m^3/d

$P_{gas,air}$ = air pressure at reading point, bar

$P_{gas.H2O}$ = water vapour pressure at temperature T, bar

$P_{gas,norm}$ = norm atmosphere pressure, 1.0 bar

T = absolute temperature, K

2.5.3 Liquid-solid processes

The liquid-solid processes mainly include precipitation, sediment and adsorption. Due to their complexity, ADM1 escapes these processes. The absence of these processes has no significant impacts on the simulation results under the common conditions. However, if these processes are decisive or required to be performed under the particular conditions, they can be implemented by the similar methods as dynamic liquid-liquid processes (Musvoto *et al.* 2000a, 2000b).

A general precipitation reaction is indicated in Eqn. (36):

$$M^{m+} + A^{a-} = M_a A_m(s) \tag{36}$$

According to the theory of Koutsoukos *et al.* (1980), the rate of mineral precipitation can be expressed as Eqn. (37):

$$\rho_{sp,M_aA_m} = \frac{d}{dt} M_{v+}A_{v-} = -k' \cdot s\left[\left(\left[M^{m+}\right]_t^{v+} \cdot \left[A^{a-}\right]_t^{v-}\right)^{1/v} - \left(\left[M^{m+}\right]_0^{v+} \cdot \left[A^{a-}\right]_0^{v-}\right)^{1/v}\right] \cdot n \qquad (37)$$

Where: $\rho_{sp,MaAm}$ = precipitation rate of species M_aA_m

k' = apparent precipitation rate constant

s = proptional to the total number of available growth sites on the added seed material

$[M^{m+}]_t$ and $[A^{a-}]_t$ = concentrations of crystal lattice ions in solution at time t

$[M^{m+}]_0$ and $[A^{a-}]_0$ = concentrations of crystal lattice ions in solution at time of equilibrium

v^+ = total number of cationic species

v^- = total number of anionic species

$v = v^+ + v^-$

n = determined experimentally, for divalent sparingly soluble salts n = 2

And at the equilibrium state:

$$\left[M^{m+}\right]_0^{v+} \cdot \left[A^{a-}\right]_0^{v-} = K_{sp,M_aA_m} \qquad (38)$$

Where: $K_{sp,MaAm}$ = solubility product, mole/m^3

As one of the most important precipitation substances in ADP, $CaCO_3$ is depicted here as an example.

The reaction of $CaCO_3$ and its solubility product are:

$$Ca^{2+} + CO_3^{2-} = CaCO_3(s) \qquad (39)$$

$$\text{and } \left[Ca^{2+}\right] \cdot \left[CO_3^{2-}\right] = K_{sp,CaCO_3} \qquad (40)$$

For $CaCO_3$, $k' \cdot s$ is replaced by $k_{prec,CaCO3}$, which is the single precipitation rate constant; v+ =1, v- = 1, and v = 2; so the total dynamic reaction rate of $CaCO_3$ is acquirable by transforming the Eqn. (37) to Eqn. (41):

$$\rho_{prce,CaCO_2} = -k_{prec,CaCO_2}\left(\left(S_{CO_3^{2-}} \cdot S_{Ca^{2+}}\right)^{1/2} - K_{sp,CaCO_3}{}^{1/2}\right)^2 \qquad (41)$$

In our model, the precipitation is not included, as it is not critical for our reactors. Nevertheless, the precipitation such as $CaCO_3$, $Mg(OH)_2$, etc. can be integrated into the model by this method.

2.5.4 Influence of temperature

Temperature is one of the key issues for all reactions. Commonly, the anaerobic microorganisms are divided into three thermal groups: psychrophiles, mesophiles and

thermopiles, with optimum temperature at < 20°C, 25~40°C, and >45°C, respectively. Figure 5 shows the relations between growth rates of methanogens and temperature for each group (van Lier *et al.* 1997). Our lab-scale AD plant performs in the mesophilic conditions at temperature 38°C.

Concerning the influence of temperature to the physicochemical parameters, the van't Hoff equation is used to correct the variation of equilibria coefficients with temperature:

$$\ln\frac{K_2}{K_1}=\frac{\Delta H^0}{R}\left(\frac{1}{T_1}-\frac{1}{T_2}\right)\Rightarrow K_2=K_1\cdot e^{\left(\frac{\Delta H^0}{R}\left(\frac{1}{T_1}-\frac{1}{T_2}\right)\right)} \tag{42}$$

Where: K_2 = unknown constant at temperature T_2

K_1 = known constant at temperature T_1

ΔH^0 = heat of reaction at standard temperature and pressure, J/mole

R = gas law constant, here always 8.314 J/(mole·K)

T_2 = desired temperature, K

T_1 = reference temperature, K

The Henry's constants K_H and acid-base equilibrium coefficients K_a are modified by Eqn. (42). All physicochemical constants are given in Appendix F.

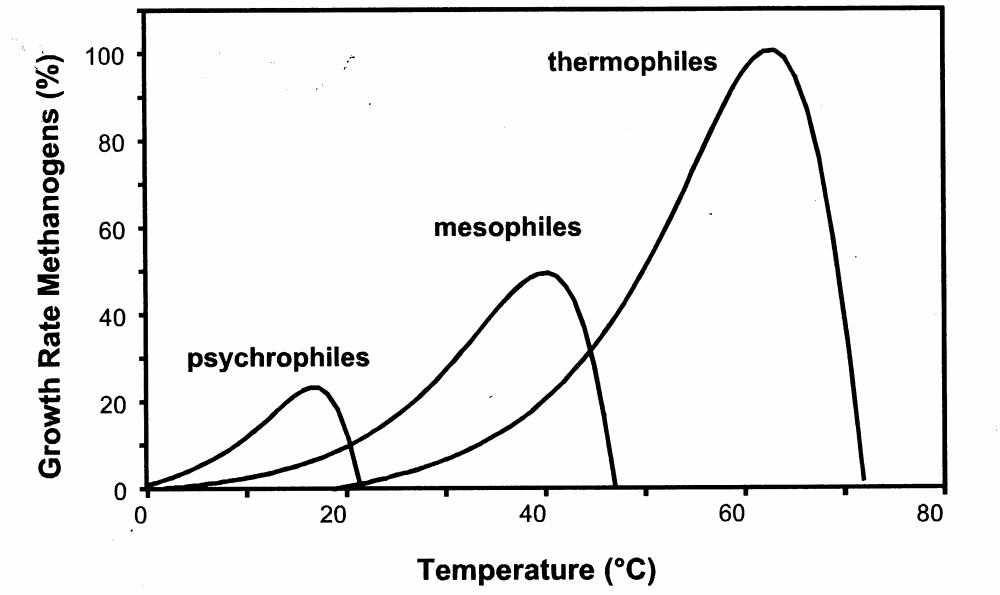

Figure 5: Relative growth rate of *methanogens* (van Lier *et al.* 1997)

2.6 Simulation Software

A differential equation solver is requisite for simulation. Currently, many software are available. AQUASIM 2.0 is chosen for our work (Reichert 1994), as ASM implemented by AQUASIM in our institute previously. This makes it possible to join two models. AQUASIM is a computer program for data analysis and simulation of aquatic systems. Besides

simulation, AQUASIM provides two powerful tools: Linear Sensitivity Analysis and Parameter Estimation.

2.7 Construction of the model by software

Our AD reactors are the single-stage Continual Stirred Tank Reactors (CSTR), so the model is implemented base on this type of reactor. Figure 6 is the scheme of a single-tank anaerobic digester.

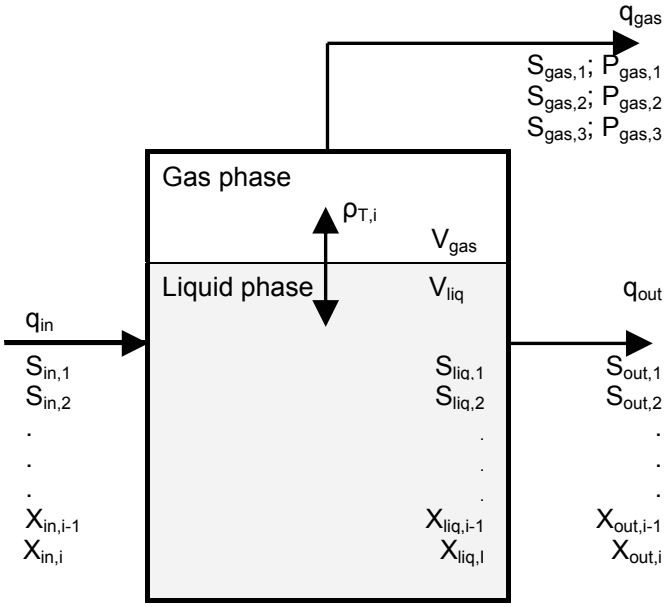

Figure 6: Scheme of a single-tank digester

2.7.1 Equations in liquid phase

According as the mass balance, the state of each component in liquid phase can be expressed as Eqn. (43):

$$\frac{dS_{liq,i}}{dt} = \frac{q_{in}S_{in,i}}{V_{liq}} - \frac{q_{out}S_{liq,i}}{V_{liq}} + \sum_{j=1-19}\rho_j \nu_{i,j} \tag{43}$$

ρ_j is the reaction rate of process j which can be found in the matrix (see Appendix B). In our case, the reactor is fed discontinuously and the liquid phase volume is constant, so during the non-feeding period, the Eqn. (43) can be simplified as:

$$\frac{dS_{liq,i}}{dt} = \sum_{j=1-19}\rho_j \nu_{i,j} \tag{44}$$

2.7.2 Equations in gas phase

In gas phase, three kinds of gases CH_4, H_2 and CO_2 are dealt with. Likewise, the following equation can be obtained based on the mass balance:

$$\frac{dS_{gas,i}}{dt} = -\frac{q_{gas}S_{gas,i}}{V_{gas}} + \rho_{T,i}\frac{V_{liq}}{V_{gas}} \tag{45}$$

Where $\rho_{T,i}$ and q_{gas} are calculated by Eqn. (30) and (34), respectively. Other necessary equations are (31), (32) and (33).

As to physicochemical processes, they can be implemented as either DAE or DE set. Let us use IC as the example all along.

2.7.3 DAE set for physicochemical processes

When IC is solved as DAE set, still from the mass balance in liquid phase, the following equation can be obtained:

$$\frac{dS_{liq,IC}}{dt} = \frac{q_{in}S_{in,IC}}{V_{liq}} - \frac{q_{out}S_{liq,IC}}{V_{liq}} + \sum_{j=1-19}\rho_j \nu_{IC,j} - \rho_{T,CO_2} \tag{46}$$

where $\rho_{T,CO2}$ comes from Eqn. (30): $\rho_{T,i} = k_L a \cdot \left(S_{liq,i} - K_{H,i}P_{gas,i}\right)$ for CO_2 transfer between liquid and gas phases. Together with Eqn. (22): $S_{H_xCO_3} = S_{IC} - S_{HCO_3^-}$ and Eqn. (23): $S_{HCO_3^-} - \frac{K_{a,CO_2} \cdot S_{IC}}{K_{a,CO_2} + S_{H^+}} = 0$, the equations are soluble.

2.7.4 DE set for physicochemical processes

When IC is solved as DE set, the following equations are needed:

$$\frac{dS_{liq,CO_2}}{dt} = \frac{q_{in}S_{in,CO_2}}{V_{liq}} - \frac{q_{out}S_{liq,CO_2}}{V_{liq}} + \sum_{j=1-19}\rho_j \nu_{IC,j} - \rho_{T,CO_2} + \rho_{A/B,CO_2} \tag{47}$$

$$\text{and } \frac{dS_{liq,HCO_3^-}}{dt} = -\frac{q_{out}S_{liq,HCO_3^-}}{V_{liq}} - \rho_{A/B,CO_2} \tag{48}$$

With Eqn. (29): $\rho_{A/B,CO_2} = k_{A/B,CO_2}\left(S_{HCO_3^-} \cdot S_{H^+} - K_{a,CO_2} \cdot S_{H_2CO_3}\right)$ for acid-base dynamic processes and Eqn. (30) for CO_2 transfer, the equations are soluble.

In AQUASIM, besides all necessary parameters and variables, as well as processes (both biochemical and physicochemical processes), the model further contains two compartments, i.e. the reactor and the headspace, which represent the liquid phase and headspace, separately. One diffusive link is established between the reactor and the headspace to transfer the biogases.

So far all processes and obligatory items of the model, which are included in our model, have been presented. Please consult the ADM1 (Batstone *et al.* 2002) for some additional explanations.

The model has been built up as individual AQUASIM files for every case. The file with the name *ADM_1_2004-03.31-04.20_refer_ohne_va.aqu* is used as the matrix. Others are derivatives of this file. The specification of this file can be found out in Appendix G.

3 Verification and Calibration

The model is calibrated by the data from our lab-scale AD plant, so first of all the AD plant is introduced. Afterwards the verification experiments of biochemical kinetics parameters are presented. And then three scenarios are worked out. The prediction of the AD plant performance by the model is carried out in succession too.

3.1 Materials and methods

As introduced in previous chapter, the blackwater anaerobic digestion (BWAD) treatment can be a very important step of the Ecological Sanitation (ECOSAN). The BW can be further treated together with kitchen refuse (KR) by ADP (e.g. Zeeman and Lettinga 1999). As mentioned before, we mainly focus on BWAD. The BW from vacuum toilets is obtained from the ECOSAN pilot project in Lübeck-Flintenbreite, Germany (Otterpohl 2001). It contains human feces, urine, toilet paper and flushing water. Due to the very low flushing water consumption (0.7~1.0 l water per flush) and the separation sewerage system, the BW has relative high COD. Normally it is in the range from 6,000 g COD/m^3 to 13,000 g COD/m^3. Currently this BW is treated by one on-site anaerobic digester. It is intending to put KR into the digester in order to get more economic profits. One lab-scale AD plant was built up according to the on-site anaerobic digester in the Institute of Wastewater Management, the Hamburg University of Technology (TUHH). The investigation of the lab-scale AD plant aims to improve the performance of the on-site digester so that it could bring the maximum ecological and economical benefits.

The lab-scale AD plant consists of three parallel Continual Stirred Tank Reactors (CSTR). Each reactor is a 10.0 l PVC cylinder with the dimension of 19.0cm inner diameter and 35.5cm height. Each reactor is filled with 8.0 l sludge and BW, where 2.0 l is retained as the headspace. The reactors are operated at mesophilic conditions (around 38°C) with discontinuous feeding, which are the same conditions as the on-site anaerobic digester. The hydraulic retention time (HRT) and the sludge retention time (SRT) are the same of 20 days (Wendland *et al.* 2004). Figure 7 displays the sketch of the lab-scale plant. Hose pump is used to feed and discharge the reactors. U-tube is for precise control of feeding and discharge. The reactors are continuously stirred by electric motors. A water tub is used to keep the temperature of the reactors at 38°C.

The biogas production, biogas pressure and pH were measured on-line. Total COD, Total Suspended Solids (TSS), Volatile Solids (VS), N-NH_4, Total Nitrogen (TN), Total Organic Carbon (TOC) and Total Inorganic Carbon (TIC) were checked every week. The VFA were measured by gas chromatography (GC) aperiodically. The specification of analysis methods for our experiments can be found from Ivanova (2003, pp46-48).

The lab-scale AD plant had been operated stably for two years, and some different operation conditions have been tested. Our model was calibrated based on these data. The

flexibility and reliability of the model were tested by these different operation conditions. The modelling results are shown in Sec. 3.4 for scenario studies.

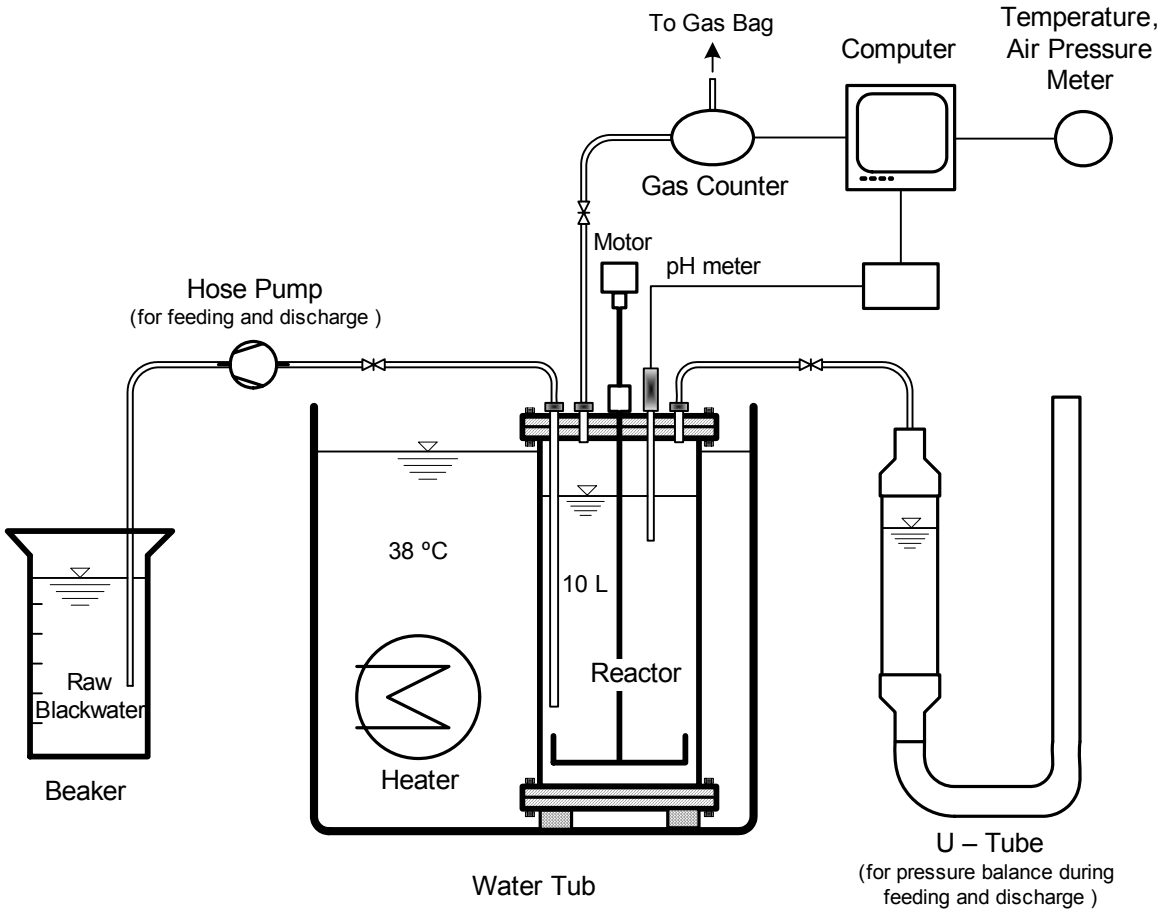

Figure 7: The sketch of the lab-scale AD plant

In order to perform the model accurately it is necessary to know the composition of the BW, especially human feces. Though the composition of the feces is pretty much depending on what human beings eat, it still can be generalized, and will be very helpful for our model later on. Feces has been fermented and decayed in our large intestines. It contains the undigested food, the indigestible cellulose from food and undigested secretion from stomach and intestine, etc. Commonly, 65% of feces is moisture, and 35% is solids. Inside the solids, one third can be bacteria, but most of them are dead; meanwhile 2~3% solids are proteins, 10~20% solids are mineral salts, and around 30% solids are undigested food[8]. Kujawa-Roeleveld *et al.* (2003) made particular analyses of both human feces and KR for their decentralized sanitation and reuse (DESAR) project, and it could be a good reference.

[8] http://www.bioon.com/health/wholehealth/medicine/constipation/200405/24285.html

3.2 Verification of kinetics parameters

The model contains more than 130 variables, parameters and coefficients. Therefore, although the ADM1 suggests the values for biochemical kinetics parameters, and those values from literatures are available too, it is still worth to verify some kinetics parameters in order to setup the model correctly. Therefore the additional batch experiments were carried out for verifying k_m and K_S (Eqn. (2)).

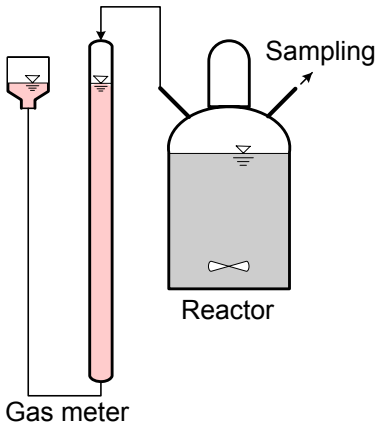

Figure 8: The sketch of the batch experiment

500 ml sludge from the lab-scale AD reactors was utilised for each batch experiment. A defined amount of SCFA (HAc, HPr and HBu) was added into the 600 ml bottle together with 500 ml sludge. The headspace was flushed by pure N_2 gas for about 2 minutes before the experiment starts. Afterwards the experiments were executed under the same conditions as lab-scale AD plant. Figure 8 is the sketch of the batch experiment. The biogas products were measured by gas meter, where the variations of SCFA were analysed by GC. The samples were stored at -20°C for several days before analysed by GC.

The first experiment was carried out by adding sodium acetate (NaAc) and HPr together. 10.0 l of 19,219 g/m^3 NaAc (equivalent to 15,000 g COD/m^3) and 10.0 ml of 7,928 g/m^3 HPr (equivalent to 12,000 g COD/m^3) were added. The transformation of units between g/m^3 weight and g COD/m^3 for each SCFA can be figured out according to the redox reactions. (See Sec. 0 for details.)

Likewise, in the second experiment the kinetic parameters of HBu were tested. In this experiment, besides 5,500 g/m^3 HBu (equivalent to 10,000 g COD/m^3), the same amounts of NaAc and HPr as experiment one were added. Because the HAc and HPr are the following metabolic substrates in the ADP, it has no effects on the previous metabolic substrate HBu.

The results of both experiments were estimated by AQUASIM, and shown in the graph A and B in Figure 9, respectively. The estimated values of k_m and K_S for these three acids are displayed in the Table 3. Meanwhile, according to the ADM1, the butyrate and valerate are utilised by the same kind of degraders, so the kinetics parameters for butyrate uptake rates are also used for valerate. However, it can be argued. Further discussions are presented in the section Sec. 4.3.

Table 3: Verified kinetics parameters

	Acetate	Propionate	Butyrate	Unit
k_m	13	14	18	d^{-1}
K_S	160	120	110	g COD·m^{-3}

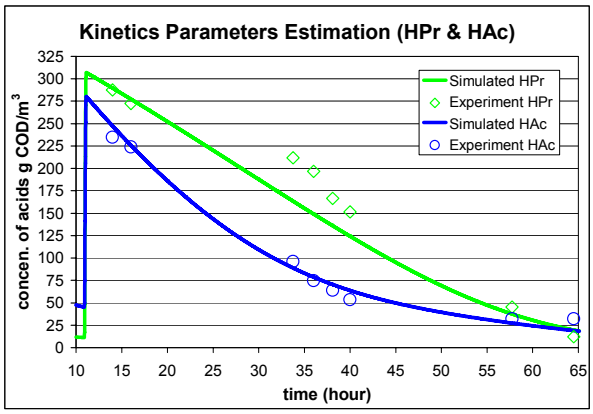

Graph A

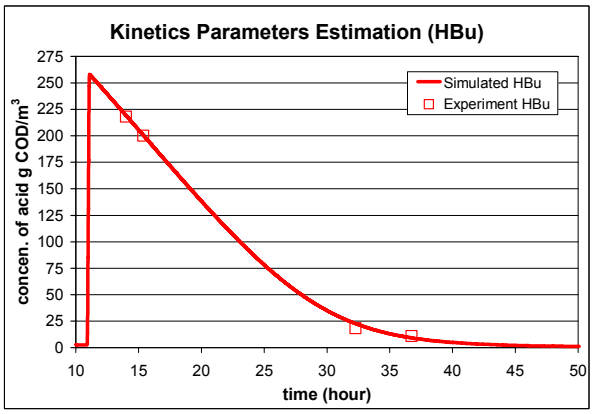

Graph B

Figure 9: Kinetics parameters verification (for HAc, HPr and HBu)

Besides HBu, HPr and HAc, the kinetics parameters for the uptake rates of sugars, AA, fats and hydrogen also need to be set up. However, when the intermediate steps are not rate-limiting, they have no significant effects on the final results. Hence, the kinetics parameters for those four substrates were set up by the recommended values from ADM1. Further, the estimation tool supported by AQUASIM can be used to adjust the kinetics parameters in the purpose of optimizing the output of the model. As the important factor, the decay rates of all seven species were estimated by AQUASIM based on the experimental data. The values of decay rates from literatures were also concerned.

All used values of kinetics parameters are listed in Appendix E. The suggested values by ADM1 and variation ranges of these parameters from literatures are shown in Appendix E simultaneously. Based on these values the scenario studies were performed.

3.3 Mass calculation

3.3.1 Units Transformation for SCFA and biogases

The unit of g/m^3 must be used for operating the experiments, whereas the unit of g COD/m^3 is used in the model. Therefore, the transformation of units is necessary. According to the redox reaction the units can be easily transformed from g/m^3 to g COD/m^3:

$$\underset{60}{CH_3COOH} + \underset{64}{2O_2} \rightarrow 2CO_2 + 2H_2O \tag{49}$$

$$\Rightarrow 1\,g\,HAc = \frac{64}{60}\,g\,COD \tag{50}$$

$$\underset{74}{CH_3CH_2COOH} + \frac{7}{2}\underset{112}{O_2} \rightarrow 3CO_2 + 3H_2O \tag{51}$$

$$\Rightarrow 1\,g\,HPr = \frac{112}{74}\,g\,COD \tag{52}$$

$$\underset{88}{CH_3CH_2CH_2COOH} + \underset{160}{5O_2} \rightarrow 4CO_2 + 4H_2O \tag{53}$$

$$\Rightarrow 1\,\text{g HBu} = \frac{160}{88}\,\text{g COD} \tag{54}$$

$$\underset{102}{CH_3CH_2CH_2CH_2COOH} + \underset{208}{\frac{13}{2}O_2} \rightarrow 5CO_2 + 5H_2O \tag{55}$$

$$\Rightarrow 1\,\text{g HVa} = \frac{208}{102}\,\text{g COD} \tag{56}$$

The unit transformation of CH_4 and H_2 is also needed when the gas pressure is calculated in headspace. The unit is transformed from g COD/m^3 to mole/m^3 as follows.

$$\underset{2}{H_2} + \underset{16}{\frac{1}{2}O_2} \rightarrow H_2O \tag{57}$$

$$\Rightarrow 1\,\text{g COD}\,H_2 = \frac{1}{16}\,\text{mole}\,H_2 \tag{58}$$

$$\underset{16}{CH_4} + \underset{64}{2O_2} \rightarrow CO_2 + 2H_2O \tag{59}$$

$$\Rightarrow 1\,\text{g COD}\,CH_4 = \frac{1}{64}\,\text{mole}\,CH_4 \tag{60}$$

The unit of IC is kept as mole/m^3 in both liquid and gas phases.

3.3.2 Methane convert coefficients

As mentioned above, the common units used in wastewater treatment are g COD and g C. Nonetheless, when biogases are obtained finally, we expect them presented as volume instead of g COD or g C. The convert coefficients of CH_4 between different units are calculated here. The coefficients can be used to quickly appraise methane products.

At the standard condition: (1.013 bar, 273k), the volume occupied by 1 mole gas is:

$$V = \frac{nRT}{P} = \frac{1\,\text{mole} \cdot 0.08312\,(\text{bar} \cdot \text{l})/(\text{mole} \cdot \text{K}) \cdot 273\,\text{K}}{1.013\,\text{bar}} = 22.4\,\text{l/mole} \tag{61}$$

The molecular weight of CH_4 is 60 g/mole. The relation between COD and mole for CH_4 can be attained by Eqn. (60), so the convert coefficient of CH_4 under the standard conditions is:

$$\text{when the unit is g COD: } \Gamma_{STD,CH_4} = \frac{22.4\,\text{l/mole}}{64\,\text{g COD/mole}} = 0.35\,(\text{l gas})/(\text{g COD}) \tag{62}$$

And one mole CH_4 contains one mole C (carbon), therefore:

$$\text{when the unit is g C: } \quad \Gamma_{STD,CH_4} = \frac{22.4\,\text{l/mole}}{12\,\text{g C/mole}} = 1.87\,(\text{l gas})/(\text{g C}) \tag{63}$$

When the temperature is not the standard condition, the coefficient can be changed by the following equation:

$$\Gamma'_{T,CH_4} = \Gamma_{STD,CH_4} \cdot \frac{T}{273.15\,K} \quad (64)$$

Where: T = expected temperature, K

3.3.3 Methane production

The mass balance is one of the most important laws. The biogas products of methane can be calculated by mass balance. And this is used to check the validity and veracity of our measurement data as well as the output of the model. Since COD and C are two common used parameters, two mass balances can be employed.

The measurement data on 14th April 2004 from Reactor One is used as the example. The data are shown in Table 4.

Table 4: Measurement data on 14.04.2004 and 21.04.2004

Time	Name	COD (g COD/m^3)	TOC (g C/m^3)	TIC (g C/m^3)
14.04.2004	Input	6,460	1,920	800
21.04.2004	Reactor 1	2,570	888	1,060

Two mass balances are calculated as:

1. COD balance

   $\Delta COD = (6{,}460 - 2{,}570)$ g COD/m^3 = 3,890 g COD/m^3

Each time 1.0 l raw BW is fed into the reactor,

$V_{CH4} = 3{,}890$ g COD/m^3 · 0.001m^3 · 0.35 l gas/(g COD) = 1.36 l/feeding

From the experiment data, the ratio of CH_4 in gas flow is around 71.3%.

Therefore, the biogas products are

$V_{norm} = 1.36$ l / 71.3% = 1.90 l/feeding

2. Carbon balance

   $\Delta TC = (1{,}920 - 888) + (800 - 1{,}060) = 772$ g C/m^3, where TC is total carbon.

And in the same way, each time 1.0 l raw BW is added into the reactor:

$V_{norm} = 772$ g TC/m^3 · 0.001m^3 · 1.87 l gas/(g C)/ 70% = 1.44 l/feeding

Due to CO_2 has been included in the total carbon balance, consequentially, the above results is the biogas products including CH_4 and CO_2.

Obviously the biogas products from two mass balances show a relatively big difference. The error is (1.90 – 1.44) / 1.90 = 24%. Therefore the accuracy of our measurement should be improved.

3.4 Scenario studies

Based on the experimental data from our lab-scale AD plant, three scenarios studies were performed:

1. Reference conditions

The temperature of all CSTR reactors was kept at 38°C. The reactor was discontinuously fed with 1.0 l raw BW on Monday, Wednesday and Friday. Before feeding, the raw BW was heated up to 38°C. SRT (as well as HRT) is 20 days. This reactor had been stably operated for two years, and regarded as the reference reactor, which it is named Reactor One. The parameters and coefficients of the model were calibrated and verified based on the performance of this reference reactor. The same parameters and coefficients were use for rest scenario studies later on.

2. Different feeding frequencies

In this scenario, the reactors were fed in different frequencies. Feeding once per 24 hours and once per 12 hours were investigated. Reactor One and Reactor Two executed these two tasks separately in the same period. All the other conditions are the same as the reference reactor.

3. High concentration of NH_4^+

The concentration of NH_4^+ in raw BW was artificially increased in order to observe the inhibition of ammonia to *methanogens*.

In all three scenarios, before simulating the real data the model had been always running for 60 days with the average-level input under the default conditions in order to reach the steady-state. In general, the model is fitted in with three scenarios quite well.

3.4.1 Scenario one: Reference conditions

In order to make the report concise and pellucid, only 6 typical and crucial graphs are shown in Figure 10 with only eight days data.

The Graph 1 in Figure 10 is the simulation of biogas production rate (BPR). The specific biogas production rate is used that is the absolute biogas production rates divided by the volume of reactor. It reflects the capacity of the reactor from the certain angle. Another often used specific biogas production rate is the absolute biogas production rates divided by the organic loading. Here the first specific rate is chosen.

In Graph 1, one half-bell-shape is formed for BPR after each feeding. The whole half-bell-shape can be classified into three periods. The first period (P1 in Graph 1) is at the peak of the half-bell-shape which has a highest biogas production rate, and the rate decreases slowly. This period occurs is because of high amount of acetate already existing in the BW. The analysis of raw BW shows that the acetate is normally around 20% of total COD. Total SCFA in raw BW can be up to 30%. This period lasts in the average time of 10 to 12 hours. Afterwards the second period (P2) comes up where the BPR is drop down very quickly. During this period, *methanogens* start to use the acetate produced by previous metabolic stages. With the

decreasing of acetate, the BPR are increasingly limited by the previous processes (e.g. hydrolysis, LCFA degradation, etc.). The second period persists around 13 to 17 hours. Finally the processes enter the third period (P3) where biogas production rate is very low and decreases tardily. Together period two and three it is the typical shape of Michaelis-Menten Kinetics. Obviously our model fits into these three periods quite well.

In the BPR simulation curve, BPR drop down to zero after each feeding. The reason is that the raw BW has lower concentration of CO_2 than it in liquid phase in the reactor. So that after feeding, the CO_2 in headspace will be dissolved back into the liquid phase. This phenomenon can not be reflected by the gas counter, but it is clearly observed by the bar meter.

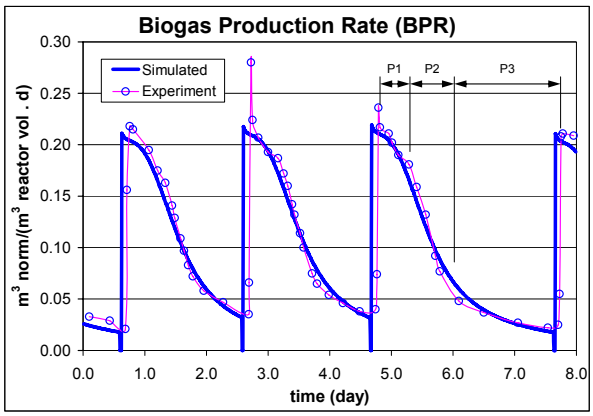

Graph 1

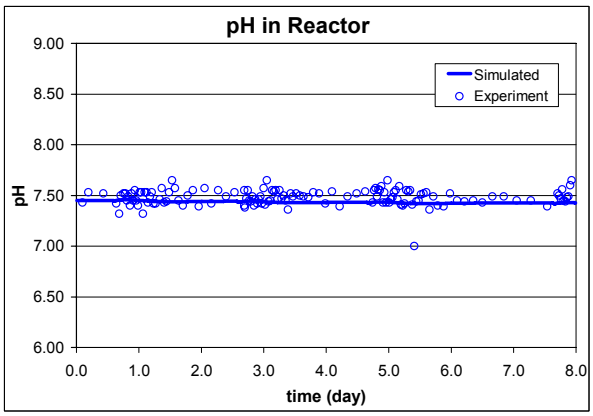

Graph 2

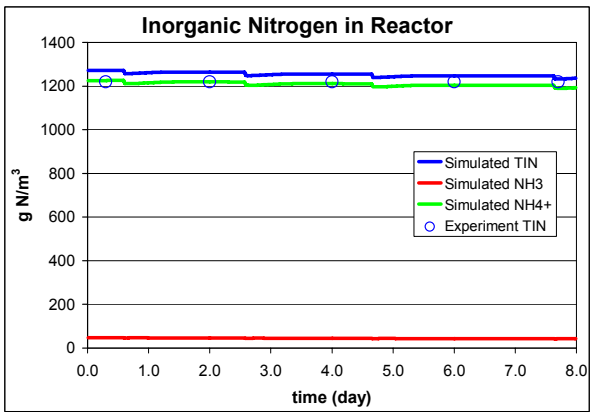

Graph 3

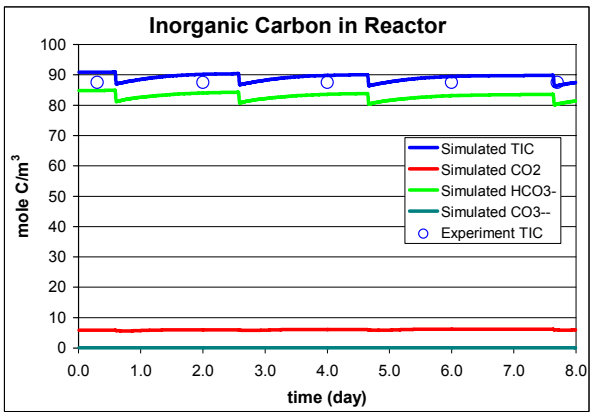

Graph 4

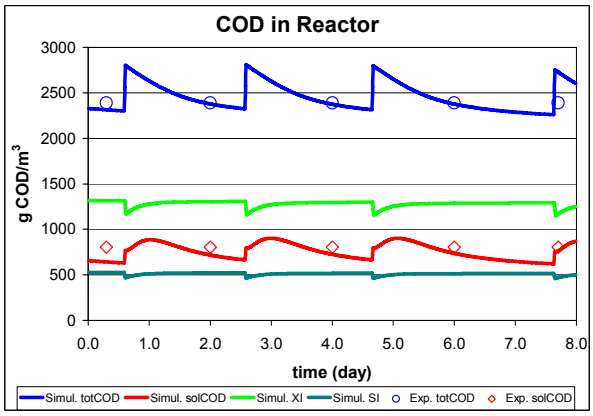

Graph 5

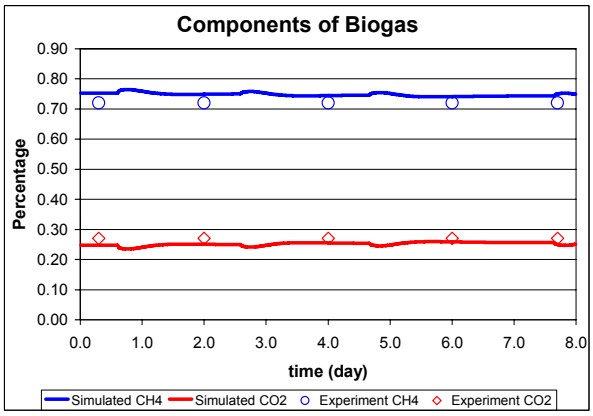

Graph 6

Figure 10: Simulation results of the reference reactor

However, in the reality the highest BPR appear around 2 hours later after feeding. This is a quite common delay phase as bacteria need time to adapt into the new conditions. Nevertheless, the model can not simulate this kind of delay. So the peaks always appear around 1 hour earlier than the measurement.

Graph 2 in Figure 10 is the simulation of pH. Because of the accuracy and errors, the measurement data are distributed in between 7.3 and 7.6. The simulation is relatively stiff, but it falls into the experimental area. The result is satisfied.

Because many parameter (e.g. IN, IC and COD, etc.) were measured only once per week, so the dynamic variation of this parameters can not be displayed. The measurement was done before feeding (for the raw BW) and after discharging (for the reactor state), so that the experimental data only represent one single state. In order to make the Graphs easier to read, more circles are generated in the graphs during simulation period. Hereby, the circles representing the experimental data in Graph 3 to Graph 6 are more or less only symbolic.

IN components are simulated in Graph 3. TIN was measured and it is simulated correctly. The free ammonia concentration in liquid phase is very important because of its inhibitory effects. In the reference reactor, the simulated NH_3 is around 45 g NH_3-N/m^3 (see Graph 37 in Figure 19). The concentration of NH_3 can also be calculated by the empirical Eqn. (65) based on the states of NH_4^+ and pH (Mitsdörffer 1991), which results in 44 g NH_3-N/m^3. Two results corroborate each other very well.

$$S_{NH_3} = S_{NH_4^+} \cdot \frac{10^{pH}}{e^{\left(6344/(273+T)\right)} + 10^{pH}} \tag{65}$$

Meanwhile, due to very high concentration of NH_4^+ (1000~2000 g NH_4^+-N/m^3) in liquid phase, the transfer of NH_3 to headspace was also tested by the model. However, with relative high solubility NH_3 is almost undetectable in headspace, so there is no need to include NH_3 in liquid-gas processes.

Similarly, Graph 4 is the simulation of the IC components in the reactor. TIC, H_2CO_3, HCO_3^- and CO_3^{2-} are simulated. Only the experimental data of TIC are available, and they are well recurred by the model.

The simulation of COD is shown in Graph 5. Total COD and soluble COD are represented properly by simulation. The soluble inerts (SI) and particulate inerts (XI) are also shown in Graph 5, which could be important for the post treatment of the effluent. Further, the amount and ration of SI and XI can be regulated by the distribution coefficients (see Appendix E).

Graph 6 displays the composition of biogas. It seems that the ratio of CH_4 is a little overestimated, whereas the CO_2 is a bit underestimated. However, the errors are within 5%, which are tolerable. It is also found that the variation of the biogas components does not have a significant influence on the BPR. This might be due to the numerical characters of the model. Further, it can be adjusted by varying the pH slightly, as CO_2 is very sensitive to pH in the liquid phase.

Base on above, one can say that the model simulated different aspects of the BWAD reactor quite well. All simulation results from this scenario are reasonable and acceptable. Hence, the further scenarios were worked out.

3.4.2 Scenario two: Different feeding frequencies

In this scenario two different kinds of feeding methods were tested, namely, once per 24 hours (tested by the Reactor One) and once per 12 hours (tested by the Reactor Two). Both have the same SRT of 20 days as the reference reactor. The model simulated two cases properly. The simulation results are shown in Figure 11 and Figure 12, separately. The same parameters with the same sequence as Figure 10 are displayed. First, let us look at the case of feeding once per 24 hours.

3.4.2.1 Feeding once per 24 hours

BPR (Graph 7 in Figure 11) are basically modelled well, whereas from day 0 to day 2.5 are not fitted in entirely. As mentioned before, the measurement was executed once per week. These 2.5 days belong to the last week. In view of other reactors' performance, the error might also come from the measurement.

Meanwhile, due to exactly the same reason as the reference reactor, BPR have a big fluctuation after feeding. But this time BPR go higher because of the higher CO_2 content in input. The delay phase still can not be simulated, and it makes the whole simulation curve shift to left side referring to the measurement data.

The simulated pH (Graph 8, Figure 11) is also in the measurement range. The pH goes down due to the changes of IC and IN in input. In this 8 days simulation, the decreasing of pH from experimental data can not be observed (due to the mechanical errors and amplified curves), but it is obviously laid out in the whole view (21 days simulation).

Graph 9 and 10 (Figure 11) represent IN and IC too, which are also well modelled. As discussed above, some measurement data are not on-line, so in Graph 11 the experimental data of total COD are quite rigid. One also can say that the simulation of COD is appropriate.

The experimental data of biogas components were measured irregularly. Hence, the circles in Graph 12 are symbolistic too. For the simulation curves, the decrease of CH_4 percentage is because of the increase of IC in input, which also causes the decrease of the pH (see Graph 8 Figure 11).

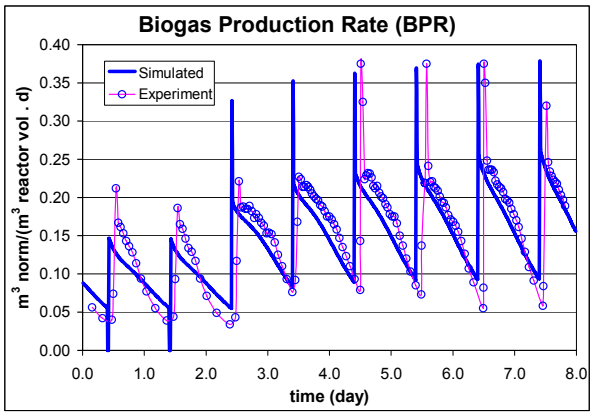

Graph 7

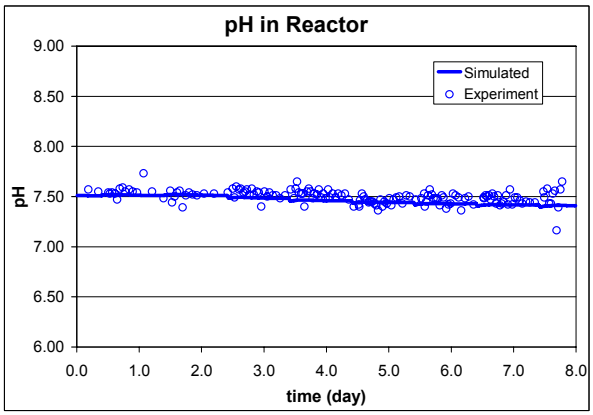

Graph 8

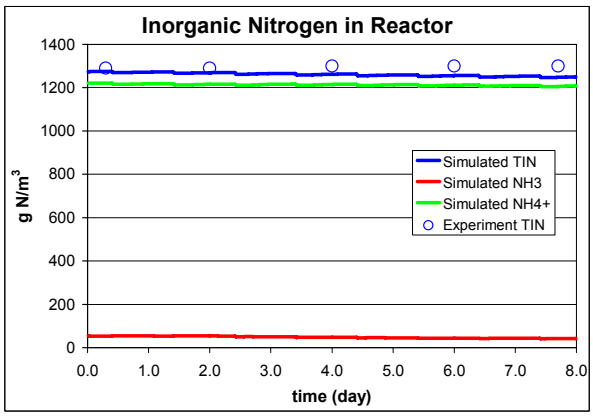

Graph 9

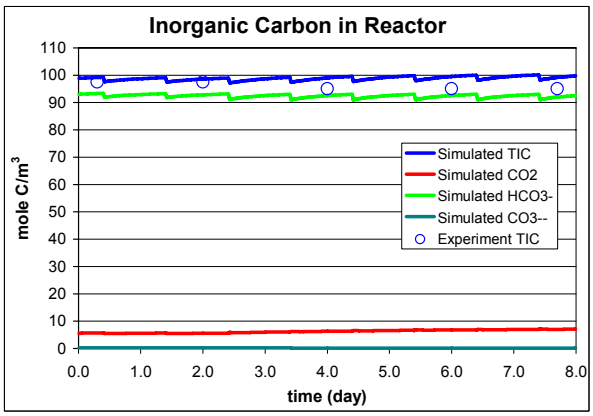

Graph 10

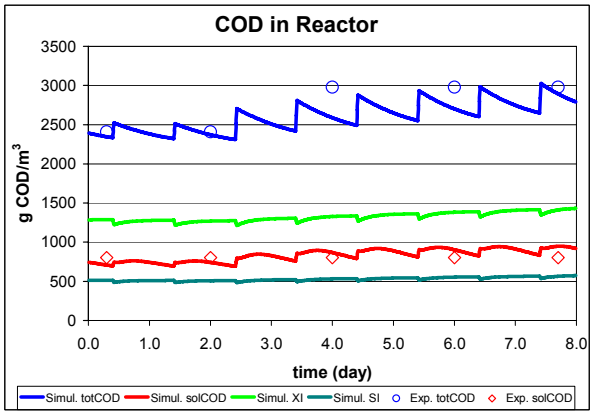

Graph 11

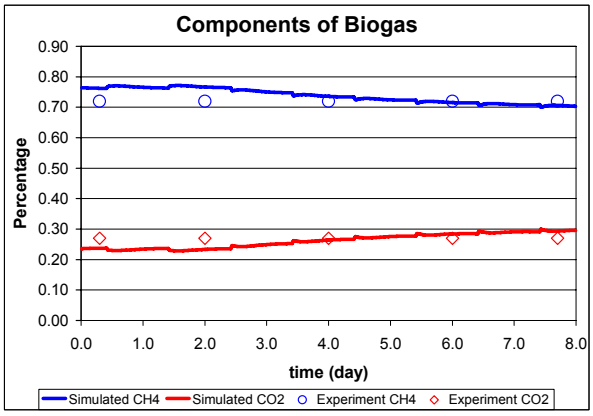

Graph12

Figure 11: Simulation results of different feeding frequency (once per 24 hr)

3.4.2.2 Feeding once per 12 hours

Regarding another feeding frequency, the simulation results are displayed in Figure 12.

Likewise, BPR are recurred by the model, but relatively too strained, and the curves are more distorted than former two cases. The reason might be that with the high feeding frequency the delay phase is amplified, whereas the mathematical model is not so flexible. Actually, even with high feeding frequency, the real BPR still vividly show three periods with the half-bell-shape.

Unfortunately, the pH on-line measurement was not available (instead of redox potential) during the certain period for this reactor. Only the rough range is obtained. Therefore, the

circles in Graph 14 are only indicators. Because the same BW was fed into both the Reactor One and the Reactor Two, the same decreasing tendency of pH as former case is attained.

The curves of IN and IC are good as always (Graph 15 and 16, Figure 12). But the total COD in reactor seems to be underestimated during the first 2.5 days (Graph 17). The problem still could come from measurement as discussed in the first feeding case. It seems that the data of that week are abnormal. In the same period the same raw BW was fed into all reactors, so the CH_4 percentage in biogas was decreased due to the same reason as mentioned above (Graph 18).

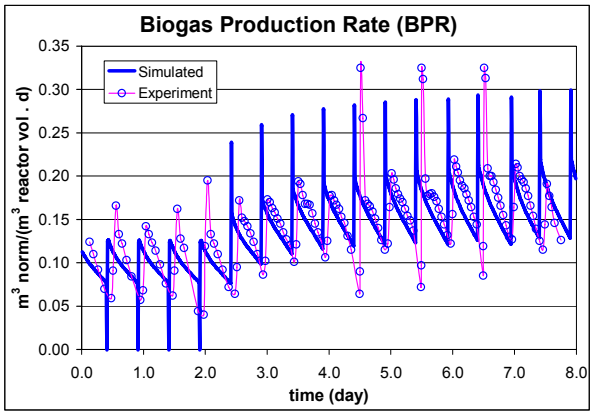

Graph 13

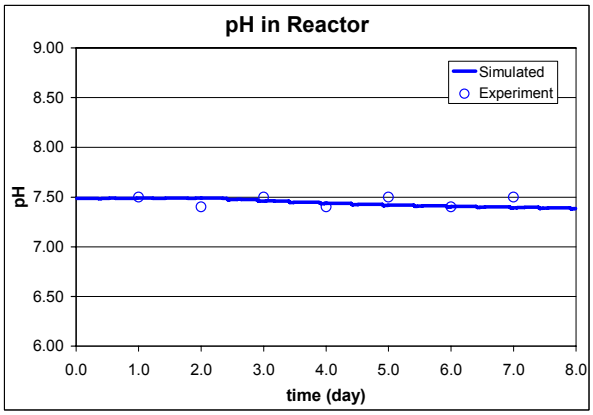

Graph 14

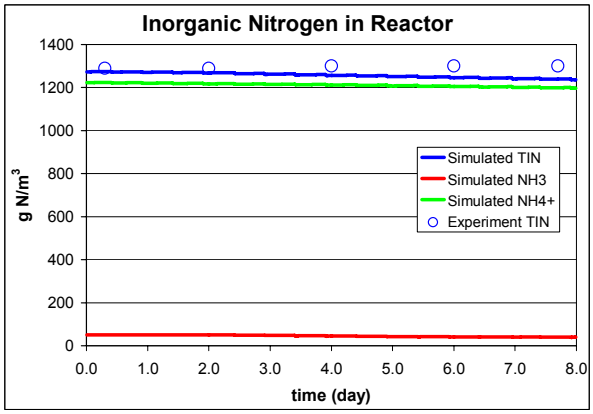

Graph 15

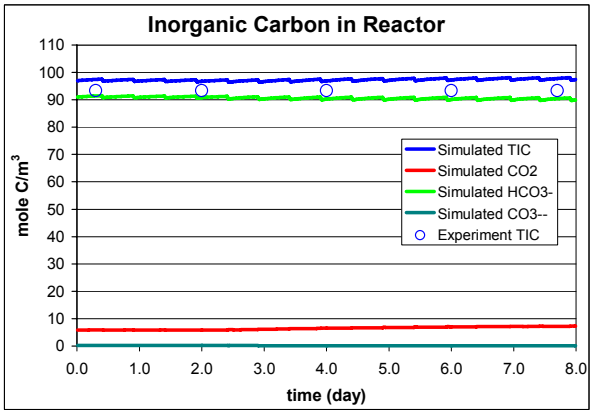

Graph 16

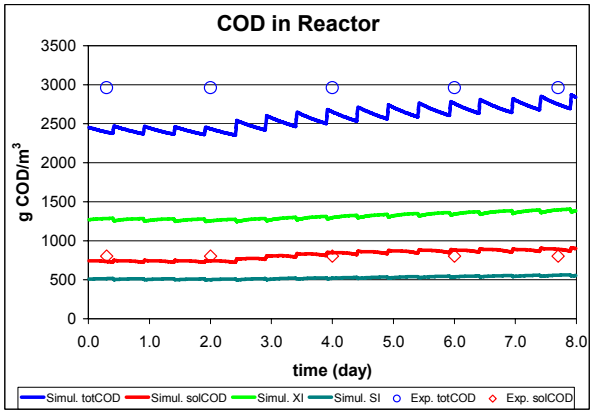

Graph 17

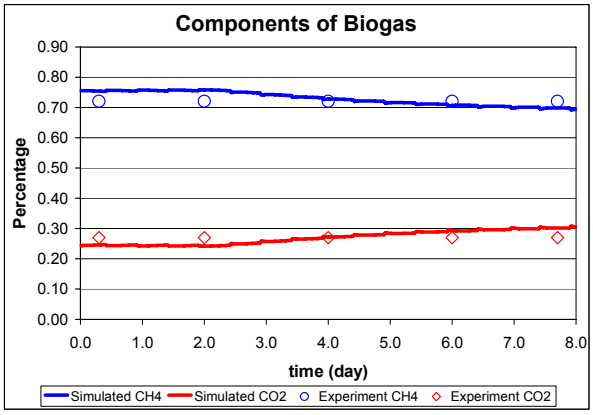

Graph 18

Figure 12: Simulation results of different feeding frequency (once per 12 hr)

General saying, the model simulated the real cases properly. However, the simulation of BPR is a little bit too strained. The modelled BPR of Reactor One (feeding once per 24 hr) is fitted in better than it of Reactor Two (feeding once per 12 hr).

3.4.3 Scenario three: With high concentration of NH_4^+

In the BW system, NH_4^+ concentration is holding at a very high level due to the existence of urine. Thereby, the impact of NH_4^+ to ADP needs to be understood.

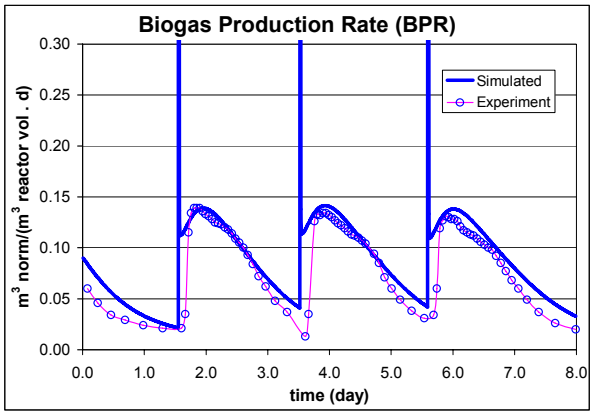

Graph 19

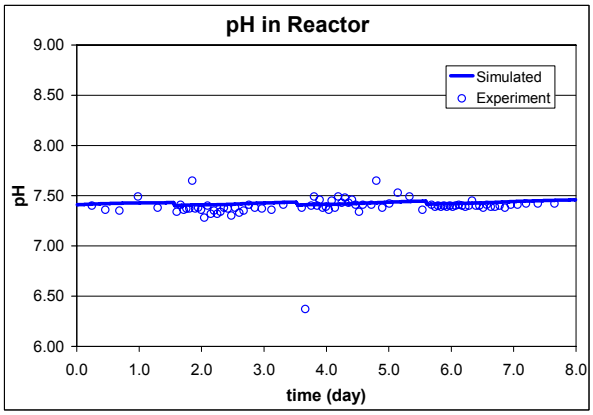

Graph 20

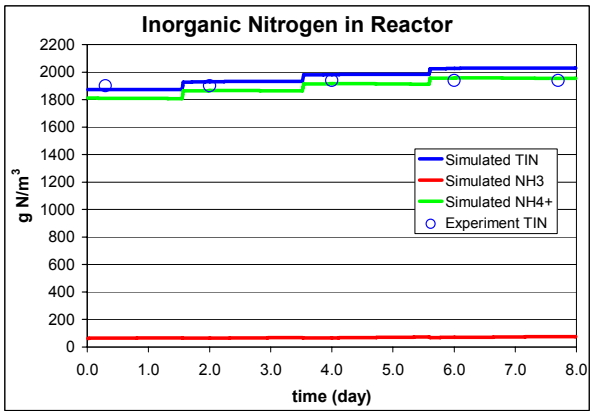

Graph 21

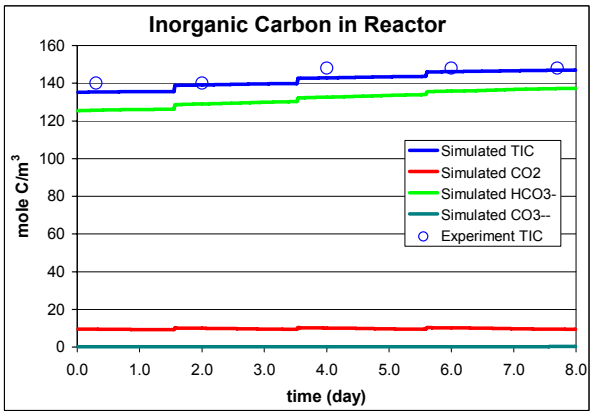

Graph 22

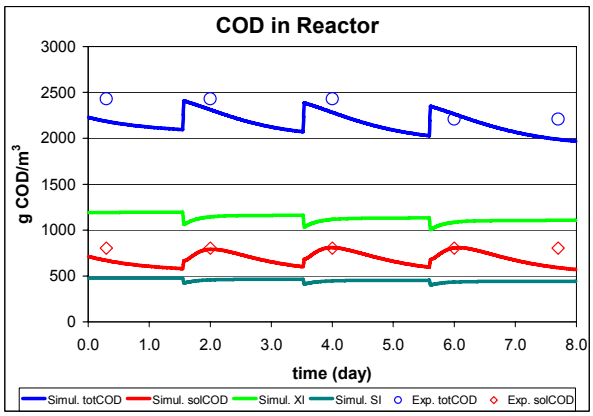

Graph 23

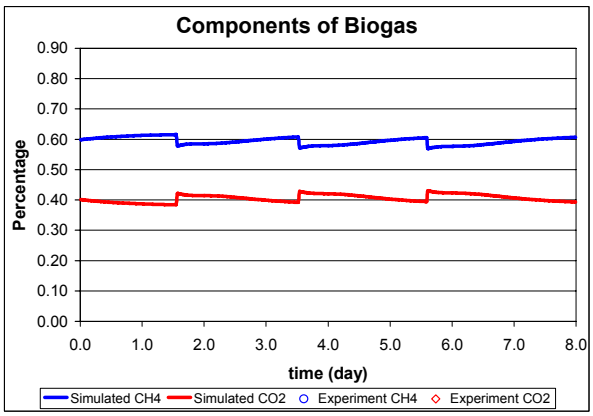

Graph 24

Figure 13: Simulation results with high NH_4^+ concentration

In order to raise the NH_4^+ concentration, the certain ammonium salts were chosen and added into the raw BW. The NH_4^+ concentration in reactor was increased from 1000 g N/m^3 to 2000 g N/m^3 step by step (L. Jean Emmanuel G. 2004). The NH_4^+ concentration in the

model was also raised up gradually trying to simulate the reality. At this high NH_4^+ concentration (NH_3 is around 65~70 g N/m^3), the free ammonia inhibition to *methanogens* is distinct comparing to the reference reactor, especially at high BPR (during the first period in the half-bell-shape). The simulation results are shown in Figure 13.

In order to get right BPR curves (Graph 19 in Figure 13), the half inhibitory concentration of ammonia to *methanogens* had to be changed much smaller comparing to the reference. It is assumed that there is a threshold of ammonia inhibition. Below this threshold, almost no inhibition acts on *methanogens*. Only when ammonia concentration is higher than the threshold, the inhibition occurs and can be described by Eqn. (13). This could be the reason that two half inhibitory concentrations are needed for two cases. Further discussion is achieved in the next chapter (Sec. 4.4.1).

In this scenario, the IC is increased to around 140 mole C/m^3 correspondingly (Graph 22). The percentage of CO_2 in biogas is also raised up to 40% (Graph 24). The simulation of total COD is reasonable too, and the soluble COD is always keeping at the similar level in all scenarios (Graph 23).

So far, our model achieves the scenario studies successfully. The model can simulate the reality properly. Based on this, the further step work was taken.

3.5 Prediction of BWAD plant by the model

Building up a rational as well as controllable model to simulate the real situation is just the first step. One can use the model to try a lot of possibilities without risks, without extra costs and with very little time consuming. For the BWAD plant, we are interested in several questions, i.e. what is the maximum capacity of our reactors, what is the optimal loading for the reactors, and how the reactors behaviour under the shock loading. Based on these requirements, two virtual scenarios were carried out.

3.5.1 Virtual scenario one: With different SRT

In this scenario, the capacity of the reactors is checked by reducing SRT but keeping the effluent at the same quality. The reactor was fed three times per week, but with different amount of raw BW. Besides 20 days, 10 days, 7.5 days and 6 days of SRT were tested, which are corresponding to 2.0 l, 2.5 l and 3.0 l BW per feeding. All other conditions were the same as the reference reactor. The average COD level of BW 6,500 g COD/m^3 was used as input. The performance of the reactor was examined and compared from different aspects.

The simulation shows that pH, IC, IN and biogas components, etc. are kept in the same level although the SRT are quite different. Only total COD in the reactor and BPR are significantly varied and, herewith, the relevant simulation results are displayed in Figure 14.

Obviously the more input, the more biogas products, as well as the more COD in the effluent. Even with SRT at 6 days, the total COD in effluent is only around 2,800 g COD/m^3 (Graph 25 in Figure 14), which means the total COD removal rate is still around 55~60%, where this remove rate is 60~65% with SRT 20 days. This indicates that the reactor has a

quite big capacity when it treats BW. Finally, the SRT of 10 days is recommended, as the shock loading has to be coped with, where the total COD in input is in the big range from 4,500 g COD/m^3 to 1,3000 g COD/m^3. The higher BPR are observed with short SRT, which indicates that more biogas is produced (Graph 26).

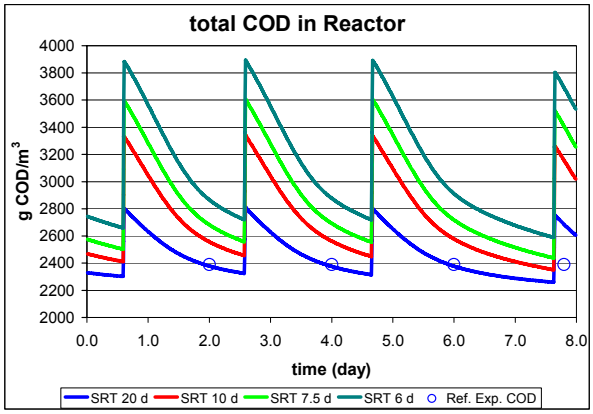

Graph 25

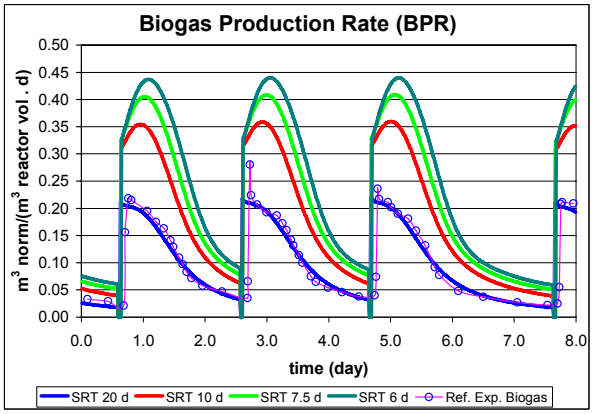

Graph 26

Figure 14: Simulation results with different SRT

From this simulation, it is concluded that the reactor has big unused capacity. Hereby, we can either giving the reactors higher organic loading, or reducing the volume of reactors. Subsequently, the next scenario was performed.

3.5.2 Virtual scenario two: With kitchen refuse

Based on the virtual scenario one, the second case with high organic loading was tried out. In the real case, the concentration of BW is fixed by the sanitation system, so the biowaste can be put into the raw BW in order to increase the organic loading. KR is the ideal biowaste to be digested together with BW. This kind of sanitation approach can be the good option for ECOSAN (Otterpohl *et al.* 1999). In recent years, the DESAR concept are also developed (Lens *et al.* 2001), and digesting BW and KR together had been investigated within the DESAR concept (Kujawa-Roeleveld *et al.* 2003).

The biodegradability of the KR is one of the key issues. It is quite diverse. But if it is classified collected, it has stably high biodegradability (e.g. in Germany the rubbish is strictly collected in the assorted tanks, and this makes the decentralized BWAD system plus KR more possibly). In this virtual scenario study, 0.8 is chosen as the biodegradable ratio. It is also supposed to have the similar distribution ratios among carbohydrates, proteins and lipids (25:25:30).

In order to integrate the digestion of KR properly into the model, the hydrolysis rate of KR should be figured out prudently. Veeken and Hamelers (1999) compared the hydrolysis rates of six different wastes (wholewheat bread, leaves, bark, straw, orange peelings, grass and filter paper), and found that the hydrolysis rates of these biowaste are in the range from 0.10 to 0.35 d^{-1}. It is also concluded that the biowaste collected indoors will be degraded faster and to a higher extent than biowaste collected outdoors (Veeken and Hamelers 1999).

Hereby, the hydrolysis rate 0.30 in chosen for our model. It assumes that carbohydrates, proteins and lipids have the same hydrolysis rates.

The KR should be cut into small pieces in order to get higher and even hydrolysis rates. Meanwhile, it is concerned that as solids KR will be dissolved into liquid phase gradually. So only the dissolved part (i.e. hydrolysed) can be used by microorganisms and will be accounted in the total COD in reactor, and the undissolved part will be not flushed out with the effluent. If the pre-storage tank is available for BW, it is recommended to put KR in this tank one or two days before it is fed into the digester. The higher hydrolysis rate will be benefited. If it is needed in real case, the above key parameters should be tested by experiments.

The SRT was kept at 20 days with 3 times BW feeding per week. All other conditions were kept the same as the reference reactor. Due to its quite low hydrolysis rate comparing to BW, KR was fed in less frequency. Two KR feeding methods were proposed, i.e. once per week and once every two weeks. Based on these situation and assumptions, two KR feeding cases were simulated and compared.

3.5.2.1 Kitchen refuse (KR) feed once per week

KR was fed into the AD reactor together with BW once per week. Three kinds of organic loading were tested, 0.75, 1.0 and 1.5 kg COD KR/(m^3 reactor · week). The simulation results of several important parameters are shown in Figure 15. This simulation was generated based on the 90 days pre-running of the model. The simulation and the experimental data of the reference reactor are also displayed in Figure 15 in order to make a clear-cut comparison. Regarding the legend, *1.5 kg/(m^3.week)* indicates the case with the organic loading 1.5 kg COD KR/(m^3 reactor · week); *1 kg/(m^3.week)* and *0.75 kg/(m^3.week)* have the same signification with different organic loading; *no add. KR* indicates the simulation of the reference reactor that has no additional KR; and *Exp.* means the experimental data of the reference reactor. In Graph 29, the experimental data of BPR is not shown, as the simulated curve of the reference reactor completely represents it under this scale. F1 with arrow in graphs indicates the KR feeding time.

According to the assumption, only dissolved KR will be accounted in the total COD in liquid phase, so two graphs were made for the total COD and residual KR respectively (Graph 27 and 28, in Figure 15). For one week time, the KR can be decreased to the similar level in all three kinds of organic loading (in Graph 28, around 250 g COD/m^3, it is the equivalent concentration because the residual KR is concerned as solids). But the total COD in liquid phase (Graph 27) are evidently increased, which means the effluent contains more COD. The effluent becomes worse especially with the BW feeding next the last BW + KR feeding. The BPR is increased certainly (Graph 29). The highest BPR appears also after the BW feeding next the last BW + KR feeding. This is because KR feeding boosts up the population of microorganisms. The CH_4 ratio is decreased in biogas products (Graph 30), although the more organic loading, the more biogas products. But the quality of biogas is still very good. Due to the simulation accuracy of the biogas components, Graph 30 tries showing the tendency instead of the precise percentages.

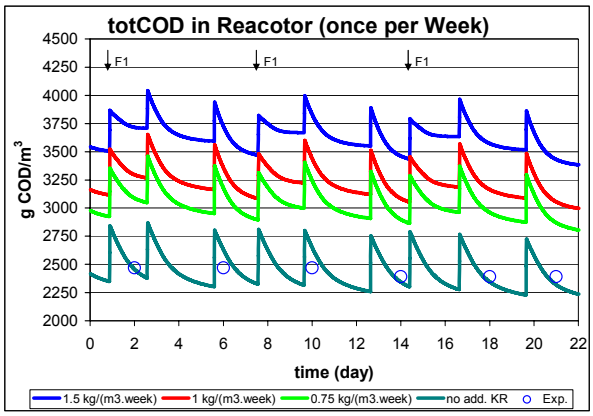

Graph 27

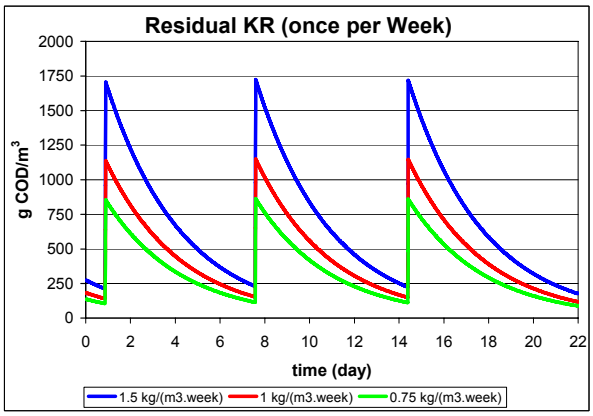

Graph 28

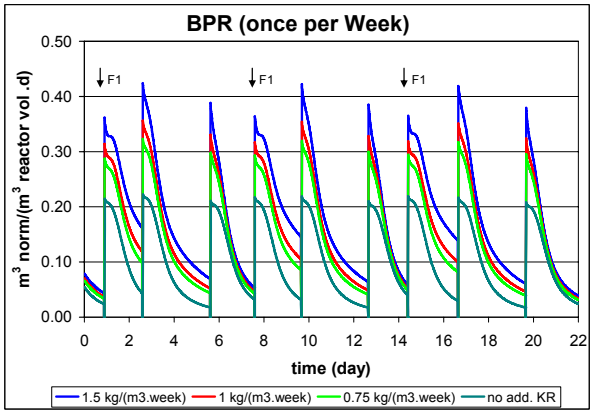

Graph 29

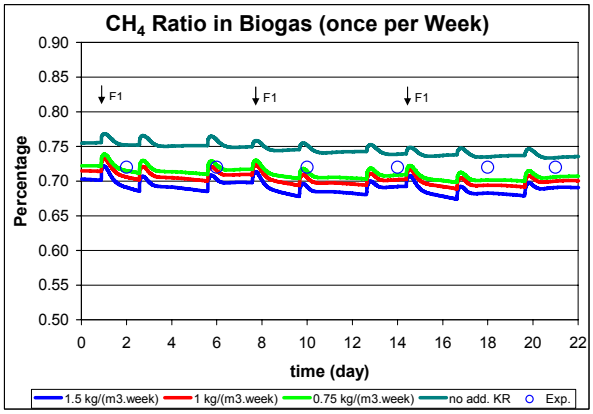

Graph 30

Figure 15: Simulation results KR feed once per week

The basic concepts the performance of BW + KR anaerobic digestion can be reached by this simulation.

3.5.2.2 KR feed once per two weeks

The parallel KR feeding method was checked out as well. The KR was fed into the reactor one every two weeks. When less KR is produced per week, this option could make sense. Also it is helpful to find out the optimized operation course. The same as before, the organic loading 0.75, 1.0 and 1.5 kg COD KR/(m^3 reactor · week) were simulated. The results are shown in Figure 16, and the same kind of legend and form are used. F2 with arrow in graphs indicates the KR feeding time with the feeding frequency once per two weeks. This time the simulation was generated based on the 120 days pre-running of the model.

In this case the KR can be reduced below 50 g COD/m^3 after two weeks (Graph 32), but the effluent is even worse during the first week (Graph 31). The effluent is very changeable during non-KR-feeding period in all three kinds of organic loading, which might not be expected. The COD in effluent are mostly undegradable parts from BW and KR, as well as biomass. However, if the next treatment step (e.g. chemical processes) that requires higher solids concentrations, it could benefit from this high COD concentration in effluent.

The influence of KR on the biogas is much bigger. More biogas certainly obtained in the first week after KR feeding. But it is decreased to almost the same level at the end of two-

week period (Graph 33). The highest BPR appear after the BW feeding next the last BW + KR feeding as well, and this phenomenon is further enhanced.

Likewise, even bigger undulation of CH_4 ratio in biogas takes place, but the biogas quality it keeps in a good level in principle (Graph 34).

In both two KR feeding cases, the variation trends are observed from 0.75 to 1.5 kg COD KR/(m^3 reactor · week). Which organic loading is more acceptable can be decided by the concrete requirements. The other special conditions can also be checked by the model if they are expected.

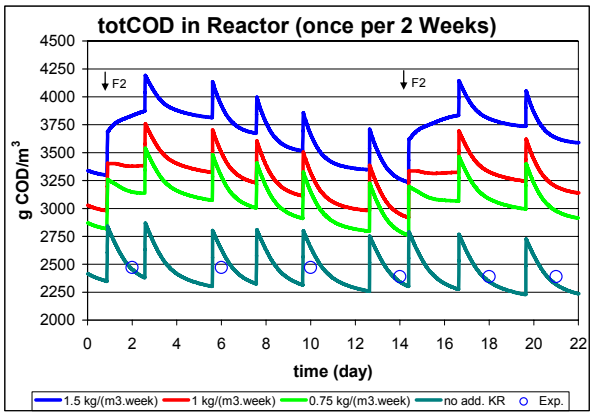

Graph 31

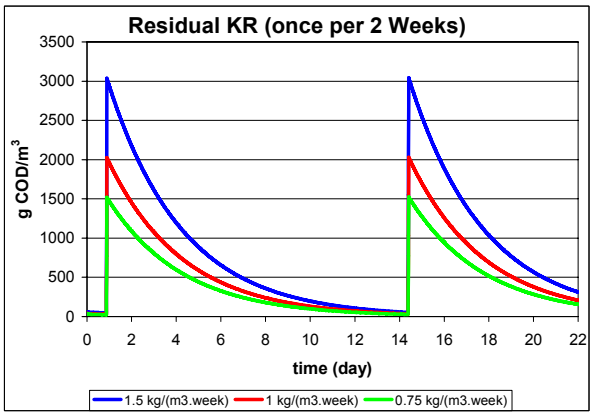

Graph 32

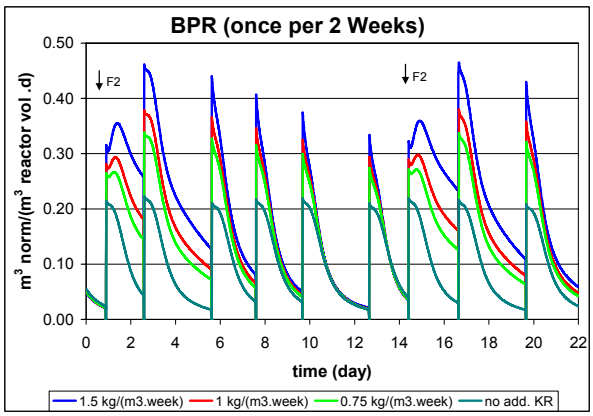

Graph 33

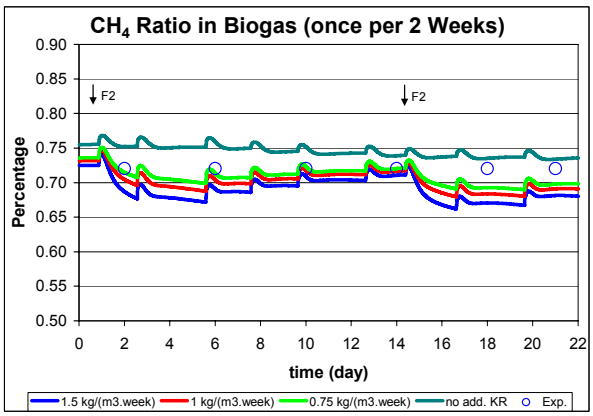

Graph 34

Figure 16: Simulation results of KR feed once per two weeks

Meanwhile the comparison between these two KR feeding ways was further figured out in order to give some instructional idea for the operation of the BWAD plant.

3.5.2.3 Comparison between two KR feeding methods

The organic loading 1.0 kg COD KR/(m^3 reactor · week) is chosen for this study. Two of the most important parameters are compared, i.e. total COD and BPR. The method of the KR feed once per week is called F1, and the KR feed once every two weeks is called F2. The comparison is shown in Figure 17 with the same Legend as above.

Using two-week-period as the frame of reference, the total COD with F1 is obviously lower than it with F2 after KR feeding in the first week, but it is reversed in the next week (Graph 35 in Figure 17). This is quite understandable. The effluents of both cases are around

800 to 100 g COD/m^3 higher than the reference reactor. The comparison of BPR shows that the more stable BPR is obtained with F1. The similar amounts of biogas product are gained from both KR feeding methods within two-week period deservedly (Graph 36).

Therefore, F1 should be more desired in common case. Which option is better still depends the real situation. Moreover, the biogas products as energy resource and its economic profit can be easily calculated based on the simulations, so more aspects can be easier taken into account when different plans are compared.

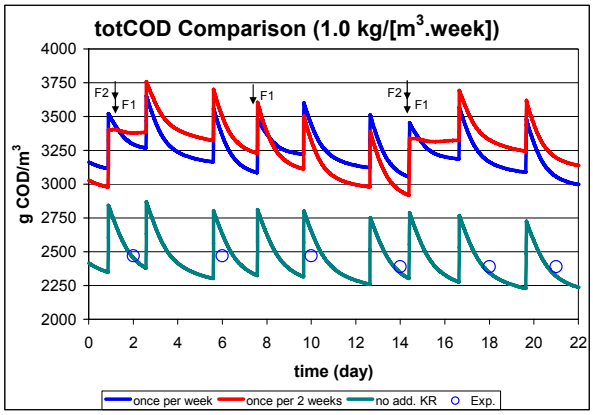

Graph 35

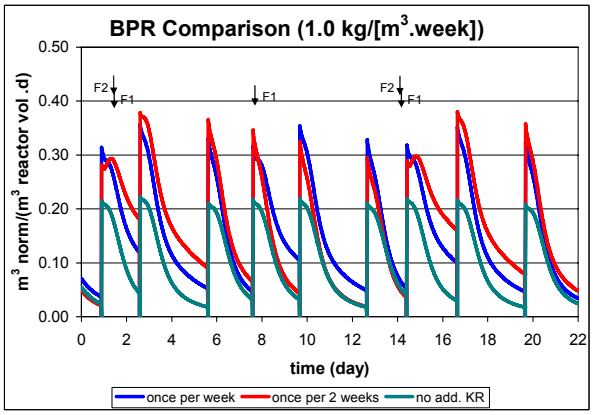

Graph 36

Figure 17: Simulation results of comparison between two KR feed methods

So far the model has been simulated three real cases and two virtual cases appropriately. It comes into the conclusion that the model is successfully applied to the BWAD. As a powerful tool, the model can predict the results of desired experiments.

At the same time, during constructing and applying the AD model, many aspects and factors of the model were checked and tested. Some of them are quite critical for understanding and manipulating the model. Of necessity, the discussion is carried out in the next chapter.

4 Discussion

In this part, discussion is performed in the same sequence as the chapter 2 in order to make the report easier to understand.

4.1 Characterization of the raw blackwater

In order to get reliable and reasonable simulation results, the raw BW must be characterized properly. For example, in our case, the raw BW already contains around 20% to 30% SCFA, which are mainly acetate. If this amount of SCFA is not presented in raw BW, the first period (see Sec. 3.4.1 Graph 1 in Figure 10) of BPR can never be obtained correctly.

As also discussed in the ADM1, the biodegradability of raw BW is one of the key issues. The ADM1 advises the methods from Pavlostathis *et al.* (1986) and Gossett *et al.* (1982) to determine the inert fraction (D) of the total input COD. However, those two methods mainly deal with the sludge from wastewater treatment plants, which are obviously unlike BW. Therefore, the biodegradability of BW has to be examined individually. One characterization of BW was presented by Kujawa-Roeleveld *et al.* (2003). Also the simple test can be achieved to determine the inert fraction, i.e. let the certain amount of input be digested adequate long time, and then the fraction D can be calculate by either checking the amount of biogas methane or calculating the mass balance. From the medical description as well as the testing results by our model, the inert part of BW is around 20 to 30%. In our simulation, 25% of total input COD is treated as the inert part.

Another important issue is the distribution ratio among carbohydrates, proteins and lipids. As one can see in Figure 3, after disintegration, the composites will be distributed to four portions. This distribution ratio was regarded as the critical point, because carbohydrates, proteins and lipids have different hydrolysis rates. Although it is costly and time-consuming to analyse the ratio of these components in input, it is, generally, necessary to determine this ratio of input in order to make the model execute correctly and accurately. However, it is found that this distribution ratio is not so crucial in BWAD, as:

1. the hydrolysis rates of the BWAD are not critical.

One observed phenomenon might prove this conjecture. In order to check the hygiene conditions of BW after AD, one reactor were fed with cooked BW. BW was heated at 70°C degree for an hour. Afterwards it was cooled down to 38°C and fed into the reactor. This heating step can dramatically increase hydrolysis rates. However, Cooked and uncooked BW have the same BPR and biogas products, which might implicit that hydrolysis is not rate-limiting step for the BWAD.

2. the existence of SCFA (especially acetate) in raw BW further decreases the impacts of hydrolysis to the final output.

Therefore, the model is not sensitive to the distribution ratio of carbohydrates, lipids and proteins at least for BW in our case. From the mathematical point of view, It shows that the variation of the ratio can be 20 ~ 30%, whereas the total biogas production rates are only slightly different.

At the same time, the existence of SCFA in raw BW makes the model more sensitive to the raw BW, because SCFA are utilised by the downstream microorganisms directly and exert an influence on the final output immediately. Therefore, instead of knowing the composition of raw BW, the amount of SCFA must be determined.

In our case, the ratio of carbohydrates : proteins : lipids is set as 20:20:25 excluding SCFA. Around 28% of total COD in raw BW is SCFA, where acetate accounts for 20%.

Generally, some microorganisms already exist in the input but showing at very small quantity. ADM1 initially does not consider this amount of biomass. If this biomass needs to be taken into account, it can be roughly assumed by the ratios from Torre and Stephanopoulos (1986), which are given as the percentages of the total input COD for each species to.

4.2 Disintegration and hydrolysis

As the first stage of ADP, these two steps are often rate-limiting, e.g. ADM1 was successfully applied to the AD of sludge in two wastewater treatment plants (WWTP), and it was proved that the disintegration is the rate-limiting step (Shang *et al.* 2004). Therefore, their reaction rates have been investigated extensively. As mentioned in Sec. 2.4.1, these two steps are not separated in most literatures, and the processes are investigated in the term of hydrolysis. Due to the great diversity, different substrates under different conditions have dissimilar rates, which make the problem more complicated.

First, let us look into the disintegration. It can be quite different from case to case. The ADM1 suggests several values for disparate ADP, e.g. k_{dis} = 0.4 d^{-1} for mesophilic high-rate solids and 0.5 for mesophilic solids. However, k_{dis} for our BW is ten times bigger than these values. After extensively testing by the model, it was found that k_{dis} has to be set as 4.5 d^{-1}, otherwise the correct curves of BPR can never be obtained. Moreover, with this k_{dis} = 4.5 d^{-1}, hydrolysis rates of carbohydrates, lipids and proteins all were set up as 10 d^{-1}, which are also the recommended values from ADM1 for mesophilic solids AD.

It is probably because the components of our BW are mainly human feces, which are already digested by human's digestive system. Also the substances in BW are nearly always in water phase, this can make them easier to hydrolysis. Meanwhile, before the BW is transported from on-site to laboratory it has been keeping in the container at least one or two days, it provides more time to perform hydrolysis. This also can be the reason that the raw BW contains such high amount of SCFA.

Normally, the carbohydrates are relative easier hydrolysed and lipids are slowler hydrolysed, where proteins is in between (Pavlostathis and Giraldo-Gomez 1991). However, the ADM1 gives the same hydrolysis rates to three substrates for the mesophilic solids AD, with much higher rates (up to 10 d^{-1}) than the common levels (between 0.01 and 1.0 d^{-1}). The

ADM1 does not give any reason. Therefore, the following cause is presumed. Under certain situations the hydrolysis rates of carbohydrates, lipids and proteins are not significantly different, so the same rate can be used. Hence, they are set up with adequately high values (e.g. 10 d^{-1}) in order to make the disintegration become the rate-limiting step. With this high rate, the influence from hydrolysis step to the whole ADP can be neglected at all in the model.

Therefore, from pure mathematical point of view, the advantage of containing disintegration and hydrolysis two steps also come into view. Just as discussed above, either disintegration or hydrolysis can be set as the rate-limiting step, so that the reaction rates of three substances can be set either same or different. This makes the model easier to manipulate. When three substances have the same hydrolysis rates, it further makes the model less sensitive to the distribution ratio (Sec. 4.1). And this causes the model more controllable and flexible. In our case, the disintegration and hydrolysis are not rate-limiting steps (at least not the sole rate-limiting step), so the even higher values were used for both.

4.3 Parameters of Michaelis-Menten Kinetics (k_m and K_S)

ADM1 includes 7 different species which utilise 8 different kinds of substrates, where valerate and butyrate are utilised by the same degraders. All kinetics parameters are figured out based upon their respective total concentrations in reactor. Actually Brühl (1991) proved that only undissolved SCFA can be taken by microorganisms, and determined k_m and K_S based on the concentration of undissolved SCFA. Nonetheless, so far most literatures consider the whole concentration instead of the undissolved form of SCFA, the uptake rates of SCFA in our work are treated as the function of the whole concentration of SCFA, too.

In particular, being a key step of ADP, the kinetics of acetate uptake (or say the biochemical kinetics of *methanogens)* should be investigated and set up carefully, in respect that it determines the biogas production.

4.3.1 Estimation of parameters

The batch experiments were executed in our studies in order to obtain the kinetics parameters of butyrate, propionate and acetate (valerate was on the plan but it was not practiced). However, from practical point of view, not all kinetics of all species need to be tested by experiment, because faster utilised intermediates has insignificant or no influence on the final results.

From mathematical point view, theses kinetics parameters can be slightly adjusted by mathematical tools in order to optimize the output. AQUASIM offers one tool of Parameter Estimation which can achieve this requirement. As a powerful and useful tool, the Parameter Estimation tool can estimate values of constant variables according to the measurement data. Ozkan-Yucel and Gokcay (2004) made use of ADM1 with AQUASIM to simulate sludge digestion of a WWTP, and estimated biochemical kinetics parameters by this estimation tool. However, it is not recommended to estimate so many parameters only depending on one or

two measurements (e.g. the biogas production). Only some sort of adjustment within the reasonable range can be done based on the performance of AD reactors.

In addition, the Parameter Estimation tool are effective and efficient to assess the particular kinetics based on the corresponding measurement, for example, the estimation of $k_{m,ac}$ and $K_{S,ac}$ based on the variation of S_{ac} in the reactor was achieved in our studies.

4.3.2 Kinetics for valerate and butyrate

As to valerate and butyrate, AMD1 uses one species with a single kinetics parameters set to utilise both of them with the competition inhibition. This is probably for simplifying the model. However, it is easily to be doubted and argued.

Batstone *et al.* (2003) estimated the kinetics of valerate and butyrate together with their allotropes (n-butyrate, i-valerate), and discussed how to set up kinetics parameters for valerate and butyrate in an optimum way. Different kinetics parameters of valerate and butyrate were observed, and it was concluded that in a mixed-feeding system with mixed culture, the assumption of using a single set of parameters and biomass for two acids is reasonable (Batstone *et al.* 2003). However, we recommend that valerate and butyrate should be utilised with two independent kinetics sets no matter by either one or two kinds of species. The reason is, when they are not critical steps, both can be skipped; when either one or both of them are critical, they have to be described precisely in order to truly reflect their impacts to the ADP. Moreover, with one more biochemical process the calculation speed of the model is not impaired.

4.3.3 Modification of the model

Concerning the conclusion to valerate and butyrate, two more simulations were made in order to check the influence from valerate and butyrate on the processes, as well as the flexibility of the model.

4.3.3.1 Skip valerate

In this simulation, valerate was skipped. The biochemical stoichiometric coefficients, which control the mass flux from one metabolic stage to the next, were modified in order to keep the same mass flux as the original ADM1 (which contains 7 species utilising 8 substances). The comparison of BPR is shown in Figure 18 together with the experimental data. As to the legend, *original* indicates the model with the uptake steps of both valerate and butyrate; *without va* indicates the model skips valerate; *without va & bu* means both valerate and butyrate are skipped and *Exp. Biogas* represents the experimental data of BPR. It is clear that BPR are nearly the same no matter with or without the utilization step of valerate. The difference of pH is invisible (the curves are not shown, as the curves are totally overlapped with this scale). Therefore, its impact to the whole system is so small that valerate can be skipped at all. In real situation, valerate concentration in reactors remains at a low level, which is around 20 to 40 g COD/m^3 in the raw BW, and it is undetectable 3 hours later after feeding until the next feeding.

Established upon this conclusion, the model was modified further to skip both valerate and butyrate.

4.3.3.2 Skip both valerate and butyrate

As the intermediates with a relative low concentration too, butyrate could be also skipped. In the same way, the model was tested without both valerate and butyrate this time. The simulation results are shown in Figure 18, too. Obviously, without the uptake steps of butyrate and valerate the biogas production rate will be faster, and the BPR will be kept in higher level longer. But it is tolerable. Furthermore, it can be compensated by adjusting the uptake rates of upstream substances or by changing the biochemical stoichiometric coefficients. These kinds of adjustment have been successfully done (the simulation results are not shown).

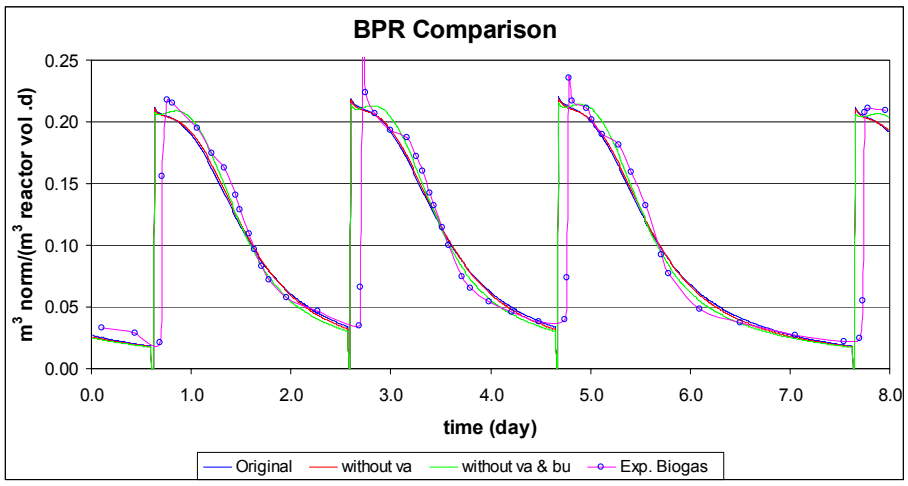

Figure 18: comparison of the model with different sorts of degraders

Grounded on these two possibilities studies, one can say that the uptake of valerate and butyrate are optional steps, and they can be included or excluded depending on their situations or the simulation purpose. In the common case, both of them can be skipped. Concerning our simulation, valerate is skipped but butyrate is kept attempting to keep the capacity of the model. In this report, if it is not specified, the simulation results are carried out based on the model with butyrate but without valerate.

Similarly to other SCFA, when they are not the critical steps, they can be skipped at all. Whether they are critical steps or not can be simply checked by measuring their concentrations in the reactor. The continuous low concentrations can prove that they are faster utilised intermediates, which are less important to the whole ADP. If go further from this point of view, new substrates can be easily added into the model so that the model becomes more applicable. It has been reported that the alcohol is added into ADM1 as a key intermediate and successfully simulated the realities (Ruiz *et al.* 2004).

4.3.4 Delay phenomenon

When the organisms enter the new situation, they need certain time to response this change first, instead of start utilising substances at once. This kind of delay phenomenon was observed in our lab-scale AD plant, and already shown in Sec. 3.4. It is the nature of organisms, but it can not be simulated by Michaelis-Menten kinetics. Batstone *et al.* (2003) observed the same phenomenon of the unitization of valerate. Especially for valerate in ADP, Batstone *et al.* (2003) assumed some reasons, tried compensating it by decreasing maximum uptake rate (k_m). But it does not work in our case, since the delay comes from the utilization of acetate. When $k_{m,ac}$ is decreased, the right peak value of BPR can not be obtained. Hereby, it needs to be studies further.

Based on the extensive testing, in our model, the kinetics parameters of sugar, amino acid and LCFA are set up with the recommended values by AMD1, where some small adjustment was made. Butyrate, propionate and acetate were coped with in virtue of experimental data. Valerate is skipped. The values for each set are listed in Appendix E.

4.4 Inhibition

The inhibition function is one of the most important aspects of ADP. The main inhibitors are ammonia, pH and hydrogen. It also comes from sulphide and heavy metals, etc. Here the ammonia and pH inhibition were discussed from the angle of mathematical model.

4.4.1 Ammonia inhibition

It is widely accepted that high level of free ammonia nitrogen (FAN) are more inhibitory to the anaerobic processed than the ammonium ion itself, and the inhibitory effects of FAN influences mostly only on *methanogenesis* (Stronach *et al.* 1986, pp74). Nonetheless, many literatures reported the inhibition as total ammonium nitrogen (TAN). Meanwhile, the *methanogens* can be acclimated in the higher concentration FAN, so the inhibition thresholds fall into a big variation from 1,900~2,000 g NH_4^+-N/m^3 (Moen 2000) to 5,000~8,000 g NH_4^+-N/m^3 (van Velsen 1977). The total TAN inhibition concentrations can be as high as 10,000 g NH_4^+-N/m^3 regardless of acclimation factors (Liu and Sung 2002). It is reported that after acclimation to higher level of TAN, the *methanogens* become less sensitive to the change both of TAN and pH (Liu and Sung 2002). This kind of acclimation can not be simulated anyway.

Back to our simulation, in scenario One (Sec. 3.4.1), the TAN is 1,000~1,200 g NH_4^+–N/m^3 concomitantly with 45 g NH_3-N/m^3 FAN. In order to fit in with the measurement data, the half inhibitory coefficient $K_{I,NH3,ac}$ (the concentration that 50% methanogenic activity is inhibited by FAN)has to be set around 200 g NH_3-N/m^3. In scenario Three (Sec. 3.4.3), the TAN and FAN are raised to 2,000~2,200 NH_4^+-N/m^3 and 70 g NH_3-N/m^3, respectively. This time $K_{I,NH3,ac}$ has to be decreased to 50 g NH_3-N/m^3, otherwise the measurement data never can be matched. The reason for this strange situation was hypothesized as follows. There is a threshold for ammonia inhibition, the inhibitory effects occur only when the FAN above this

threshold. The non-competitive inhibition equation (Eqn. (13)) correctly describes the ammonia inhibition, but it does not reflect the changes over the threshold. Lay *et al.* (1998) found that up to 50 g NH_3-N/m^3 until 500 g NH_3-N/m^3 the ammonia inhibition is increased. This could illustrate what happened in our simulation. The recommended $K_{I,NH3,ac}$ value from ADM1 is 1.4 g NH_3-N/m^3, which seems a little bit too small. With this value, in the reference reactor the *methanogenesis* will be inhibited 70%, which obviously does not reflect the reality. Furthermore, the acclimation of methanogens makes this problem more complex, and it needs to be further studied as well.

TAN and FAN have direct relation to pH, which is also the inhibitor to anaerobic processes. The fraction of NH_3 at pH 7 is close to 1% of TAN and increases to 10% at pH 8 (Kayhanian 1999). The relation between ammonia inhibition and pH inhibition will be explained in the next section.

4.4.2 pH inhibition

pH has inhibition function to most anaerobic microorganisms. In ADM1 two empirical equations (Eqn. (11) and (12)) are introduced for pH inhibition. Eqn. (11) takes into account both upper and lower pH inhibition, where Eqn. (12) considers only lower pH inhibition. ADM1 suggests that only Eqn. (12) should be used for the pH inhibition to *methanogenesis* when the ammonia inhibition is included. One conjectural reason is that at high pH level the high concentration of ammonia will be formed, so the inhibition will be present by the inhibition term of ammonia. This also could be the reason that $K_{I,NH3,ac}$ from ADM1 is relative too small.

If , however, big number is used for $K_{I,NH3,ac}$ or TAN has very low concentration, free ammonia will bring no inhibition at high pH. Therefore, we advise to use Eqn. (11) together with ammonia inhibition and $K_{I,NH3,ac}$ needs to be modified. Regarding to Eqn. (11) itself, the tests results showed that it is too sensitive or too stiff, e.g. I = 1 at pH= 7.0, and I = 0.59 at pH =7.5 (pH_{LL} = 6.0 and pH_{UL} = 8.0), notwithstanding Veeken and Hamelers (1999) found that the highest methanogenic activity occurs in between 7.0 ~7.5 of pH.

The inhibition from pH and VFA on hydrolysis of organic solid wastes was studied by Veeken *et al.* (2000), and it was found that only pH (in the range of 6 ~ 7) primarily effects on the hydrolysis rates, whereas either total VFA or dissociated VFA has no significant impact to hydrolysis. The VFA causes severe inhibition to hydrolysis only when it is up to 30,000 g/m^3 (ten Brummeler *et al.* 1991).

4.5 Comparison of equilibrium and dynamic processes

Liquid-liquid processes can be implemented as either equilibrium or dynamic processes. The same results are obtained by these two kinds of methods, and the simulation speeds are similar, too.

As an example, NH_4^+ was implemented by these two methods in two independent models. In order to make the results comparable, other acid-bases processes stick to one method (CO_2

and HCO_3^- as dynamic processes, and organic acids as equilibrium processes). The simulation results of NH_3 and CO_2 by both methods are shown in Graph 37 of Figure 19. Clearly, both methods work out the exactly the same results of free NH_3 in the reactor, and identically, the CO_2 simulated by both methods are also the same. For pH, only after input there is a visible difference between two implementation methods with very high resolution (Graph 38). And this difference is so small that it can be ignored certainly. The TIN and NH_4^+ in the reactor are compared in Graph 39. Also only very small difference is observed. As the corresponding substance, the simulation of TIC and HCO_3- is shown as well in Graph 40. All simulation results in Figure 19 illustrate that two methods almost give the same results, where the dynamic process generates more stiff curves for NH_3. CO_2, HCO_3^- and HAc were tested by both methods too, and the same conclusion was obtained. Concerning dynamic processes, two implementation methods (the dynamic process is implemented as either one integrated process or two double-direction processes, see Sec. 2.5.1) were tested as well, and exactly the same results were gained.

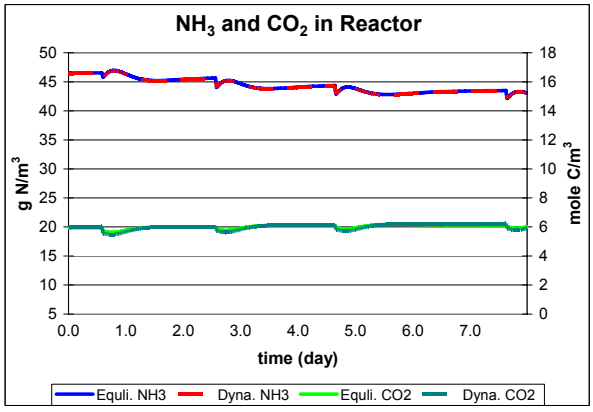

Graph 37

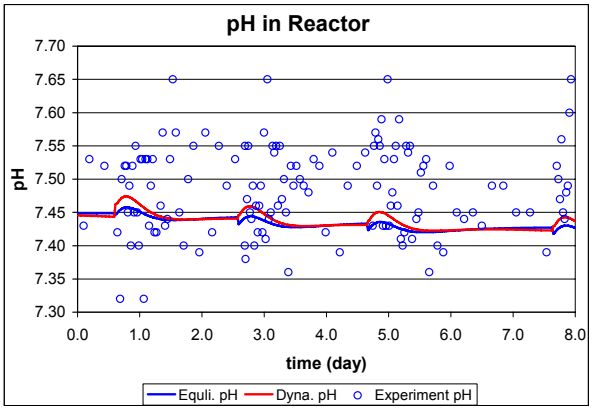

Graph 38

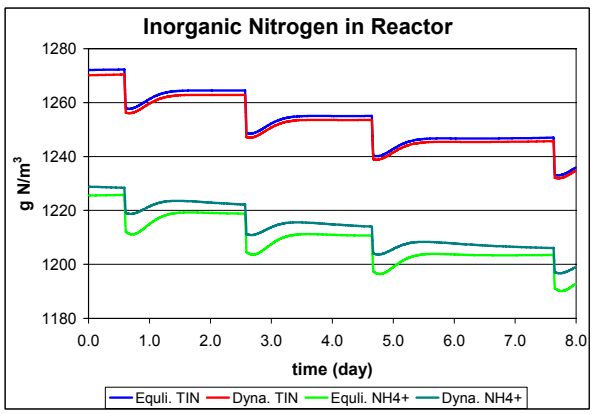

Graph 39

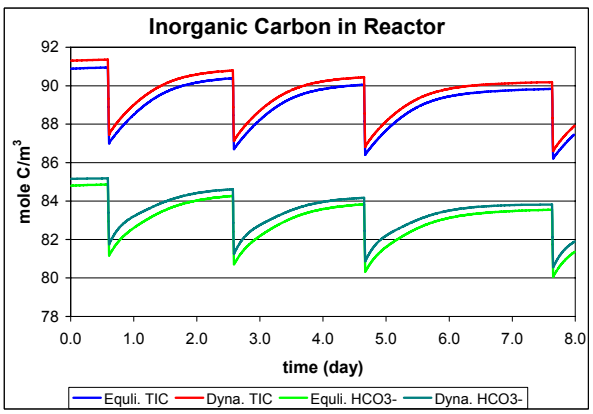

Graph 40

Figure 19: Comparison of different implementation methods for liquid-liquid processes

So when acid-base processes need to be implemented in the model, these two methods can be chosen arbitrarily. In our model, CO_2 and HCO_3^- are achieved as dynamic processes, where NH_4^+ and organic acids are achieved as equilibrium processes. As to liquid-solid processes, it is reported that the precipitation of $CaCO_3$ was successfully integrated in the ADM1 as a dynamic processes with Eqn. (41) to simulate and predict a real AD plant (Batstone and Keller 2003).

4.6 Coefficients of physicochemical processes

4.6.1 $k_{A/B,i}$ and $k_{prec,i}$

$k_{A/B,i}$ and $k_{prec,i}$ are the coefficients of dynamic processes for implementing liquid-liquid and liquid-solid processes, respectively. They fall into a big range from 10^7 to 10^{14}, which lead to the same simulation results. One thing is found during our tests. When processes were transformed from equilibrium processes to dynamic processes, some variables could become inactive (in AQUASIM, and the reason is unknown). Therefore, $k_{A/B,i}$ needs a very small value ($<10^4$) in order to get right pH value, but FAN can not simulated correctly in any case. Under this situation, the new variable must be established to replace the old one, although the new one is exactly the same as the old one.

4.6.2 k_La

K_La describes the transfer rates of gases from liquid phase to gas phase. It is affected by many boundary conditions, such as temperature, gas pressure, liquid quality, reactor type and stirring methods, and so forth.

Pauss *et al.* (1990) investigated k_La of CH_4, H_2 and CO_2 with the different types of reactors, and reported k_La of CH_4 and H_2 as 2.64 ± 0.48 and 2.16 ± 0.24 d^{-1} for anaerobic processes with CSTR, respectively. Siegrist *et al.* (2002) found the $k_La_{,CO2}$ was above 100 d^{-1} in their lab. Merkel and Krauch (1999) gave the superficial gas velocity relationship which can be used to estimate k_La:

$$k_La = 9.43 \cdot \left(u^0_{gas}\right)^{0.83} \tag{66}$$

Where: u^0_{gas} = superficial gas-flow velocity, m/d

With Eqn. (66) the temperature correction needs to be involved by van't Hoff Eqn. (42).

However, from the mathematical point of view, k_La is not sensitive. The values of k_La from 1.0 to 1000 result in the same BPR that all can fit in with the measurements. Only when it is smaller than 1.0, the BPR starts to be impaired. The reason can be that k_La and the concentrations of substrates are in different magnitudes, so when differential equations are calculated, k_La has much shorter response time. When it is magnified or dwindled, the results will not be influenced. Therefore k_La can be easier set up.

In the normal case, k_La for all three gases can have the same arbitrary value. ADM1 also recommends using the same k_La value for all gases. In our model, k_La is 20 d^{-1}.

4.6.3 k_p

k_p is the pipe resistance coefficient for calculating the gas flow, when the headspace pressure is variable (Batstone *et al.* 2002). Due to the same reason as k_La, it is not sensitive in the mathematical model, too. Only when k_p is smaller than 0.5, the biogas flowrate is diminished. Herewith, it can be set up optionally as well. Nevertheless, in order to keep the

offset $\Delta P < 0.01$ bar, k_p should be 100 time bigger than $P_{tot,average}$ (total average gas pressure in headspace, as unit of bar) (Siegrist *et al.* 2002). In our model, k_p is 100 $m^3/(d \cdot bar)$.

4.6.4 Cations and anions

Cations and anions represent ions of strong base and acid slats in liquid phase. Though they do not contribute any H^+ or OH^-, they still influence on pH due to the charge balance (Eqn.(18)). So cations and anions also need to be dealt with advisably. Based on the charge balance, the pH is increased when anions is decreased with all others being constants. This could be useful when pH has to be modulated.

4.6.5 Startup of the model

As sensitive and frail processes, the startup of real AD plant can take months or even fail. Surprisingly, the startup of AD model can be frustrated too. This is caused by minus value in the logarithm of pH that is brought on by improper initial values. Therefore, the initial values of IN, IC, SCFA, cations and anions need to be set discreetly. As discussed above, anions or cations could be a good handle.

Subsequent upon the startup, the simulation period is the next key issue. In order to reach the steady-state, it is suggested that the model should be running at least three SRT before simulating realities. In order to get microorganisms in reactors, the initial value of microorganisms (e.g. 7 degraders) should be bigger them 0, otherwise the input should contain certain amount of these microorganisms. The proper initial biological conditions of reactors can results in less time consuming to achieve the steady-state. Therefore, the model can be running 5 or 6 SRT firstly so that the steady-state can be surely reached, and then change the initial conditions of model to this steady-state. Consequentially, next time the model needs much shorter running time (e.g. only 2 SRT) to achieve the steady-state.

5 Conclusion

The mathematical model is an effective, efficient and economic method to design and control systems. ADM1 was successfully implemented and applied to the BWAD plant. Our targets were commendably achieved. Meanwhile, ADM1 was further tested and improved. Batstone and Keller (2003) illustrated that a high accuracy of all model predictions is not required in such cases, when only a limited number of simulation outputs are of relevance, and the accuracy of these can be estimated very well with some practical considerations. ADM1 satisfies these requirements quite well.

As a generic ADM platform, ADM1 tries to comprise information and items as much as possible. Therefore, the ADM1 should be modified (either simplification or complication) for each instance in order to get the optimum model. ADM1 is very easy to add or subtract new or old processes due to its structure.

Based on our studies, it is found that the distribution ratio from input composites to carbohydrates, proteins and lipids are not so sensitive, whereas the percentage of SCFA (e.g. acetate and propionate) in the input is more important instead. The SCFA are much easier to be characterized than the composition of input.

ADM1 includes disintegration and hydrolysis two steps, and it makes the model more flexible. In mesophilic digestion of BW, the disintegration and the hydrolysis are not the rate-limiting steps (at least not the sole rate-limiting step).

Although the model is not so sensitive to k_m and K_S, it is still worth to test those parameters of acetate, which is more convincible and reliable.

As one of the key issues, the inhibition function is implemented in the model. However, its credibility and validity need to be further investigated.

The physicochemical processes work also well. The coefficients of $k_{A/B,i}$, $k_{prec,i}$, k_La and k_P are not sensitive to the mathematical model, so they can be arbitrarily set up. The particular experiments to examine them are not necessary.

Cations and anions can influent the pH value significantly, so that they need to be worked out correctly. The startup of the model should be paid attention to, as inappropriate initial conditions can lead the model entirely failed.

In addition, because each cycle of the batch experiments (or discontinuous feeding operation) goes though nearly all biological status (e.g. high food to biomass ratio (F/M), low F/M and starving phase, etc.), it is stricter to mathematical model. Meanwhile, when acetate exists in input, it also requires more functional and precise model. Therefore, these two kinds of circumstance can be very good benchmark or higher criterion for examining mathematical models.

6 Next step work

The work that has been accomplished is just a favourable outset. The model can be further improved, and more significative and valuable work can be done based on the model. The tasks that could be further performed in the next step are outlined as follow:

1. further study the inhibition function

The interrelations between inhibitors need to be further understood. The acclimation to the higher NH_4^+ and the threshold can not be reflected by current model.

2. explore the decay of biomass

The real case shows that bacteria have faster decay rates, as after weekend (three days starving) the highest biogas production rates on Monday are much lower than on Friday (the reactors are fed on Monday Wednesday and Friday). However, the model is a bit less sensitive to this, though different decay rates had been tested. This phenomenon should be studied further from the mathematical point of view.

3. simulate the delay phenomenon of biochemical processes

This phenomenon can not be simulated so far, although it is nature behaviour of organisms.

4. simulate more types of reactors

In this work, only CSTR was modelled, more types of reactors should be modelled, e.g. UASB reactor.

5. simulate more AD treatment processes

The AD treatment is a powerful method to deal with wastes and wastewater. More processes can be modelled, e.g. the ammonia removal in ADP (van Dongen *et al.* 2001), the sulphate reduction in ADP (Ristow and Hansford 2001), etc.

References

Angelidaki, I., Ellegaard, L. and Ahring, B.K., 1993. A mathematical model for dynamic simulation of anaerobic digestion of complex substrates: Focusing on ammonia inhibition. Biotech. Bioeng. Vol 42: 159-166

Barker, H.A., 1956. Biological Formation of Methane. In: Bacterial Fermenttions. John Wiley & Sons, Inc., New York, U.S.

Batstone, D.J., Keller, J., Angelidaki, I.., Kalyuzhnyi, S., Pavlostathis, S.G., Rozzi, A.., Sanders, W., Siegrist, H. and Vavilin, V. (IWA Task Group for Mathematical Modelling of Anaerobic Digestion Processes), 2002. Anaerobic Digestion Model No. 1 (ADM1). IWA Publishing, London, U.K.

Batstone, D.J. and Keller, J., 2003. Industrial applications of the IWA anaerobic digestion model No. 1 (ADM1). Wat. Sci. Tech. Vol 47, No 12: 199-206

Batstone, D.J., Pind, P.F. and Angelidaki, I., 2003. Kinetics of thermophilic, anaerobic oxidation of straight and branched chain butyrate and valerate. Biotech. Bioeng. Vol 84, No 2: 195-204

Brühl, A.S., 1991. Anaerobe Abwasserreinigung in neuen Bioreaktoren mit Polyurethan-Schaumstoffpartikeln zur Immobilisierung der Bakterien. VDI Verlage GmbH, Düsseldorf. Fortschrittberichte, Reihe 15, Nr. 85: Umwelttechnik. in German

Chen, Y.R. and Hashimoto, A.G., 1980. Substrate utilization kinetic model for biological treatment process. Biotech. Bioeng. Vol 22, No 10: 2081-2095

Eastman, J.A. and Ferguson, J.F., 1981. Solubilization of particulate organic carbon during the acid phase of anaerobic digestion. J. Wat. Poll. Cont. Fed. Vol 53: 352-266

Gavala H.N., Angelidaki, I., Ahring, B.K., 2003. Kinetics and Modeling of anaerobic digestion process. Adv. Biochem. Eng. Biotechnol. Vol 81: 57-93

Gossett, J.M. and Belser, R.L., 1982. Anaerobic digestion of waste activated sludge, J. Environ. Eng. ASCE Vol 108: 1101-1120

Haldane, J.B.S., 1930. Enzymes. Longman Green and Co., London, U.K.

Henze, M., Gujer, W., Mino, T. and van Loosdrecht, M., (IWA Task Group on Mathematical Modelling for Design and Operation of Biological Wastewater Treatment), 2000. Activated Sludge Models ASM1, ASM2, ASM2d and ASM3. IWA Publishing, London, U.K.

Hobson, P.N., 1983. The kinetics of anaerobic digestion of farm wastes. J. Chem. Tech. Biotechnol. Vol 33B: 1-20

Ivanova, M., 2003. Untersuchungen zur Vergärung von Schwarzwasser aus Vakuumtoiletten mit zugegebenen Bioabfällen. Master Thesis, Hamburg University of Technology (TUHH), Germany. in German

Jöbses, I.M.L., 1986. Modelling of anaerobic microbial fermentations – the production of alcohols by Zymomonas mobilis and Clostridium beijerinckii. Krips Repro Meppel

Kayhanian, M., 1999. Ammonia inhibition in high solids biogasification: an overview and practical solutions. Environ. Technol. Vol 20: 355

Koutsoukos, P., Amjad, Z., Tomson, M.B. and Nancollas G.H., 1980. Crystallization of calcium phosphates: a constant composition study. J. Am. Chem. Soc. Vol 27: 1553-1557

Kujawa-Roeleveld, K., Elmitwalli, T., Gaillard, A., van Leeuwen, M. and Zeeman, G., 2003. Co-digestion of concentrated black water and kitchen refuse in an accumulation system within the DESAR (decentralized sanitation and reuse) concept. Wat. Sci. Tech. Vol 48 No 4: 121–128

L. Jean Emmanuel G., N., 2004. Impact of Mixing, Feeding Frequency and High Nitrogen Concentrations on the Anaerobic Digestion of Blackwater. Master Thesis, Hamburg University of Technology (TUHH), Germany

Lay, J.J., Li, Y.Y., Noike, T., 1998. The influence of pH and ammonia concentration on the methane production in high-solids Digestion Processes. *Water Environment Research* Vol 70:1075-1082

Lehninger, A., Nelson, D. and Cox, M., 1993. Principles of biochemistry. 2nd ed., Worth Publishers, New York, U.S.

Lens, P., Zeeman, G., Lettinga, G., 2001. Decentralised sanitation and reused: Concepts, systems and implementation. IWA publishing, London, U.K.

Lettinga, G., Van Velsen, A.F.M., Hobma, S.W., De Zeeuw, W. and Klapwijk, A., 1980. Use of the upflow sludge blanket reactor concept for biological waste water treatment, especially for anaerobic treatment. Biotech. Bioeng. Vol 22: 699–734.

Lema, J.M. and Omil, F., 2001. Anaerobic treatment: a key technology for a sustainable management of wastes in Europe. Wat. Sci. Tech. Vol 44, No 8: 133-140

Lide, D., 2001. CRC Handbook of chemistry and physics. 82nd ed. CRC Press, Boca Raton, FL.

Liu, T. and Sung, S., 2002. Ammonia inhibition on thermophilic aceticlastic methanogens. Wat. Sci. Tech. Vol 45 No 10: 113-120

Madigan, M.T., Martinko, J.M., and Parker, J., 2003. Brock biology of microorganisms. Upper Saddle River, NY: Prentice Hall, 10th ed., International Edition

McCarty, P.L, 2001. The development of anaerobic treatment and its future. Wat. Sci. Tech. Vol 44, No 8: 149-156

Merkel, W. and Krauth, K., 1999. Mass transfer of carbon dioxide in anaerobic reactors under dynamic substrate loading conditions Wat. Res. Vo 33, No 9: 2011-2020

Metcalf, L. and Eddy, H.P., 1915. American Sewerage Practice, III. Disposal of Sewage. 1st ed., McGraw-Hill Book Company, Inc., New York, U.S.

Metcalf & Eddy, 2003. Wastewater Engineering: Treatment and Reuse. 4th ed., McGraw-Hill, Inc.

Michaelis, L. and Menten, L., 1913. Die Kinetik der Invertinwirkung. Biochem. Z. Vol 49: 334-369

Mitsdörffer, R., 1991. Charakteristika der zweistufigen thermophilen/mesophilenSchlammfaulung unter Berücksichtigung kinetischer Ansätze; Berichte aus Wassergüte-und Abfallwirtschaft, TU München

Moen, G.M., 2000. A comparison of the performance and kinetics of thermophilic and mesophilic anaerobic digestion. Master of Science Thesis, Dapartment of Civil and Environmental engineering, University of Washington, Seattle, WA.

Mosey, F., 1983. Mathematical modelling of the anaerobic digestion process: regulatory mechanisms for the formation of short chain volatile fatty acids from glucose. Wat. Sci. Tech. Vol 15, No 8/9: 209-232

Musvoto, E.V., Wentzel, M.C., Loewenthal, R.E. and Ekama, G.A., 2000a. Integrated chemical-physical processes modelling – I. Development of a kinetic-based model for mixed weak acid/base systems. Wat. Res. Vol 34: 1857-1867

Musvoto, E.V., Wentzel, M.C., Loewenthal, R.E. and Ekama, G.A., 2000b. Integrated chemical-physical processes modelling – II. Development of a kinetic-based model for mixed weak acid/base systems. Wat. Res. Vol 34: 1869-1880

NRC, 1995. The Role of Technology in Environmentally Sustainable Development. National Academy Press, Washington D.C., U.S.

Otterpohl, R., Grottker, M. and Lange, J., 1997. Sustainable water and waste management in urban areas. Wat. Sci. Tech. Vol 35, No 9: 121-133

Otterpohl, R., Albold, A. and Oldenburg, M., 1999. Source control in urban sanitation and waste management: ten systems with reuse of resources. Wat. Sci. Tech. Vol 39, No 5: 153-160

Otterpohl, R., 2001. Black, brown, yellow, grey - the new colours of sanitation. Water 21, October, 2001. Magazine of the International Water Association. IWA Publishing, London, U.K.

Otterpohl, R., Braun, U. and Oldenburg, M., 2002. Innovative Technologies for Decentralised Wastewater Management in Urban and Peri-Urban Areas. Keynote presentation at IWA Small2002, Istanbul, Sept 2002

Ozkan Yucel, U.G. and Gokcay C.F., 2004. Modeling a full-scale anaerobic digester. The 10th World Congress on Anaerobic Digestion (AD10), proceedings, Montreal, Canada

Pauss, A., Andre, G., Perrier,M., Guiot, S.R., 1990. Liquid-to-Gas Mass Transfer in Anaerobic Processes: Inevitable Transfer Limitations of Methane and Hydrogen in the Biomethanation Process. Appl. Environ. Microbiol. Vol 56, No 6: 1636-1644

Pavlostathis, S.G. and Gossett, J.M, 1986. A kinetic Model for anaerobic digestion of biological sludge. Biotech. Bioeng. Vol 28, No 10: 1519-1530

Pavlostathis, S.G., and Giraldo-Gomez, E., 1991. Kinetic of anaerobic treatment. Wat. Sci.Technol. Vol 24, No 8: 35-59

Peterson, E.E., 1965. Chemical reaction analysis. Prentice-Hall, Englewood Cliffs, NJ, U.S.

Ramsay, I.R., 1997. Modelling and control of high-rate anaerobic wastewater treatment systems. Ph.D. thesis, University of Queensland, Brisbane, Australia

Reichert, P., 1994. Aquasim - a tool for simulation and data-analysis of aquatic systems. Wat. Sci. Tech. Vol 30 No 2: 21-30

Reichert, P. 1998. Aquasim 2.0 – User Manual, computer program for the identification and simulation of aquatic systems. EAWAG: Dübendorf, Switzerland, ISBN 3 906484 16 5

Ristow, N.E. and Hansford, G.S., 2001. Modelling of a falling sludge bed reactor using AQUASIM. Water SA Vol. 27 No. 4: 445-454

Ruiz, G., Rodriguez, J., Roca, E. and Lema, J.M., 2004. Modification of the IWA-ADM1 for application to anaerobic treatment of ethanolic wastewater from wine factories. The 10th World Congress on Anaerobic Digestion (AD10), proceedings, Montreal, Canada

Shang, Y., Johnson, B.R. and Sieger, R., 2004. Application of the IWA Anaerobic Digestion Model (ADM1) for simulating full-scale anaerobic sewage sludge digestion. The 10th World Congress on Anaerobic Digestion (AD10), proceedings, Montreal, Canada

Siegrist, H., Vogt, D., Garcia-Heras, J.L. and Gujer, W., 2002. Mathematical model for meso- and thermophilic anaerobic sewage sludge digestion. Environ. Sci. Technol. Vol 36 Issue 5: 1113-1123

Stronach, S.M., Rudd, T. and Lester, J.N., 1986. Anaerobic Digestion Process in Industrial Wastewater Treatment. Springer-Verlag, Berlin, Heidelberg, Germany

Stryer, L. 1988. Biochemistry. 3rd ed., W. H. Freeman & Co., New York, , U.S.

ten Brummeler, E., Horbach, H.C.J.M. and Koster, I.W., 1991. Dry anaerobic batch digestion of the organic fraction of municipal solid waste. J. Chem. Tech. Biotechnol. Vol 50: 191-209

Torre, A.D., Stephanopoulos, G., 1986. Mixed culture model of anaerobic digestion: Application to the valuation of startup procedures. Biotech. Bioeng. Vol 28: 1106-1118

van Dongen, U., Jetten, M.S.M. and van Loosdrecht, M.C.M., 2001. The SHARON®-Anammox® process for treatment of ammonium rich wastewater. Wat. Sci. Tech. Vol 44, No 1: 153-160

van Lier, J.B., Rebac, S. and Lettinga, G., 1997. High-rate anaerobic wastewater treatment under psychrophilic and thermophilic conditions. Wat. Sci. Tech. Vol 35, No 10: 199-206

van Velsen, A.F.M., 1977. Anaerobic digestion of piggery waste. Netherlands Journal of Agricultural Science Vol 25: 151

Vavilin, V.A., Rytov, S.V. and Lokshina, L.Y., 1996. A description of hydrolysis kinetics in anaerobic degradation of particulate organic matter. Biores. Tech. Vol 56: 229-237

Veeken, A. and Hamelers, B., 1999.Effect of temperature on hydrolysis rates of selected biowaste components. Biores. Technol. Vol 69, No 3: 249-254

Veeken, A., Kalyuzhyi, S., Scharff, H. and Hamelers, B., 2000. Effect of pH and VFA on hydrolysis of organic solid waste. J. Environ. Eng. Vol 126, No 12: 1076-1081

Wendland, C., Deegener, S., Behrendt, J. and Otterpohl, R., 2004. Anaerobic digestion of blackwater from vacuum toilets. The 10th World Congress on Anaerobic Digestion (AD10), proceedings, Montreal, Canada

Whitman, W.G., 1923. The two-film-theory of absorption. Chem. Met. Eng. Vol 29: 147

Zeeman, G. and Lettinga, G., 1999. The role of anaerobic digestion of domestic sewage in closing the water and nutrient cycle at community level. Wat. Sci. Tech. Vol 39, No 5: 187-194

Appendix

Appendix A : The list of symbols and abbreviations

Abbreviation	Description	Abbreviation	Description
AA	amino acids	HVa	valeric acid
Ac^-	acetate	IC	Inorganic Carbon
AD	anaerobic digestion	IN	Inorganic Nitrogen
ADP	anaerobic digestion process	LCFA	long chain fatty acids
BPR	biogas production rate	MS	monosaccharides
Bu^-	butyrate	NH_3-N	ammonia nitrogen
BWAD	blackwater anaerobic digestion	NH_4-N	ammonium nitrogen
CH_4	methane	Pr^-	propionate
CO_2	carbon dioxide	SCFA	short chain fatty acids
COD	Chemical Oxygen Demand	Sec.	section
CSTR	Continual Stirred Tank Reactor	SI	soluble inerts
DAE	Differential-Algebraic Equation	SRT	sludge retention time
DE	Differential Equation	TAN	total ammonium nitrogen
DESAR	decentralized sanitation and reuse	TC	Total Carbon
ECOSAN	ecological sanitation	TIC	Total Inorganic Carbon
Eqn.	equation	TIN	Total Inorganic Nitrogen
F1	KR feed once per week	TN	Total Nitrogen
F2	KR feed once per two weeks	TOC	Total Organic Carbon
FAN	free ammonia nitrogen	TSS	Total Suspended Solids
F/M	Food biomass ratio	TUHH	Hamburg University of Technology
GC	gas chromatography	Va^-	valerate
HAc	acetic acid	VFA	Volatile fatty acids
HBu	butyric acid	VS	Volatile Solids
HPr	Propionic acid	WWTP	wastewater treatment plants
HRT	hydraulic retention time	XI	particulate inerts

* The mathematical symbols and their units can be found in Table 1, on page 8.

Appendix B : The matrix of biochemical processes (modified from ADM1)

	Component i →	1	2	3	4	5	6	7	8	9	10	11	12	Reaction rate: ρ_j, g COD/(m^3·d)
j	Process j ↓	S_{su}	S_{aa}	S_{fa}	S_{va}	S_{bu}	S_{pro}	S_{ac}	S_{h2}	S_{ch4}	S_{IC}	S_{IN}	S_I	
C_i	C content	C_{su}	C_{aa}	C_{fa}	C_{va}	C_{bu}	C_{pro}	C_{ac}		C_{ch4}	C_{IC}		C_{SI}	
N_i	N content		N_{aa}									C_{IN}	N_{SI}	
0	raw $X_{c,raw}$				$f_{va\_xc,raw}$	$f_{bu\_xc,raw}$	$f_{pro\_xc,raw}$	$f_{ac\_xc,raw}$						
1	Disintegration										$\sum_{i=1\sim9,11\sim24} C_i \nu_{i,1}$		$f_{SI,Xc}$	$\rho_{dis} = k_{dis} X_c$
2	Hydrolysis Carbohydrates	1.0									$\sum_{i=1\sim9,11\sim24} C_i \nu_{i,2}$			$\rho_{hyd,ch} = k_{hyd,ch} X_{ch}$
3	Hydrolysis of Proteins		1.0								$\sum_{i=1\sim9,11\sim24} C_i \nu_{i,3}$			$\rho_{hyd,pr} = k_{hyd,pr} X_{pr}$
4	Hydrolysis of Lipids	1-$f_{fa,li}$		$f_{fa,li}$							$\sum_{i=1\sim9,11\sim24} C_i \nu_{i,4}$			$\rho_{hyd,li} = k_{hyd,li} X_{li}$
5	Uptake of Sugars	-1.0				(1-Y_{su}) $f_{bu,su}$	(1-Y_{su}) $f_{pro,su}$	(1-Y_{su}) $f_{ac,su}$	(1-Y_{su}) $f_{h2,su}$		$\sum_{i=1\sim9,11\sim24} C_i \nu_{i,5}$	- (Y_{su}) N_{biom}		$\rho_{su} = k_{m,su} \frac{S_{su}}{K_{S,su} + S_{su}} X_{su} \cdot I_1$
6	Uptake of Amino Acids		-1.0		(1-Y_{aa}) $f_{va,aa}$	(1-Y_{aa}) $f_{bu,aa}$	(1-Y_{aa}) $f_{pro,aa}$	(1-Y_{aa}) $f_{ac,aa}$	(1-Y_{aa}) $f_{h2,aa}$		$\sum_{i=1\sim9,11\sim24} C_i \nu_{i,6}$	N_{aa}- (Y_{aa})N_{biom}		$\rho_{aa} = k_{m,aa} \frac{S_{aa}}{K_{S,aa} + S_{aa}} X_{aa} \cdot I_1$
7	Uptake of LCFA			-1.0				(1-Y_{fa}) 0.70	(1-Y_{fa}) 0.30		$\sum_{i=1\sim9,11\sim24} C_i \nu_{i,7}$	- (Y_{fa}) N_{biom}		$\rho_{fa} = k_{m,fa} \frac{S_{fa}}{K_{S,fa} + S_{fa}} X_{fa} \cdot I_2$
8	Uptake of Valerate				-1.0		(1-Y_{c4}) 0.54	(1-Y_{c4}) 0.31	(1-Y_{c4}) 0.15		$\sum_{i=1\sim9,11\sim24} C_i \nu_{i,8}$	- (Y_{c4}) N_{biom}		$\rho_{va} = k_{m,c4} \frac{S_{va}}{K_{S,c4} + S_{va}} X_{c4} \cdot \frac{S_{va}}{S_{va} + S_{bu}} \cdot I_2$
9	Uptake of Butyrate					-1.0		(1-Y_{c4}) 0.80	(1-Y_{c4}) 0.20		$\sum_{i=1\sim9,11\sim24} C_i \nu_{i,9}$	- (Y_{c4}) N_{biom}		$\rho_{bu} = k_{m,c4} \frac{S_{bu}}{K_{S,c4} + S_{bu}} X_{c4} \cdot \frac{S_{bu}}{S_{bu} + S_{va}} \cdot I_2$
10	Uptake of Propionate						-1.0	(1-Y_{pro}) 0.57	(1-Y_{pro}) 0.43		$\sum_{i=1\sim9,11\sim24} C_i \nu_{i,10}$	- (Y_{pro}) N_{biom}		$\rho_{pro} = k_{m,pro} \frac{S_{pro}}{K_{S,pro} + S_{pro}} X_{pro} \cdot I_2$
11	Uptake of Acetate							-1.0		(1-Y_{ac})	$\sum_{i=1\sim9,11\sim24} C_i \nu_{i,11}$	- (Y_{ac}) N_{biom}		$\rho_{ac} = k_{m,ac} \frac{S_{ac}}{K_{S,ac} + S_{ac}} X_{ac} \cdot I_3$
12	Uptake of Hydrogen								-1.0	(1-Y_{h2})	$\sum_{i=1\sim9,11\sim24} C_i \nu_{i,12}$	- (Y_{h2}) N_{biom}		$\rho_{h2} = k_{m,h2} \frac{S_{h2}}{K_{S,h2} + S_{h2}} X_{h2} \cdot I_1$
13	Decay of X_{su}													$\rho_{dec,Xsu} = k_{dec,Xsu} X_{su}$
14	Decay of X_{aa}													$\rho_{dec,Xaa} = k_{dec,Xaa} X_{aa}$
15	Decay of X_{fa}													$\rho_{dec,Xfa} = k_{dec,Xfa} X_{fa}$
16	Decay of X_{c4}													$\rho_{dec,Xc4} = k_{dec,Xc4} X_{c4}$
17	Decay of X_{pro}													$\rho_{dec,Xpro} = k_{dec,Xpro} X_{pro}$
18	Decay of X_{ac}													$\rho_{dec,Xac} = k_{dec,Xac} X_{ac}$
19	Decay of X_{h2}													$\rho_{dec,Xh2} = k_{dec,Xh2} X_{h2}$
		Mono-saccharides (g COD/m^3)	Amino acids (g COD/m^3)	LCFA (g COD/m^3)	Total valerate (g COD/m^3)	Total butyrate (g COD/m^3)	Total propionate (g COD/m^3)	Total acetate (g COD/m^3)	Hydrogen gas (g COD/m^3)	Methane gas (g COD/m^3)	Inorganic carbon (mole C/m^3)	Inorganic nitrogen (g N/m^3)	Soluble inerts (g COD/m^3)	Inhibition factors: $I_1 = I_{pH} \cdot I_{IN,lim}$ $I_2 = I_{pH} \cdot I_{IN,lim} \cdot I_{h2}$ $I_3 = I_{pH} \cdot I_{IN,lim} \cdot I_{NH3,ac}$

The matrix of biochemical processes (Continued)

	Component i →	13	14	15	16	17	18	19	20	21	22	23	24	25	Reaction rate: ρ_j, g COD/(m^3·d)
j	Process j ↓	X_c	X_{ch}	X_{pr}	X_{li}	X_{su}	X_{aa}	X_{fa}	X_{c4}	X_{pro}	X_{ac}	X_{h2}	X_I	$X_{c,raw}$	
C_i	C content	C_{Xc}	C_{ch}	C_{pr}	C_{li}	C_{biom}	C_{biom}	C_{biom}	C_{biom}	C_{biom}	C_{biom}	C_{biom}	C_{XI}	$C_{Xc,raw}$	
N_i	N content	N_{Xc}		N_{pr}			N_{biom}	N_{biom}	N_{biom}	N_{biom}	N_{biom}	N_{biom}	N_{XI}	$N_{Xc,raw}$	
0	raw $X_{C,raw}$	$f_{xc\_xc,raw}$												-1	
1	Disintegration	-1.0	$f_{ch,Xc}$	$f_{pr,Xc}$	$f_{li,Xc}$								$f_{XI,Xc}$		$\rho_{dis} = k_{dis} X_c$
2	Hydrolysis Carbohydrates		-1.0												$\rho_{hyd,ch} = k_{hyd,ch} X_{ch}$
3	Hydrolysis of Proteins			-1.0											$\rho_{hyd,pr} = k_{hyd,pr} X_{pr}$
4	Hydrolysis of Lipids				-1.0										$\rho_{hyd,li} = k_{hyd,li} X_{li}$
5	Uptake of Sugars					Y_{su}									$\rho_{su} = k_{m,su} \frac{S_{su}}{K_{S,su} + S_{su}} X_{su} \cdot I_1$
6	Uptake of Amino Acids						Y_{aa}								$\rho_{aa} = k_{m,aa} \frac{S_{aa}}{K_{S,aa} + S_{aa}} X_{aa} \cdot I_1$
7	Uptake of LCFA							Y_{fa}							$\rho_{fa} = k_{m,fa} \frac{S_{fa}}{K_{S,fa} + S_{fa}} X_{fa} \cdot I_2$
8	Uptake of Valerate								Y_{c4}						$\rho_{va} = k_{m,c4} \frac{S_{va}}{K_{S,c4} + S_{va}} X_{c4} \cdot \frac{S_{va}}{S_{va} + S_{bu}} \cdot I_2$
9	Uptake of Butyrate								Y_{c4}						$\rho_{bu} = k_{m,c4} \frac{S_{bu}}{K_{S,c4} + S_{bu}} X_{c4} \cdot \frac{S_{bu}}{S_{bu} + S_{va}} \cdot I_2$
10	Uptake of Propionate									Y_{pro}					$\rho_{pro} = k_{m,pro} \frac{S_{pro}}{K_{S,pro} + S_{pro}} X_{pro} \cdot I_2$
11	Uptake of Acetate										Y_{ac}				$\rho_{ac} = k_{m,ac} \frac{S_{ac}}{K_{S,ac} + S_{ac}} X_{ac} \cdot I_3$
12	Uptake of Hydrogen											Y_{h2}			$\rho_{h2} = k_{m,h2} \frac{S_{h2}}{K_{S,h2} + S_{h2}} X_{h2} \cdot I_1$
13	Decay of X_{su}	1.0				-1.0									$\rho_{dec,Xsu} = k_{dec,Xsu} X_{su}$
14	Decay of X_{aa}	1.0					-1.0								$\rho_{dec,Xaa} = k_{dec,Xaa} X_{aa}$
15	Decay of X_{fa}	1.0						-1.0							$\rho_{dec,Xfa} = k_{dec,Xfa} X_{fa}$
16	Decay of X_{C4}	1.0							-1.0						$\rho_{dec,Xc4} = k_{dec,Xc4} X_{c4}$
17	Decay of X_{pro}	1.0								-1.0					$\rho_{dec,Xpro} = k_{dec,Xpro} X_{pro}$
18	Decay of X_{ac}	1.0									-1.0				$\rho_{dec,Xac} = k_{dec,Xac} X_{ac}$
19	Decay of X_{h2}	1.0										-1.0			$\rho_{dec,Xh2} = k_{dec,Xh2} X_{h2}$
		Composites (g COD/m^3)	Carbohydrates (g COD/m^3)	Proteins (g COD/m^3)	Lipids (g COD/m^3)	Sugar degraders (g COD/m^3)	Amino acid degraders (g COD/m^3)	LCFA degraders (g COD/m^3)	Valerate and butyrate degraders (g COD/m^3)	Propionate degraders (g COD/m^3)	Acetate degraders (g COD/m^3)	Hydrogen degraders (g COD/m^3)	Particulate inerts (g COD/m^3)	Raw input (g COD/m^3)	Inhibition factors: $I_1 = I_{pH} \cdot I_{IN,lim}$ $I_2 = I_{pH} \cdot I_{IN,lim} \cdot I_{h2}$ $I_3 = I_{pH} \cdot I_{IN,lim} \cdot I_{NH3,ac}$

Appendix C : The DE implementation for acid-base processes

Acid-base processes are implemented as dynamic processes

	Component i →	**4a**	**4b**	**5a**	**5b**	**6a**	**6b**	**7a**	**7b**	**10a**	**10b**	**10c**	**11a**	**11b**	
j	**Process j ↓**	S_{HVa}	S_{Va-}	S_{HBu}	S_{Bu-}	S_{HPro}	S_{Pro-}	S_{HAc}	S_{Ac-}	S_{CO2}	S_{HCO3-}	S_{CO3--}	S_{NH4+}	S_{NH3}	**Reaction rate: ρ_j, g COD/(m^3·d)**
AB-1	**Valerate**	1	-1												$k_{A/B,HVa}\left(S_{Va^-}\cdot S_{H^+} - K_{a,va}\cdot S_{HVa}\right)$
AB-2	**Butyrate**			1	-1										$k_{A/B,HBu}\left(S_{Bu^-}\cdot S_{H^+} - K_{a,bu}\cdot S_{HBu}\right)$
AB-3	**Propionate**					1	-1								$k_{A/B,HPro}\left(S_{Pro^-}\cdot S_{H^+} - K_{a,pro}\cdot S_{HPro}\right)$
AB-4	**Acetate**							1	-1						$k_{A/B,HAc}\left(S_{Ac^-}\cdot S_{H^+} - K_{a,ac}\cdot S_{HAc}\right)$
AB-5	**Carbon dioxide**									1	-1				$k_{A/B,CO_2}\left(S_{HCO_3^-}\cdot S_{H^+} - K_{a,CO_2}\cdot S_{H_2CO_3}\right)$
AB-5	**Bicarbonate**										1	-1			$k_{A/B,HCO_3^-}\left(S_{CO_3^{2-}}\cdot S_{H^+} - K_{a,HCO_3^-}\cdot S_{HCO_3^-}\right)$
AB-7	**Ammonium**												1	-1	$k_{A/B,NH_4^+}\left(S_{NH_3}\cdot S_{H^+} - K_{a,NH_4^+}\cdot S_{NH_4^+}\right)$
		Valeric acid (g COD/m^3)	Valerate (g COD/m^3)	Butyric acid (g COD/m^3)	Butyrate (g COD/m^3)	Propionic acid (g COD/m^3)	Propionate (g COD/m^3)	Acetic acid (g COD/m^3)	Acetate (g COD/m^3)	Carbon-dioxide (mole C/m^3)	Bicarbonate (mole C/m^3)	Carbonate (mole C/m^3)	Ammonium (g N/m^3)	Ammonia (g N/m^3)	* $k_{A/B,i}$ (m^3·$mole^{-1}$·d^{-1}) can be in between 10^7 and 10^{14}, and generally the same results will be attained. ** For each acid-base this process can not be implemented together with its process in Append E

Appendix D : The DAE implementation for acid-base processes

Acid-base processes are implemented as equilibrium processes

	Equation	Variable
1	$S_{cat^+} + S_{NH_4^+} + S_{H^+} - S_{HCO_3^-} - 2 \times S_{CO_3^{2-}} - \frac{S_{Ac^-}}{64} - \frac{S_{Pro^-}}{112} - \frac{S_{Bu^-}}{160} - \frac{S_{Va^-}}{208} - S_{OH^-} - S_{an^-} = 0$	S_{H^+}
2	$S_{OH^-} - \frac{K_W}{S_{H^+}} = 0$	S_{OH^-}
3	$S_{Va^-} - \frac{K_{a,va} \cdot S_{va,total}}{K_{a,va} + S_{H^+}} = 0$	S_{Va^-}
4	$S_{Bu^-} - \frac{K_{a,bu} \cdot S_{bu,total}}{K_{a,bu} + S_{H^+}} = 0$	S_{Bu^-}
5	$S_{Pro^-} - \frac{K_{a,pro} \cdot S_{pro,total}}{K_{a,pro} + S_{H^+}} = 0$	S_{Pro^-}
6	$S_{Ac^-} - \frac{K_{a,ac} \cdot S_{ac,total}}{K_{a,ac} + S_{H^+}} = 0$	S_{Ac^-}
7	$S_{HCO_3^-} - \frac{K_{a,CO_2} \cdot S_{IC}}{K_{a,CO_2} + S_{H^+}} = 0$	$S_{HCO_3^-}$
8	$S_{CO_3^{2-}} - \frac{K_{a,HCO_3^-} \cdot S_{HCO_3^-}}{K_{a,HCO_3^-} + S_{H^+}} = 0$	$S_{CO_3^{2-}}$
9	$S_{IC} - S_{CO_2} - S_{HCO_3^-} - S_{CO_3^{2-}} = 0$	S_{CO_2}
10	$S_{NH_4^+} - \frac{S_{H^+} \cdot S_{IN}}{K_{a,NH_4} + S_{H^+}} = 0$	$S_{NH_4^+}$
11	$S_{IN} - S_{NH_3} - S_{NH_4^+} = 0$	S_{NH_3}

Appendix E : The values of biochemical processes parameters

1. Carbon content (C_i) and Nitrogen content (N_i) of each component

j	*Name*	*Description*	*C content*	*mole C/g COD*	*N content*	*g N/g COD*	*Remark*
1	S_{su}	monosaccharides	C_{su}	6/192	N_{su}	0	
2	S_{aa}	amino acids	C_{aa}	0.0300	N_{aa}	0.098	
3	S_{fa}	total LCFA	C_{fa}	0.0217	N_{fa}	0	
4	S_{va}	total valerate	C_{va}	5/208	N_{va}	0	
5	S_{bu}	total butyrate	C_{bu}	4/160	N_{bu}	0	
6	S_{pro}	total propionate	C_{pro}	3/112	N_{pro}	0	
7	S_{ac}	total acetate	C_{ac}	2/64	N_{ac}	0	
8	S_{h2}	hydrogen	C_{h2}	0	N_{h2}	0	
9	S_{ch4}	methane	C_{ch4}	1/64	N_{ch4}	0	
10	S_{IC}	inorganic carbon	C_{IC}	-	N_{IC}	0	
11	S_{IN}	inorganic nitrogen	C_{IN}	0	N_{IN}	1	
12	S_I	soluble inerts	C_{SI}	0.0300	N_{SI}	0.028	
13	X_c	composite	C_{Xc}	0.0279	N_{Xc}	0.028	
14	X_{ch}	carbohydrates	C_{ch}	0.0313	N_{ch}	0	
15	X_{pr}	proteins	C_{pr}	0.0300	N_{pr}	0.098	
16	X_{li}	lipids	C_{li}	0.0217	N_{li}	0	
17~23	$X_{su\sim h2}$	biomass	C_{biom}	5/160	N_{biom}	0.0875	biomass
24	X_I	particulate inerts	C_{XI}	0.0300	N_{XI}	0.028	
0	$X_{c,raw}$	raw input	$C_{Xc,raw}$	0.0217	$N_{Xc,raw}$	0.028	

* The values partly come from ADM1, and partly come from Mr. Batstone by personal contact.

** The number in the first column is the number of processes in Appendix B. The following tables have the same arrangement.

*** Normally IC refers CO_2 and its derivatives, which have 0 g COD content, so the carbon content coefficient of IC is not given here. It is also unnecessary.

2. The values of stoichiometric parameters for mass flux

No	Name	Description	ADM1	Without va	Without va & bu	Remark
	f_{sl_xc}	soluble inert from composites	0.1	0.1	0.1	$1-f_{ch\_xc}-f_{li\_xc}-f_{pr\_xc}-f_{xl\_xc}$
	f_{xl_xc}	particulate inert from composites	0.25	0.25	0.25	
	f_{ch_xc}	carbohydrates from composites	0.2	0.2	0.2	
	f_{pr_xc}	proteins from composites	0.2	0.2	0.2	
	f_{li_xc}	lipids form composites	0.25	0.25	0.25	
	f_{su_li}	sugars from lipids	0.05	0.05	0.05	$1-f_{fa\_li}$
	f_{fa_li}	LCFA from lipids	0.95	0.95	0.95	
	f_{h2_su}	hydrogen from sugars	0.1906	0.1906	0.2172	$0.33*\eta_{1,su}+0.17*\eta_{3,su}$
	f_{bu_su}	butyrate from sugars	0.1328	0.1328	-	$0.83*\eta_{3,su}$
	f_{pro_su}	propionate from sugars	0.2690	0.2690	0.2690	$0.78*\eta_{2,su}$
	f_{ac_su}	acetate from sugars	0.4076	0.4076	0.5138	$0.67*\eta_{1,su}+0.22*\eta_{2,su}$
	f_{h2_aa}	hydrogen from amino acids	0.06	0.08	0.1465	$1-f_{va\_aa}-f_{bu\_aa}-f_{pro\_aa}-f_{ac\_aa}$
	f_{va_aa}	valerate from amino acids	0.23	-	-	
	f_{bu_aa}	butyrate from amino acids	0.26	0.26	-	
	f_{pro_aa}	propionate from amino acids	0.05	0.1742	0.1742	
	f_{ac_aa}	acetate from amino acids	0.4	0.4858	0.6793	
	$\eta_{1,su}$	sugar gradation coefficient 1	0.495	0.495	-	$1-\eta_{2,su}-\eta_{3,su}$
	$\eta_{2,su}$	sugar gradation coefficient 2	0.345	0.345	-	
	$\eta_{3,su}$	sugar gradation coefficient 3	0.16	0.16	-	
	$f_{xc\_xc,raw}$	from raw blackwater to X_C	0.72	0.73	0.74	
	$f_{va\_xc,raw}$	valerate in raw blackwater	0.01	0	0	
	$f_{bu\_xc,raw}$	butyrate in raw blackwater	0.02	0.02	0	
	$f_{pro\_xc,raw}$	propionate in raw blackwater	0.05	0.05	0.06	
	$f_{ac\_xc,raw}$	acetate in raw blackwater	0.20	0.20	0.20	

* The data partly come from ADM1, and partly come from Mr. Batstone by personal contact.

** Other fixed coefficients can be found directly from Peterson Matrix in Appendix B.

*** The coefficients for cases of "without va" and "without va & bu" are figured out based on the values from ADM1.

**** The raw blackwater ($X_{C,raw}$) is first distributed to composites (X_C) and SCFA, as it contains quite a few amount of SCFA.

3. The values of biochemical kinetics parameters

j	*Name*	*Description*	*ADM1*	*Used*	*Min*	*Max.*	*Unit*
	disintegration and hydrolysis rates						
1	k_{dis}	disintegration rate of composites	0.5	4.5	0.013	0.700	d^{-1}
2	k_{hyd_ch}	hydrolysis rate of carbohydrates	10	10			d^{-1}
3	k_{hyd_pr}	hydrolysis rate of proteins	10	10			d^{-1}
4	k_{hyd_li}	hydrolysis rate of lipids	10	10			d^{-1}
	biomass decay						
13	k_{S_su}	sugar degraders	0.02	0.03	0.010	0.800	d^{-1}
14	k_{dec_aa}	amino acid degraders	0.02	0.03	0.010	0.800	d^{-1}
15	k_{dec_fa}	LCFA degraders	0.02	0.02	0.010	0.060	d^{-1}
16	k_{dec_c4}	valerate and butyrate degraders	0.02	0.03	0.010	0.030	d^{-1}
17	k_{dec_pro}	propionate degraders	0.02	0.04	0.010	0.060	d^{-1}
18	k_{dec_ac}	acetate degraders	0.02	0.04	0.010	0.050	d^{-1}
19	k_{dec_H2}	hydrogen degraders	0.02	0.04	0.009	0.300	d^{-1}
	Maximum uptake rate						
5	k_{m_su}	sugar degraders	30	30	27.0	5067.0	d^{-1}
6	k_{m_aa}	amino acid degraders	50	50	27.0	53.0	d^{-1}
7	k_{m_fa}	LCFA degraders	6	6	1.9	363.0	d^{-1}
8~9	k_{m_c4}	valerate and butyrate degraders	20	18	5.3	41.0	d^{-1}
10	k_{m_pro}	propionate degraders	13	14	11.0	23.0	d^{-1}
11	k_{m_ac}	acetate degraders	8	13	6.4	19.0	d^{-1}
12	k_{m_H2}	hydrogen degraders	35	35	25.0	44.0	d^{-1}
	half saturation concentration						
5	K_{S_su}	sugar degraders	500	500	50	1280	g COD/m^3
6	K_{S_aa}	amino acid degraders	300	300	50	1198	g COD/m^3
7	K_{S_fa}	LCFA degraders	400	400	100	9210	g COD/m^3
8~9	K_{S_c4}	valerate and butyrate degraders	300	110	13	280	g COD/m^3
10	K_{S_pro}	propionate degraders	300	120	20	373	g COD/m^3
11	K_{S_ac}	acetate degraders	150	160	40	384	g COD/m^3
12	K_{S_H2}	hydrogen degraders	0.007	0.007	0.001	0.6	g COD/m^3
11	$K_{S\_NH3\_all}$	IN limitation to all degraders	1.4	1.4			g N/m^3
	yield from substrates to degraders						
5	$Y_{\_su}$	sugar degraders	0.1	0.1	0.07	0.17	COD/COD
6	$Y_{\_aa}$	amino acid degraders	0.08	0.08	0.058	0.15	COD/COD
7	$Y_{\_fa}$	LCFA degraders	0.06	0.06	0.004	0.055	COD/COD

j	*Name*	*Description*	*ADM1*	*Used*	*Min*	*Max.*	*Unit*
8~9	Y_{c4}	valerate and buterate degraders	0.06	0.06			COD/COD
10	Y_{pro}	propionate degraders	0.04	0.04	0.019	0.055	COD/COD
11	Y_{ac}	acetate degraders	0.05	0.05	0.027	0.076	COD/COD
12	Y_{h2}	hydrogen degraders	0.06	0.06	0.05	0.06	COD/COD
	50% inhibitory concentration						
7	$K_{I\_H2\_fa}$	hydrogen to LCFA uptake	0.005	0.005			g COD/m^3
8~9	$K_{I\_H2\_c4}$	hydrogen to bu and va uptake	0.01	0.01			g COD/m^3
10	$K_{I\_H2\_pro}$	hydrogen to propionate uptake	0.0035	0.0035			g COD/m^3
11	$K_{I\_NH3\_ac}$	Free NH_3 to acetate uptake	25.2	200 / 50			g N/m^3
	upper and lower pH of 50% inhibitory level						
5~10	$pH_{su\sim pro\_ul}$	only lower pH inhibition considered	5.5	5.5			-
5~10	$pH_{su\sim pro\_ll}$		4.0	4.0			-
11	pH_{ac_ul}	both lower and upper inhibition considered		8.0			-
11	pH_{ac_ll}			6.0			-
12	pH_{h2_ul}	only lower pH inhibition considered	6.0	6.0			-
12	pH_{h2_ll}		5.0	5.0			-

* The variation range of each parameter is summarized from the literature review of ADM1.

Appendix F : The physicochemical constants

1. Acid-base equilibrium constants

No	*Acid/base*	*pK_a (-) at 298K*	*ΔH^0 (j/mole)*	*K_a (mM) at 311K*	*Remark*
1	HAc/Ac^-	4.76	-	0.017378	
2	HBu/Bu^-	4.84	-	0.014454	
3	CO_2/HCO_3^-	6.35	7,646	0.000508	
4	HCO_3^-/CO_3^{2-}	10.33	14,850	4.93×10^{-4}	
5	$H_2O/(OH^-)$	14.00	55,900	2.08×10^{-8}	$K_a = 10^{(-pK_a+6)}$
6	NH_3/NH_4^+	9.25	51,965	1.11×10^{-6}	
7	HPr/Pr^-	4.88	-	0.013183	
8	HVa/Va^-	4.80	-	0.015849	

* The values of pK_a and ΔH^0 are gotten from Lide (2001).

** K_a is calculated by Eqn. (21): $K_a = 10^{(-pK_a+3)}$. Exponent pluses 3 because the unit is transformed from M (≡ kmole/m^3) to mM (≡ mole/m^3), and H_2O needs to plus 6 as both OH^- and H^+ are involved.

*** When ΔH^0 is available, temperature compensation is included by van't Hoff equation (42).

2. Liquid-gas transfer parameters

No	*Acid/base*	*K_H (mM_{liq}/bar_{gas}) at 298K*	*ΔH^0 (j/mole)*	*Diffusivity ($m^2/s \times 10^9$) at 311K*	*Remark*
1	H_2	0.78	-4,180	4.65	
2	CH_4	1.4	-14,240	1.57	
3	CO_2	35	-19.410	1.98	
4	NH_3	57,540			

* The values are gotten from Lide (2001).

** Normally NH_3 is not calculated in headspace due to its high K_H value.

*** When ΔH^0 is available, temperature compensation is included by van't Hoff equation (42).

Appendix G : The specification of the model file

The name of the basic model file is *ADM_1_2004-03.31-04.20_refer_ohne_va.aqu*

The file is explained in the four parts, i.e. VARIABLE, PROCESS, COMPARTMENT, and LINK, which are the same structure as AQUASIM:

1. VARIABLE

Legend:

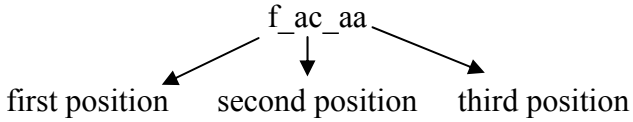

The meaning of the variable in first position:

Symbol	*Indication*	Unit	Symbol	*Indication*	Unit
C_i	carbon content of i	mole C/ g COD	**nue_i_su**	fraction of i from sugars	-
COD_S	Soluble COD	g COD/m^3	**Patm**	pressure of atmosphere	bar
COD_Tot	total COD	g COD/m^3	**Pgas_i**	partial pressure of gas i	bar
COD_X	particulate COD	g COD m^3	**Pgas_i_dried**	partial pressure of gas i (dried)	-
Exp_i	Experimental data of component i	-	**Pgas_tot**	total gas pressure	bar
f_i_j	yield of i from j	-	**pH**	pH	-
I_i_j	Inhibition of i to j	-	**pKa_i**	acid equilibrium constant of i at 298K	-
iniS_i	initial condition of i in reactor	g COD/m^3	**probeGas_S_i**	probe Variable of gas i in headspace	g COD/m^3
inPercent_xc	percentage of Xc in raw input	-	**probeLiq_S_i**	probe Variable of gas i in reactor	g COD/m^3
inQ	input flow rate	m^3/d	**Qgas**	total gas flow	m^3/d
inS_i	input concentration of i	g COD/m^3	**Qgas_Spec**	specific norm gas flow	m^3/m^3
kAB_i	kinetic constant for acid i	m^3/(mole·d)	**Qout**	effluent	m^3/d
Ka_i	dissociation constant of acid i	mole/m^3	**R**	gas law constant	bar/ (mM·K)
kdec_i	decay rate of biomass i	d^{-1}	**S_i**	concentration of soluble component i	g COD/m^3
kdis	composites disintegration rate	d^{-1}	**T**	absolute temperature	K
KH_i	non-dimensional henry's law constant	mM_{liq}/ mM_{gas}	**t**	time	d
khyd_i	Hydrolysis rate of i	d^{-1}	**V**	reactor volume	m^3
KI_i_j	inhibitory concentration of i to j	g COD/m^3	**V_reactor**	probe Variable of reactor volume	m^3
kLa	liquid-gas transfer coefficient k_La	d^{-1}	**X_i**	concentration of particulate i	g COD/m^3
km_i	maximum uptake rate of i	d^{-1}	**Y_i**	yield of biomass on uptake of i	COD/ COD
kp	pipe resistance coefficient	m^3/(bar·d)	**_inQ_dyn_i**	coefficient of input (for dynamic input)	-
Ks_i	half saturation constant of substrate i	g COD/m^3	**_inQ_vol_i**	Input volume of case i	m^3/batch
M_i	Molar weight	g/mole	**_inS_j_i**	input concen. of j at case i	g COD/m^3
mue_X_i	growth rate of biomass i	d^{-1}	**_inXc_raw_i**	The raw input concen. at case i	g COD/m^3
N_i	nitrogen content of i	g N/ g COD	**_Percent_j**	percentage of j (SCFA) in raw input	-

* Normally the unit of S_i and X_i is g COD /m^3, but S_i is mole C/m^3 and g N/m^3 for carbon and nitrogen, respectively.

** The units of experimental data are corresponding to their objects.

The meaning of the variables in second and third positions:

Symbol	*Indication*	*Symbol*	*Indication*	*Symbol*	*Indication*
aa	Amino acid	**fa**	LCFA	**NH4_p**	NH_4^+
ac	acetate	**H_p**	H^+	**OH_m**	OH^-
ac_m	acetate ion	**H2 or h2**	hydrogen	**p**	Plus (valance)
an	anions	**H2CO3**	H_2CO_3	**pr**	protein
bac	bacteria	**HCO3_m**	HCO_3-	**pro**	propionate
biom	biomass	**IN**	inorganic nitrogen	**pro_m**	propionate ion
bu	butyrate	**li**	lipids	**SI**	soluble inert
bu_m	butyrate ion	**lim**	limitation	**su**	sugar
cat	cations	**ll**	lower level	**ul**	upper level
ch4	methane	**m**	minus (valance)	**va**	valerate
CO2	CO_2	**mm**	minus 2 (valance)	**xc**	composite
CO3_mm	CO_3^{2-}	**NH3**	NH_3	**XI**	particulates inert

2. PROCESS

Symbol	*Indication*	*Symbol*	*Indication*
decay_i	decay of biomass i	**equilib_charge**	charge balance of acids, bases and salts
disintegration	disintegration of composites	**hyd_i**	hydrolysis of component i
dyn_AcidBase_i	dynamic acid-base processes of i	**uptake_i**	uptake of component i
equilib_i	equilibrium acid-base processes of i		

3. COMPARTMENT

Name	*Indication*
headspace	represent headspace; volume: 2.0 l; type: Mixed Reactor Compartment
reactor	represent liquid phase; volume: 8.0 l; type: Mixed Reactor Compartment

4. LINK

Name	*Indication*		
gas_transfer	Gas transfer between reactor and headspace; type: Diffusive Link		
Exchange Coefficients:			
Variable	**Exchange Coefficient**	**Convert Factor**	**Description**
S_CH4	k_La	KH_CH4	gas transfer of CH_4
S_H2	k_La	KH_H2	gas transfer of H_2
S_CO2	k_La	KH_CO2	gas transfer of CO_2